

HIGGS BOSONS: THEORY AND SEARCHES

Updated May 2012 by G. Bernardi (CNRS/IN2P3, LPNHE/U. of Paris VI & VII), M. Carena (Fermi National Accelerator Laboratory and the University of Chicago), and T. Junk (Fermi National Accelerator Laboratory).

- I. Introduction
- II. The Standard Model (SM) Higgs Boson
 - II.1. Indirect Constraints on the SM Higgs Boson
 - II.2. Searches for the SM Higgs Boson at LEP
 - II.3. Searches for the SM Higgs Boson at the Tevatron
 - II.4. SM Higgs Boson Searches at the LHC
 - II.5. Models with a Fourth Generation of SM-Like Fermions
- III. Higgs Bosons in the Minimal Supersymmetric Standard Model (MSSM)
 - III.1. Radiatively-Corrected MSSM Higgs Masses and Couplings
 - III.2. Decay Properties and Production Mechanisms of MSSM Higgs Bosons
 - III.3. Searches for Neutral Higgs Bosons in the CP-Conserving *CPC* Scenario
 - III.3.1. Searches for Neutral MSSM Higgs Bosons at LEP
 - III.3.2. Searches for Neutral MSSM Higgs Bosons at Hadron Colliders
 - III.4. Searches for Charged MSSM Higgs Bosons
 - III.5. Effects of *CP* Violation on the MSSM Higgs Spectrum
 - III.6. Searches for Neutral Higgs Bosons in *CPV* Scenarios
 - III.7. Indirect Constraints on Supersymmetric Higgs Bosons
- IV. Other Model Extensions
- V. Searches for Higgs Bosons Beyond the MSSM
- VI. Outlook
- VII. Addendum

NOTE: The 4 July 2012 update on the Higgs search from ATLAS and CMS is described in the Addendum at the end of this review.

I. Introduction

Understanding the mechanism that breaks electroweak symmetry and generates the masses of the known elementary particles¹ is one of the most fundamental problems in particle physics. The Higgs mechanism [1] provides a general framework to explain the observed masses of the W^\pm and Z gauge bosons by means of charged and neutral Goldstone bosons that are manifested as the longitudinal components of the gauge bosons. These Goldstone bosons are generated by the underlying dynamics of electroweak symmetry breaking (EWSB). However, the fundamental dynamics of the electroweak symmetry breaking are unknown. There are two main classes of theories proposed in the literature, those with weakly coupled dynamics—such as in the Standard Model (SM) [2]—and those with strongly coupled dynamics; both classes are summarized below.

In the SM, the electroweak interactions are described by a gauge field theory based on the $SU(2)_L \times U(1)_Y$ symmetry group. The Higgs mechanism posits a self-interacting complex doublet of scalar fields, and renormalizable interactions are arranged such that the neutral component of the scalar doublet acquires a vacuum expectation value $v \approx 246$ GeV, which sets the scale of EWSB. Three massless Goldstone bosons are generated, which are absorbed to give masses to the W^\pm and Z gauge bosons. The remaining component of the complex doublet becomes the Higgs boson—a new fundamental scalar particle. The masses of all fermions are also a consequence of EWSB since the Higgs doublet is postulated to couple to the fermions through Yukawa interactions. If the Higgs boson mass m_H is below ~ 180 GeV, all fields remain weakly interacting up to the Planck scale, M_{Pl} .

The validity of the SM as an effective theory describing physics up to the Planck scale is questionable, however, because of the following “naturalness” argument. All fermion masses and dimensionless couplings are logarithmically sensitive to the

¹ In the case of neutrinos, it is possible that the Higgs mechanism plays a role but is not entirely responsible for the generation of their observed masses.

scale Λ at which new physics becomes relevant. In contrast, scalar squared masses are quadratically sensitive to Λ . Thus, the observable SM Higgs mass has the following form:

$$m_H^2 = m_{H_0}^2 + \frac{kg^2\Lambda^2}{16\pi^2},$$

where m_{H_0} is a fundamental parameter of the theory. The second term is a one-loop correction in which g is an electroweak coupling and k is a constant, presumably of $\mathcal{O}(1)$, that is calculable within the low-energy effective theory. The two contributions arise from independent sources and one would not expect that the observable Higgs boson mass is significantly smaller than either of the two terms. Hence, if the scale of new physics Λ is much larger than the electroweak scale, unnatural cancellations must occur to remove the quadratic dependence of the Higgs boson mass on this large energy scale and to give a Higgs boson mass of order of the electroweak scale, as required from unitarity constraints [3,4], and as preferred by precision measurements of electroweak observables [5]. Most relevantly, recent results from direct Higgs searches at the Tevatron [6] and, in particular, at the LHC [7–10] strongly constrain the SM Higgs boson mass to be in the range 114–129 GeV, in excellent agreement with the indirect predictions from electroweak precision data. Thus, the SM is expected to be embedded in a more fundamental theory which will stabilize the hierarchy between the electroweak scale and the Planck scale in a natural way. A theory of that type would usually predict the onset of new physics at scales of the order of, or just above, the electroweak scale. Theorists strive to construct models of new physics that keep the successful features of the SM while curing its shortcomings, such as the absence of a dark matter candidate or a detailed explanation of the observed baryon asymmetry of the universe.

In the weakly-coupled approach to electroweak symmetry breaking, supersymmetric (SUSY) extensions of the SM provide a possible explanation for the stability of the electroweak energy scale in the presence of quantum corrections [11,12]. These theories predict at least five Higgs particles [13]. The properties of the lightest Higgs scalar often resemble those of

the SM Higgs boson, with a mass that is predicted to be less than 135 GeV [14] in the simplest supersymmetric model². Additional neutral and charged Higgs bosons are also predicted. Moreover, low-energy supersymmetry with a supersymmetry breaking scale of order 1 TeV allows for grand unification of the electromagnetic, weak and strong gauge interactions in a consistent way, strongly supported by the prediction of the electroweak mixing angle at low energy scales, with an accuracy at the percent level [22,23].

Alternatively new strong interactions near the TeV scale can induce strong breaking of the electroweak symmetry [24]. “Little Higgs” models have been proposed in which the scale of the new strong interactions is pushed up above 10 TeV [25–27], and the lightest Higgs scalar resembles the weakly-coupled SM Higgs boson.

Another approach to electroweak symmetry breaking has been explored in which extra space dimensions beyond the usual 3 + 1 dimensional space-time are introduced [28] with characteristic sizes of the fundamental Planck scale of order $(1 \text{ TeV})^{-1}$. In such scenarios, the mechanisms for electroweak symmetry breaking are inherently extra-dimensional and the resulting Higgs phenomenology can depart significantly from SM predictions [27,29].

Both in the framework of supersymmetric theories and in the strongly coupled dynamic approach there have been many studies based on effective theory approaches [18,20,21,30,31] that prove useful in exploring departures from the SM Higgs phenomenology in a more model independent way.

Prior to 1989, when the e^+e^- collider LEP at CERN came into operation, searches were sensitive only to Higgs bosons

² Larger values of the mass of the lightest Higgs boson, up to about 250 GeV, can be obtained in non-minimal SUSY extensions of the SM [15–21]. However, if the LHC’s indications of a light Higgs boson are confirmed, the main motivation for non-minimal SUSY extensions would be to obtain a Higgs boson mass in the 120–130 GeV mass range without demanding heavy top quark superpartners, and thereby avoid the so-called little hierarchy problem.

with masses of a few GeV and below [32]. In the LEP 1 phase, the collider operated at center-of-mass energies close to M_Z . During the LEP 2 phase, the energy was increased in steps, reaching 209 GeV in the year 2000 before the final shutdown. The combined data of the four LEP experiments, ALEPH, DELPHI, L3, and OPAL, were sensitive to neutral Higgs bosons with masses up to about 115 GeV and to charged Higgs bosons with masses up to about 90 GeV [33,34].

The search for the Higgs boson continued at the Tevatron $p\bar{p}$ collider, which operated at a center-of-mass energy of 1.96 TeV until its shutdown in the Fall of 2011. The two experiments, CDF and DØ, each collected approximately 10 fb^{-1} of data with the capability to probe a SM Higgs boson mass in the 90 – 185 GeV range. The combination of the results from CDF and DØ shows an excess of data events with respect to the background estimation in the mass range $115 \text{ GeV} < m_H < 135 \text{ GeV}$. The global significance for such an excess anywhere in the full mass range is approximately 2.2 standard deviations. The excess is concentrated in the $H \rightarrow b\bar{b}$ channel, although the results in the $H \rightarrow W^+W^-$ channel are also consistent with the possible presence of a low-mass Higgs boson. Other neutral and charged Higgs particles postulated in most theories beyond the SM are also searched for at the Tevatron. The Tevatron Higgs results are discussed in more detail later in this review. The final results are expected to be available by the end of 2012.

Searches for Higgs bosons are ongoing at the LHC pp collider. These searches have much higher sensitivity than the Tevatron searches and cover masses up to several hundred GeV. At present both LHC experiments, ATLAS and CMS, have searched for a SM Higgs boson produced mainly through gluon fusion, and decaying dominantly into gauge boson pairs. The initial results are compatible with the presence of a SM-like Higgs boson with a mass in the range 114–129 GeV, with most of the remaining mass values up to at least 500 GeV being excluded at the 95% C.L. by both experiments. Both LHC experiments observe small excesses, predominantly in the $\gamma\gamma$ and ZZ modes, which could be compatible with a Higgs boson with a mass near 125 GeV but are not yet conclusive. These

results are discussed in more detail later in this review. If a signal is confirmed, the next step is to understand the precise nature of such a particle by scrutinizing the coupling strengths in the different production and decay channels. Searches are also conducted by both LHC collaborations for Higgs bosons produced via vector boson fusion and in association with a W or a Z boson. Decays to $b\bar{b}$ and $\tau^+\tau^-$ are searched for in addition to the more experimentally distinct boson pair signatures. With additional data, these searches will constrain the production rates and decay branching ratios of the Higgs boson. An exciting time lies ahead in the case of the discovery of a Higgs boson since we would need to understand its nature and the underlying new physics that might be related to it. Beyond a discovery, precision measurements will be crucial to completely understand the mechanism of electroweak symmetry breaking.

II. The Standard Model (SM) Higgs Boson

In the SM, the Higgs boson mass is given by $m_H = \sqrt{\lambda/2} v$, where λ is the Higgs self-coupling parameter and v is the vacuum expectation value of the Higgs field, $v = (\sqrt{2}G_F)^{-1/2} \approx 246$ GeV, fixed by the Fermi coupling G_F , which is determined with a precision of 0.6 ppm from muon decay measurements [35]. Since λ is presently unknown, the value of the SM Higgs boson mass m_H cannot be predicted. However, besides the upper bound on the Higgs boson mass from unitarity constraints [3,4], additional theoretical arguments place approximate upper and lower bounds on m_H [36]. There is an upper bound based on the perturbativity of the theory up to the scale Λ at which the SM breaks down, and a lower bound derived from the stability of the Higgs potential. If m_H is too large, then the Higgs self-coupling diverges at some scale Λ below the Planck scale. If m_H is too small, then the Higgs potential develops a second (global) minimum at a large value of the magnitude of the scalar field of order Λ . New physics must enter at a scale Λ or below, so that the global minimum of the theory corresponds to the observed $SU(2)_L \times U(1)_Y$ broken vacuum with $v = 246$ GeV. Given a value of Λ , one can compute the minimum and maximum

allowed Higgs boson masses. Conversely, the value of m_H itself can provide an important constraint on the scale up to which the SM remains successful as an effective theory. In particular, a Higgs boson with mass in the range $130 \text{ GeV} \lesssim m_H \lesssim 180 \text{ GeV}$ would be consistent with an effective SM description that survives all the way to the Planck scale. For smaller Higgs mass values, the stability of our universe prefers new physics at a lower scale. The lower bound on m_H can be reduced to about 115 GeV [37] if one allows for the electroweak vacuum to be metastable, with a lifetime greater than the age of the universe. The main uncertainties in the stability and perturbativity bounds come from the uncertainties in the value of α_s and the top quark mass. As can be inferred from Fig. 1 [38], taking these uncertainties into account, a Higgs boson mass of about 125 GeV is close to the boundary of a SM that is consistent up to the Planck scale, and a SM that is unstable with a slow tunneling rate.

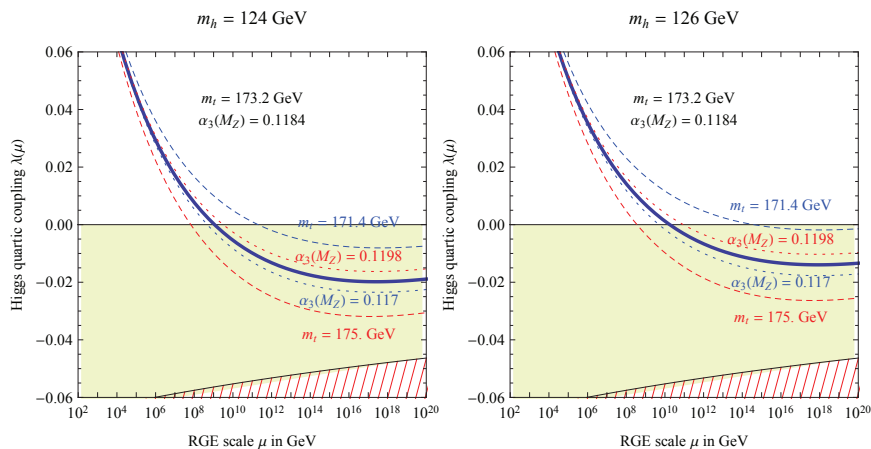


Figure 1: Renormalization group evolution of the Higgs self coupling λ , for $m_H = 124 \text{ GeV}$ (left) and $m_H = 126 \text{ GeV}$ (right), for the central values of m_t and α_S (solid curves), as well as for variations of m_t (dashed curves) and α_S (dotted curves). For negative values of λ , the lifetime of the SM vacuum due to quantum tunneling at zero temperature is longer than the age of the universe as long as λ remains above the region shaded in red. From Ref. 38.

The SM Higgs couplings to fundamental fermions are proportional to the fermion masses, and the couplings to bosons are proportional to the squares of the boson masses. In particular, the SM Higgs boson is a CP -even scalar, and its couplings to gauge bosons, Higgs bosons and fermions are given by:

$$g_{Hf\bar{f}} = \frac{m_f}{v}, \quad g_{HVV} = \frac{2m_V^2}{v}, \quad g_{HHVV} = \frac{2m_V^2}{v^2}$$

$$g_{HHH} = \frac{3m_H^2}{v} \quad g_{HHHH} = \frac{3m_H^2}{v^2}$$

where $V = W^\pm$ or Z . In Higgs boson production and decay processes, the dominant mechanisms involve the coupling of the H to the W^\pm , Z and/or the third generation quarks and leptons. The Higgs boson's coupling to gluons, is induced at leading order by a one-loop graph in which the H couples to a virtual $t\bar{t}$ pair. Likewise, the Higgs boson's coupling to photons is also generated via loops, although in this case the one-loop graph with a virtual W^+W^- pair provides the dominant contribution [13]. Reviews of the SM Higgs boson's properties and phenomenology, with an emphasis on the impact of loop corrections to the Higgs boson decay rates and cross sections, can be found in Refs. [39–45].

The main Higgs boson production cross sections at an e^+e^- collider are the Higgs-strahlung process $e^+e^- \rightarrow ZH$ [4,46], and the WW fusion process [47] $e^+e^- \rightarrow \bar{\nu}_e\nu_e W^*W^* \rightarrow \bar{\nu}_e\nu_e H$. As center-of-mass energy \sqrt{s} is increased, the cross-section for the Higgs-strahlung process decreases as s^{-1} and is dominant at low energies, while the cross-section for the WW fusion process grows as $\ln(s/m_H^2)$ and dominates at high energies [48,49,50]. The ZZ fusion mechanism, $e^+e^- \rightarrow e^+e^- Z^*Z^* \rightarrow e^+e^- H$, also contributes to Higgs boson production, with a cross-section suppressed by an order of magnitude with respect to that of WW fusion. The process $e^+e^- \rightarrow t\bar{t}H$ [51,52] can become relevant for large $\sqrt{s} \simeq 800$ GeV for SM Higgs masses in the experimentally preferred region. For a more detailed discussion of Higgs production properties at lepton colliders see for example Refs. [44] and [45], and references therein.

At high-energy hadron colliders, the Higgs boson production mechanism with the largest cross section is $gg \rightarrow H + X$.

This process is known at next-to-next-to-leading order (NNLO) in QCD, in the large top-mass limit, and at NLO in QCD for arbitrary top mass [53]. The NLO QCD corrections approximately double the leading-order prediction, and the NNLO corrections add approximately 50% to the NLO prediction. NLO electroweak corrections range between 0 and 6% of the LO term [54]. Mixed QCD-electroweak corrections $O(\alpha\alpha_s)$ are computed in Ref. [55]. In addition, soft-gluon contributions to the cross sections have been resummed at next-to-leading logarithmic (NLL), NNLL and partial NNNLL accuracy [56]. Updated predictions for the gluon fusion cross sections at NNLO or through soft-gluon resummation up to next-to-next-to-leading logarithmic accuracy (NNLL), and two-loop electroweak effects can be found in Refs. [55,57]. A better perturbative convergence is achieved by resumming the enhanced contributions arising from the analytic continuation of the gluon form factor [58]. Updated predictions to compute the gluon fusion cross sections at NNNLL in renormalization group improved perturbation theory and incorporating two-loop electroweak effects can be found in Ref. [59]. Some search strategies look for Higgs boson production in association with jets. In the heavy top quark mass limit, the Higgs boson production cross section in association with one jet is considered in Refs. [60–63] and in association with two jets in Refs. [64,65].

The other relevant Higgs boson production mechanisms at the Tevatron and the LHC are associated production with W and Z gauge bosons and vector boson fusion, and at a significantly smaller rate, the associated production with top quark pairs. The cross sections for the associated production processes $q\bar{q} \rightarrow W^\pm H + X$ and $q\bar{q} \rightarrow ZH + X$ [66,67,68] are known at NNLO for the QCD corrections and at NLO for the electroweak corrections [69,70]. The residual uncertainty is less than 5%. For the vector boson fusion processes $qq \rightarrow qqH + X$, corrections to the production cross section are known at NNLO in QCD and at NLO for the electroweak corrections and the remaining theoretical uncertainties in the inclusive cross section are approximately 2% [71], but are larger if jets are required or vetoed [43]. The cross section for the associated production

process $t\bar{t}H$ has been calculated at NLO in QCD [72], while the bottom fusion Higgs boson production cross section is known at NNLO in the case of five quark flavors [69,73,74]. The cross sections for the production of SM Higgs bosons are summarized in Fig. 2 for $p\bar{p}$ collisions at the Tevatron, and in Fig. 3 for pp collisions at $\sqrt{s} = 7$ TeV at the LHC [75,76]. Ref. [75] also includes cross sections computed at $\sqrt{s} = 8$ TeV, which are relevant for data collected in 2012.

The branching ratios for the most relevant decay modes of the SM Higgs boson as functions of m_H , including the most recent theoretical uncertainties, are shown in Fig. 4. The total decay width as function of m_H is shown in Fig. 5. Details of these calculations can be found in Refs. [40–44]. For Higgs boson masses below 135 GeV, decays to fermion pairs dominate; the decay $H \rightarrow b\bar{b}$ has the largest branching ratio and the decay $H \rightarrow \tau^+\tau^-$ is about an order of magnitude smaller. For these low masses, the total decay width is less than 10 MeV. For Higgs boson masses above 135 GeV, the W^+W^- decay dominates (below the W^+W^- threshold, one of the W bosons is virtual) with an important contribution from $H \rightarrow ZZ$, and the decay width rises rapidly, reaching about 1 GeV at $m_H = 200$ GeV and 100 GeV at $m_H = 500$ GeV. Above the $t\bar{t}$ threshold, the branching ratio into $t\bar{t}$ pairs increases rapidly as a function of the Higgs boson mass, reaching a maximum of about 20% at $m_H \sim 450$ GeV. Higgs boson decays into pairs of gluons, pairs of photons, and $Z\gamma$ are induced at one loop level. Higgs boson decay into a pair of photons is particularly relevant for the discovery potential of the LHC for a low-mass Higgs boson. In spite of the small expected signal rate, the reconstructed mass resolution provides a way to separate signal from background, a means to calibrate the background rate with a signal-free sample of events, and a precise measurement of m_H once a signal is identified.

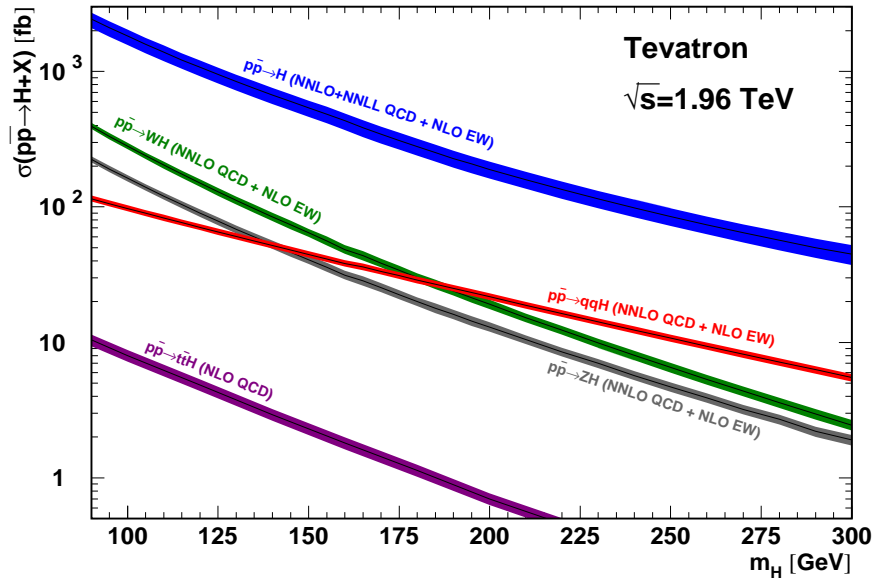


Figure 2: SM Higgs boson production cross sections for $p\bar{p}$ collisions at 1.96 TeV, including theoretical uncertainties [53,70–72].

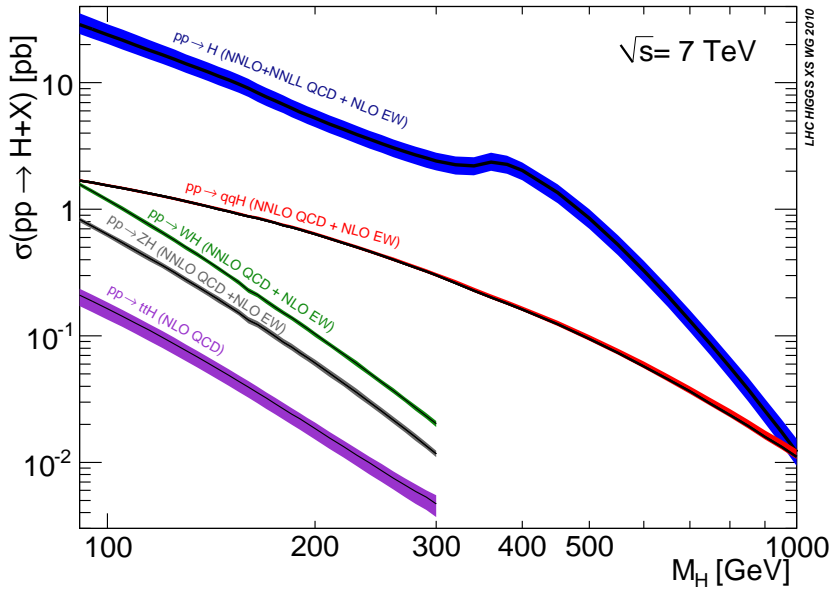


Figure 3: SM Higgs boson production cross sections for pp collisions at 7 TeV, including theoretical uncertainties [76].

II.1. Indirect Constraints on the SM Higgs Boson

Indirect experimental bounds for the SM Higgs boson mass are obtained from fits to precision measurements of electroweak observables. The Higgs boson contributes to the W^\pm and Z vacuum polarization through loop effects, leading to a logarithmic sensitivity of the ratio of the W^\pm and Z gauge boson masses on the Higgs boson mass. A global fit to the precision electroweak data accumulated in the last two decades at LEP, SLC, the Tevatron, and elsewhere, gives $m_H = 94^{+29}_{-24}$ GeV, or $m_H < 152$ GeV at 95% C.L. [5]. The top quark contributes to the W^\pm boson vacuum polarization through loop effects that depend quadratically on the top mass, which plays an important role in the global fit. A top quark mass of 173.2 ± 0.9 GeV [77] and a W^\pm boson mass of 80.385 ± 0.015 GeV [5] were used.

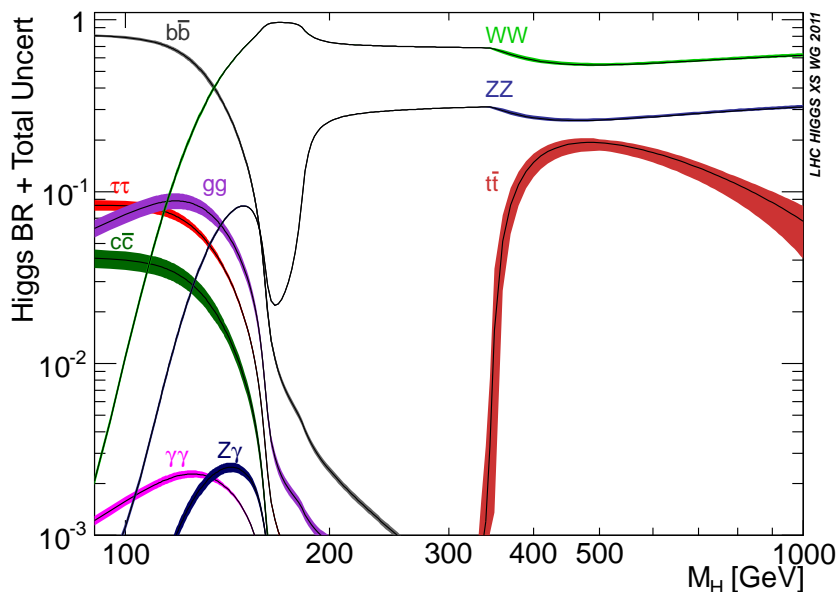


Figure 4: Branching ratios for the main decays of the SM Higgs boson, including theoretical uncertainties [40–44].

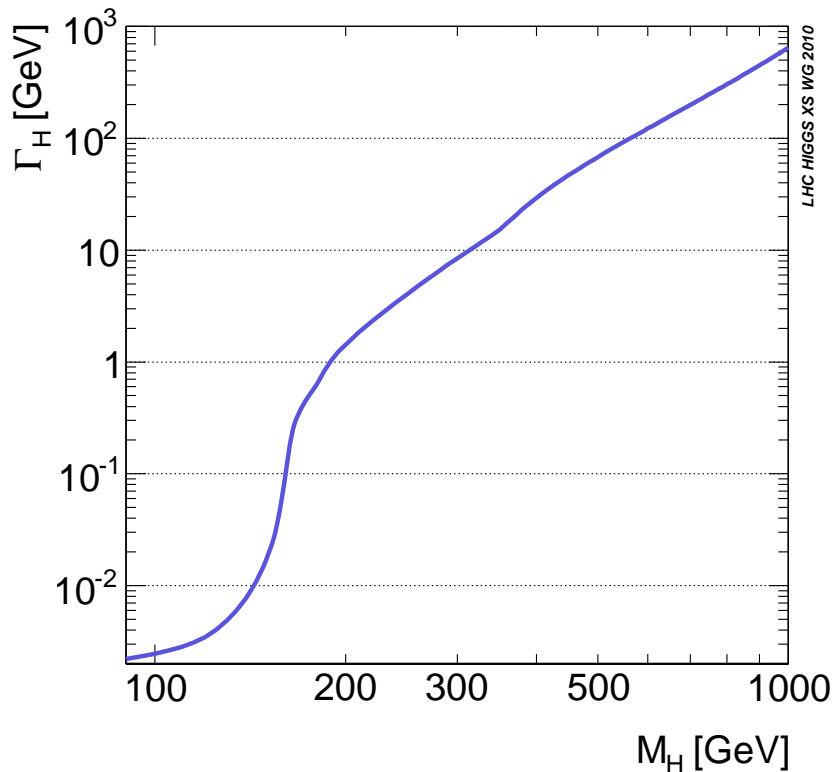


Figure 5: The total decay width of the SM Higgs boson, shown as a function of m_H [76].

II.2. Searches for the SM Higgs Boson at LEP

The principal mechanism for producing the SM Higgs boson in e^+e^- collisions at LEP energies is Higgs-strahlung in the s -channel, $e^+e^- \rightarrow HZ$. The Z boson in the final state is either virtual (LEP 1), or on mass shell (LEP 2). At LEP energies, SM Higgs boson production via W^+W^- and ZZ fusion in the t -channel has a small cross section. The sensitivity of the LEP searches to the Higgs boson depends on the center-of-mass energy, \sqrt{s} . For $m_H < \sqrt{s} - M_Z$, the cross section is of order 1 pb or more, while for $m_H > \sqrt{s} - M_Z$, the cross section is smaller by at least an order of magnitude.

During the LEP 1 phase, the ALEPH, DELPHI, L3 and OPAL collaborations analyzed over 17 million Z decays and set lower bounds of approximately 65 GeV on the mass of the SM

Higgs boson [78]. At LEP 2, substantial data samples were collected at center-of-mass energies up to 209 GeV. Data recorded at each center-of-mass energy were studied independently and the results from the four LEP experiments were then combined. The CL_s method [79] was used to compute the observed and expected limits on the Higgs boson production cross section as functions of the Higgs boson mass considered, and from that a lower bound on m_H was derived.

Higgs bosons with mass above $2m_\tau$ were searched for in four final state topologies: The four-jet topology in which $H \rightarrow b\bar{b}$ and $Z \rightarrow q\bar{q}$; the final states with tau leptons produced in the processes $H \rightarrow \tau^+\tau^-$ where $Z \rightarrow q\bar{q}$, together with the mode $H \rightarrow b\bar{b}$ with $Z \rightarrow \tau^+\tau^-$; the missing energy topology produced mainly in the process $H \rightarrow b\bar{b}$ with $Z \rightarrow \nu\bar{\nu}$, and finally the leptonic states $H \rightarrow b\bar{b}$ with $Z \rightarrow e^+e^-, \mu^+\mu^-$. At LEP 1, only the modes with $Z \rightarrow \ell^+\ell^-$ and $Z \rightarrow \nu\bar{\nu}$ were used because the backgrounds in the other channels were prohibitive. For the data collected at LEP 2, all decay modes were used.

For very light Higgs bosons, with $m_H < 2m_\tau$, the decay modes exploited above are not kinematically allowed, and decays to jets, muon pairs, pion pairs, and lighter particles dominate, depending on m_H . For very low masses, OPAL's decay-mode independent search [80] for the Bjorken process $e^+e^- \rightarrow S^0 Z$, where S^0 denotes a generic neutral scalar particle, provides sensitivity regardless of the branching fractions of the S^0 . This search is based on studies of the recoil mass spectrum in events with $Z \rightarrow e^+e^-$ and $Z \rightarrow \mu^+\mu^-$ decays, and on the final states $Z \rightarrow \nu\bar{\nu}$ and $S^0 \rightarrow e^+e^-$ or photons. Upper bounds on the $e^+e^- \rightarrow ZH$ cross section are obtained for scalar masses between 1 KeV and 100 GeV, and are below 0.05 times the SM prediction for $m_H < 80$ GeV, constraining the coupling of the Higgs boson to the Z .

The combination of the LEP data yields a 95% C.L. lower bound of 114.4 GeV for the mass of the SM Higgs boson [33]. The median limit one would expect to obtain in a large ensemble of identical experiments with no signal present is 115.3 GeV. An excess of data was seen consistent with a Higgs boson of mass $m_H \approx 115$ GeV. The significance of this excess is low,

however. It is quantified by the background-only p -value [79], which is the probability to obtain data at least as signal-like as the observed data, assuming a signal is truly absent; a small p -value indicates data that are inconsistent with the background model but are more consistent with a signal model. The background-only p -value for the excess in the LEP data is 9%.

II.3. Searches for the SM Higgs Boson at the Tevatron

As shown in Fig. 2, at the Tevatron, the most important SM Higgs boson production processes are gluon fusion ($gg \rightarrow H$) and Higgs boson production in association with a vector boson ($W^\pm H$ or ZH). Vector boson fusion (VBF) has a smaller cross section, but some search channels are optimized for it. For m_H less than about 135 GeV, the most sensitive analyses search for $W^\pm H$ and ZH with $H \rightarrow b\bar{b}$. The mode $gg \rightarrow H \rightarrow b\bar{b}$ is overwhelmed by the background from the inclusive production of $p\bar{p} \rightarrow b\bar{b} + X$ via the strong interaction. The associated production modes $W^\pm H$ and ZH allow use of the leptonic W and Z decays to purify the signal and reject QCD backgrounds.

The contribution of $H \rightarrow W^*W$ or WW is dominant at higher masses, $m_H > 135$ GeV. Using this decay mode, both the direct ($gg \rightarrow H$) and the associated production ($p\bar{p} \rightarrow W^\pm H$ or ZH) channels are explored, and the results of both Tevatron experiments, CDF and DØ, are combined to maximize the sensitivity to the Higgs boson.

The signal-to-background ratio is much smaller in the Tevatron searches than in the LEP analyses, and the systematic uncertainties on the estimated background rates are typically larger than the signal rates. In order to estimate the background rates in the selected samples more accurately, auxiliary measurements are made in data samples which are expected to be depleted in Higgs boson signal. These auxiliary samples are chosen to maximize the sensitivity to each specific background in turn. Monte Carlo simulations are used to extrapolate these measurements into the Higgs signal regions. The dominant physics backgrounds such as top-pair, diboson, $W^\pm b\bar{b}$, and single top production are estimated by Monte Carlo simulations

in this way, i.e., after having been tuned or verified by corresponding measurements in dedicated analyses, thereby reducing the uncertainty on the total background estimate. Nearly all Tevatron analyses use multivariate analysis techniques (MVA’s) to further separate signals from backgrounds and to provide the final discriminants whose distributions are used to compute limits, best-fit cross sections and uncertainties, and p -values. Separate MVA’s are trained at each m_H in all the different sub-channels.

Both Tevatron experiments have updated their main search analyses to the full analyzable data sample of approximately 10 fb^{-1} . At Higgs boson masses of 150 GeV and below, the searches for associated production, $p\bar{p} \rightarrow W^\pm H, ZH$, are performed in different channels, as follows. The $WH \rightarrow \ell\nu b\bar{b}$ searches [81–85] select events with a charged lepton ($\ell = e$ or μ), large missing transverse energy, and at least two jets, at least one of which must be b -tagged. In order to improve the sensitivity of the searches, events with one b -tag are analyzed separately from those with two, and events with three jets are analyzed separately from those with two jets. Algorithms to identify b jets provide several levels of purity for each jet, and this serves as another dimension along which to classify events. The quality and the type of the identified lepton also serves to classify events. An event with an isolated, high- p_T track is analyzed as if that track were a lepton, but such events are collected together in different sub-channels. The signals in such categories come from leptons which the detectors failed to reconstruct as leptons, and hadrons from τ lepton decay. The instrumental (“fake-lepton”) backgrounds are higher for these selections, and so samples with well-identified leptons are kept separate from the isolated-track samples.

The $ZH \rightarrow \nu\bar{\nu} b\bar{b}$ searches [86–89] seek events in which no lepton or high- p_T isolated track is found. These searches also accept signals from $WH \rightarrow \ell\nu b\bar{b}$ in which the charged lepton is either not identified or falls outside the detector acceptances. Similar b -tagging categorization is applied to these searches. The $ZH \rightarrow \ell^+\ell^- b\bar{b}$ searches [90–93] seek leptonic decays of the Z boson. These events benefit from the absence of neutrinos,

and so missing transverse energy can be interpreted as jet energy mismeasurement, and the jet energies are corrected accordingly, improving the dijet mass resolution. CDF searches for associated production and VBF in the all-hadronic mode, in which the W or the Z decays hadronically, and the H decays to $b\bar{b}$ [94,95].

A cross check of the procedures for searching for the SM Higgs boson in the $WH, ZH \rightarrow b\bar{b}$ channels, their background estimates, and combination procedures, is provided by measurements of $WZ + ZZ$ production in b -tagged final states [96,97], and their combination [98]. In these analyses, the decay $Z \rightarrow b\bar{b}$ mimics the decay $H \rightarrow b\bar{b}$, and WW production is considered a background. The measured cross section is consistent with the SM expectations, giving confidence in the Higgs boson search procedures.

Both Tevatron experiments also search for $H \rightarrow \tau^+\tau^-$ in events with one or more associated jets [99–102]. As the di-tau mass resolution is poor due to the presence of unmeasured neutrinos, the $Z \rightarrow \tau^+\tau^-$ background is large in the absence of the requirement of one or more additional jets, which purifies the sample in associated production and VBF. The process $gg \rightarrow H$ is considered as well, although the uncertainties on $gg \rightarrow H$ +jets are larger than the inclusive uncertainties.

The decay mode $H \rightarrow \gamma\gamma$ is searched for by both Tevatron collaborations [103–106]. Prompt diphoton production, $\pi^0 \rightarrow \gamma\gamma$, and fake photons are the main backgrounds. The backgrounds have a smoothly varying shape as a function of $m_{\gamma\gamma}$, while the signal mass resolution is of order 3%. All Higgs boson production mechanisms are considered, but the signal-to-background ratio at the Tevatron is not sufficient for this channel to contribute significantly to the SM search. Nonetheless, the searches for $H \rightarrow \gamma\gamma$ provide powerful tests of models with enhanced $\text{BR}(H \rightarrow \gamma\gamma)$, described later.

Another process searched for at the Tevatron is $t\bar{t}H$ production with $H \rightarrow b\bar{b}$ [107,108]. The backgrounds in this channel are low and are dominated by $t\bar{t}b\bar{b}$, but the low signal production rate and combinatoric ambiguity in assigning jets to the Higgs boson decay reduces the sensitivity.

For Higgs boson masses above 130 GeV, the searches for $H \rightarrow W^+W^- \rightarrow \ell^+\nu\ell^-\bar{\nu}$ [109–114] are the most sensitive. The candidate mass cannot be fully reconstructed in these events due to the presence of two neutrinos, but the lepton angles are correlated due to the scalar nature of the Higgs boson and the $V - A W\ell\nu$ coupling. The process $W^\pm H \rightarrow W^\pm W^+W^-$ gives rise to like-sign dilepton and trilepton final states which have very low backgrounds [110,115]. CDF also seeks $H \rightarrow ZZ \rightarrow \ell^+\ell^-\ell^+\ell^-$ [116] where $\ell = e$ or μ . The excellent mass resolution and low backgrounds help the sensitivity of the search, but low decay branching ratio for $Z \rightarrow \ell^+\ell^-$ reduces the sensitivity.

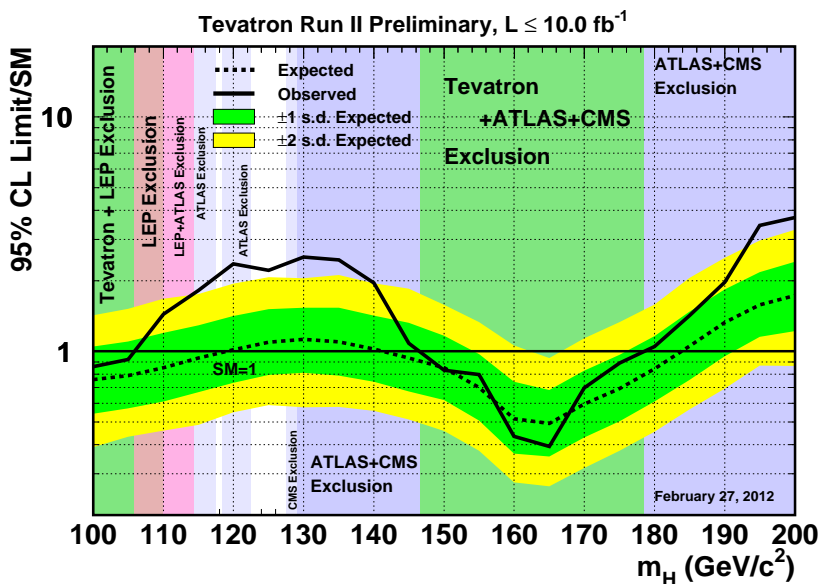


Figure 6: Observed and expected 95% C.L. upper limits on the ratios to the SM cross section, as functions of the Higgs boson mass for the combined CDF and D0 analyses [6]. The limits are expressed as a multiple of the SM prediction. The bands indicate the 68% and 95% probability regions where the limits can fluctuate, in the absence of signal. Also shown are the regions excluded by LEP, ATLAS, and CMS.

All of the searches for the SM Higgs boson at the Tevatron are combined together for maximum sensitivity [6,117,118]. The Tevatron combination excludes two ranges in m_H : between 100 GeV and 106 GeV, and between 147 GeV and 179 GeV. An excess of data is seen in the mass range $115 \text{ GeV} < m_H < 135 \text{ GeV}$, as shown in Fig. 6. with a maximum local significance of 2.7 standard deviations (sigma), at $m_H = 120 \text{ GeV}$, where the expected local significance for a SM Higgs signal is 2.0 sigma. When corrected for the look-elsewhere effect (LEE) [119], which accounts for the possibility of selecting the strongest of the several random excess which may happen in the range $115 \text{ GeV} < m_H < 200 \text{ GeV}$, the global significance of the excess is 2.2 standard deviations³. The majority of the excess is contributed by the searches for $H \rightarrow b\bar{b}$. The best-fit cross section for Higgs boson production, normalized to the SM production rate, and assuming SM decay branching ratios and SM ratios between the production mechanisms, is shown in Fig. 7.

The channels used at the Tevatron for Higgs boson masses below 130 GeV are different from those dominantly used at the LHC, and thus provide complementary information on the couplings of the Higgs boson to gauge bosons and to b quarks.

II.4. SM Higgs Boson Searches at the LHC

At the LHC, the main production processes are the same as those at the Tevatron, but with a different order of importance: gluon fusion ($gg \rightarrow H$), vector boson fusion (qqH or $q\bar{q}H$) and Higgs boson production in association with a vector boson ($W^\pm H$ or ZH) or with a top-quark pair ($t\bar{t}H$).

The higher center-of-mass energy of 7 TeV (8 TeV in 2012) and the fact that both beams consist of protons has a strong impact on the parton luminosities. The LHC experiments are sensitive to Higgs bosons with much higher masses than the Tevatron experiments. The gg luminosity is also enhanced at the LHC by the beam energy due to the large gluon PDF

³ In this Review, we use the phrase “local significance” to indicate a calculation of the significance not corrected for the LEE.

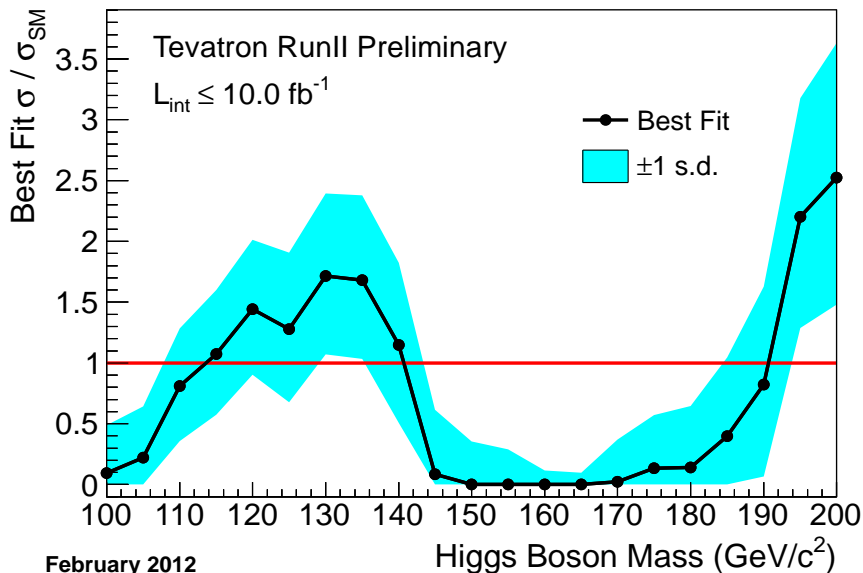


Figure 7: Best-fit cross section for the SM Higgs boson from the combined CDF and DØ searches, normalized to the SM production rates, assuming SM decay branching ratios and the SM ratio between the various production mechanisms [6]. The shaded region shows the 68% C.L. interval, as a function of the mass of the Higgs boson considered. In this fit, negative signal cross sections are not considered.

at lower parton momentum fraction x compared to that at higher x .

A variety of search channels are pursued by the LHC collaborations, ATLAS and CMS, with the channels’ relative importances changing due to the branching ratios of the SM Higgs boson as functions of m_H . At low masses, $m_H < 120$ GeV, searches for $H \rightarrow \gamma\gamma$ provide the highest sensitivity, with searches for $H \rightarrow b\bar{b}$ and $H \rightarrow \tau^+\tau^-$ contributing as well. For higher masses, $120 \text{ GeV} < m_H < 200$ GeV, searches for $H \rightarrow W^+W^- \rightarrow \ell^+\nu\ell^-\nu$ are the most sensitive, with an important contribution from $H \rightarrow ZZ \rightarrow \ell^+\ell^-\ell^+\ell^-$ between 120 GeV and 150 GeV. At even higher masses, up to $m_H = 600$ GeV, the $H \rightarrow ZZ$ searches are the most sensitive.

Both LHC collaborations seek $H \rightarrow W^+W^- \rightarrow \ell^+\nu\ell^-\nu$ production [120–122]. This channel provides high sensitivity for Higgs boson masses for which $\text{BR}(H \rightarrow W^+W^-)$ is

large, $m_H > 135$ GeV. The main SM background, nonresonant W^+W^- production, is initiated primarily by $q\bar{q}$ and thus the signal to background ratio benefits at the LHC because of the initial state. The first LHC exclusion of Higgs boson masses was obtained in this search mode. CMS also contributes a search in the mode $W^\pm H \rightarrow W^\pm W^+ W^-$ [123] in the trilepton final state. For ATLAS, the fully leptonic decay mode is supplemented with an $H \rightarrow W^+ W^- \rightarrow \ell\nu jj$ search [124].

At higher masses, $m_H > 180$ GeV, ATLAS and CMS analyses seeking $H \rightarrow ZZ$ with $ZZ \rightarrow \ell^+ \ell^- \ell^+ \ell^-$ [125,126], $ZZ \rightarrow \ell^+ \ell^- \nu\bar{\nu}$ [127,128], $ZZ \rightarrow \ell^+ \ell^- q\bar{q}$ [129,130], and $ZZ \rightarrow \ell^+ \ell^- \tau^+ \tau^-$ [131] become the most sensitive. A small excess of events in the ATLAS $\ell^+ \ell^- \ell^+ \ell^-$ channel with reconstructed masses near 125 GeV is seen, with a local significance of ≈ 2 sigma. An excess with similar significance is seen in the CMS $H \rightarrow ZZ \rightarrow 4$ leptons searches at ~ 119 GeV.

ATLAS and CMS seek the process $H \rightarrow \gamma\gamma$ including the four production mechanisms, $gg \rightarrow H$, production in association with a W or Z boson, and VBF [132–134]. Events are divided into categories depending on the reconstructed photon type (barrel calorimeter or endcap), and the presence or absence of additional jets. The reconstructed mass resolution of the selected candidates varies between 1% and 3% depending on the event category and detector. ATLAS observes an excess of events with a local significance of 2.8σ which is maximized at $m_H=126.5$ GeV, while CMS observes an excess of events with a local significance of 2.9σ which is maximized at $m_H=124$ GeV. ATLAS computes the global significance, accounting for the probability of a background fluctuation anywhere in the range $110 \text{ GeV} < m_H < 150 \text{ GeV}$ at least as significant as the observed excess, to be 1.5σ . CMS’s global significance is 1.6σ using the same range of m_H .

ATLAS and CMS seek Higgs bosons produced in association with a leptonically decaying vector boson and which decay into $b\bar{b}$ [135,136]. Although these searches benefit from the higher production cross sections at the LHC as compared to the Tevatron, the background cross sections are relatively larger, as a larger fraction of W and Z bosons at the LHC are produced

with accompanying jets, some of which contain heavy hadrons. The sensitivity of the searches is maximized by tagging jets containing B hadrons and using MVAs to separate the expected signals from the backgrounds. The achieved sensitivity, in units of the SM production rate, expressed as the 95% exclusion limit expected in the absence of a signal, varies in the range $110 \text{ GeV} < m_H < 135 \text{ GeV}$ between 2.6 to 5.1 for ATLAS and between 2.7 to 6.7 for CMS. These results are both with 4.7 fb^{-1} of analyzed data. With more data and improved analyses, the LHC will be able to measure the important decay branching ratio to $b\bar{b}$, where currently the Tevatron contributes the most.

Both ATLAS and CMS seek SM Higgs boson decays to $\tau^+\tau^-$ [137–139]. The selected events in these searches are categorized by the number of associated jets, which differentiates signals produced by $gg \rightarrow H$, associated production, and VBF from the backgrounds, which are dominated by $Z \rightarrow \tau^+\tau^-$. The reconstructed di-tau masses are used as the discriminating variables. If the tau pair has a net transverse boost, then the missing transverse energy can be projected unambiguously on the directions of the two tau leptons, and the reconstructed mass resolution is much better than in the case of little transverse boost, in which case the degree to which the neutrino momenta cancel each other is unknown. With 4.7 fb^{-1} of data, ATLAS’s expected 95% C.L. limit varies between 3.2 and 7.9 times the SM rate for Higgs bosons with $100 \text{ GeV} < m_H < 150 \text{ GeV}$, and with 4.6 fb^{-1} of data, CMS’s expected limits vary between 3.3 and 5.5 times the SM prediction for $110 \text{ GeV} < m_H < 145 \text{ GeV}$. CMS also searches for $WH \rightarrow W\tau^+\tau^-$ [140] with a 95% C.L. sensitivity between 5 and 15 times the SM prediction in the range $100 \text{ GeV} < m_H < 140 \text{ GeV}$ using 4.7 fb^{-1} of data.

Both ATLAS and CMS have combined their SM Higgs boson searches [7–10]. The most recent combination of ATLAS includes the full suite of channels mentioned above. As shown in Fig. 8, ATLAS excludes at the 95% C.L. the mass ranges $110.0 \text{ GeV} < m_H < 117.5 \text{ GeV}$, $118.5 \text{ GeV} < m_H < 122.5 \text{ GeV}$, and $129 \text{ GeV} < m_H < 539 \text{ GeV}$, and expects to exclude, in the absence of a signal, $120 \text{ GeV} < m_H < 555 \text{ GeV}$. ATLAS’s local p -values [79], computed with the likelihood ratio test statistic,

are shown as functions of the tested m_H in Fig. 9. The local significance is maximal at $m_H = 126$ GeV, with a value of 2.9σ . The global significance is 1.3σ when the interval considered for the LEE correction is $110 \text{ GeV} < m_H < 146 \text{ GeV}$, and becomes 0.5σ for the interval $110 \text{ GeV} < m_H < 600 \text{ GeV}$. The best-fit production cross section as a multiple of the SM prediction is shown in Fig. 10. The excesses seen in the $H \rightarrow \gamma\gamma$ and $H \rightarrow ZZ \rightarrow \ell^+\ell^-\ell^+\ell^-$ searches are somewhat offset by a more background-like outcome in the $H \rightarrow W^+W^-$ searches.

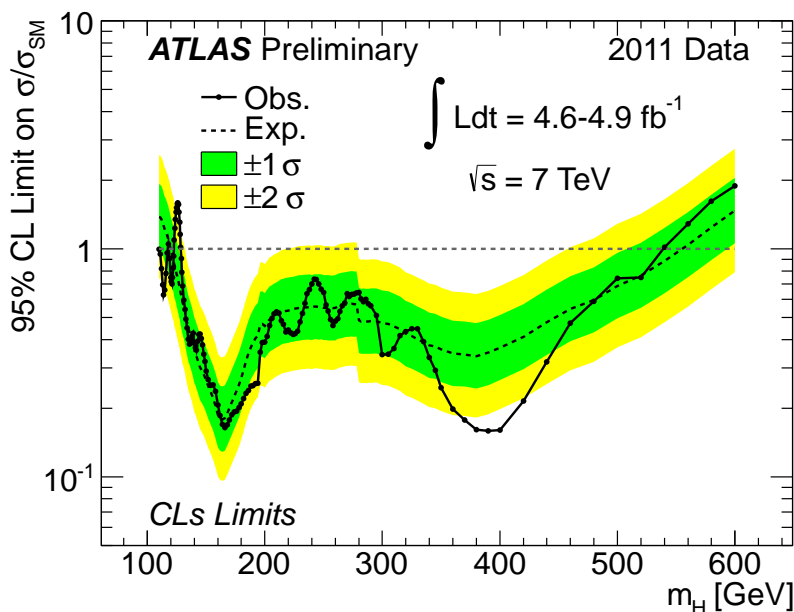


Figure 8: Observed and expected 95% C.L. upper limits on the ratios to the SM cross section, as functions of the Higgs boson mass for the combined ATLAS analyses [8].

The most recent combination of CMS includes the full suite of channels mentioned above. As shown in Fig. 11, CMS excludes at the 95% C.L. the mass range $127.5 \text{ GeV} < m_H < 600 \text{ GeV}$, and expects to exclude $114.5 \text{ GeV} < m_H < 525 \text{ GeV}$ in the absence of a signal. CMS’s local p -values [79], computed using the likelihood ratio test statistic, are shown as functions of the tested m_H in Fig. 12. The local significance is maximal at $m_H = 125$ GeV, with a value of 2.8σ . The global significance becomes 2.1σ (0.8σ) after correcting for LEE in the range

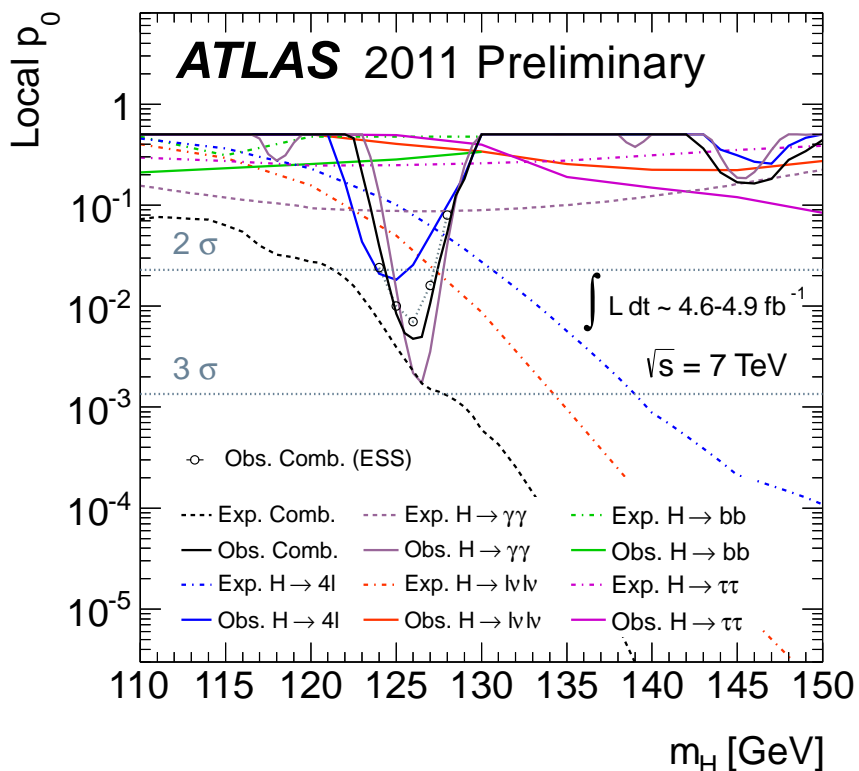


Figure 9: Local p -values for each of ATLAS’s SM Higgs boson search channels and the combination [8]. The observed p -values are shown with solid curves, and the median expected p -values assuming a signal is present at the SM strength are shown with dashed and dot-dashed curves. Dotted lines indicate the 2σ and 3σ thresholds. Hollow circles indicate p -values computed with ensemble tests taking into account energy scale systematic uncertainties (ESS).

$110 \text{ GeV} < m_H < 145 \text{ GeV}$ ($110 \text{ GeV} < m_H < 600 \text{ GeV}$). The best-fit production cross section CMS measures as a multiple of the SM prediction is shown in Fig. 13. A signal-like excess is seen in the $H \rightarrow \gamma\gamma$ and $H \rightarrow W^+W^-$ searches, but the outcome in the $H \rightarrow ZZ$ search is less signal-like at $m_H = 125 \text{ GeV}$.

In summary, beyond the region excluded by LEP, the region excluded at 95% C.L. by both ATLAS and CMS extends from 129 GeV to 539 GeV. The observed and expected limits from the two LHC collaborations and the Tevatron are listed in Table 1

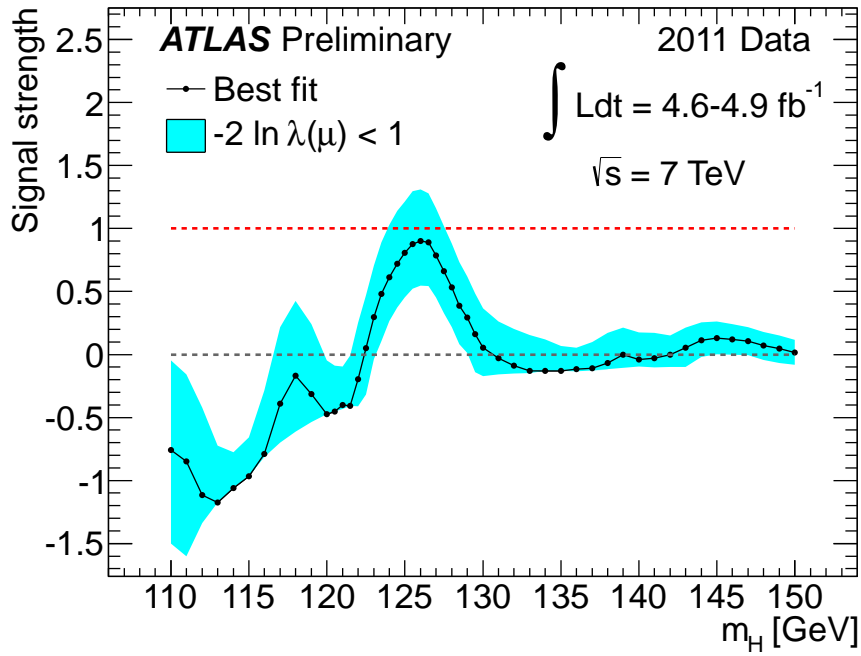


Figure 10: ATLAS SM best-fit cross sections [8].

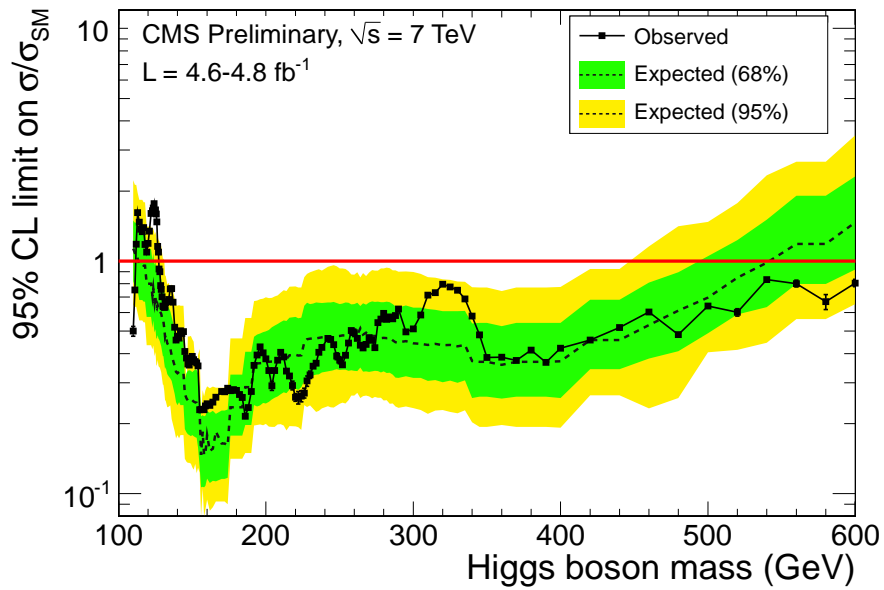


Figure 11: Observed and expected 95% C.L. upper limits on the ratios to the SM cross section, as functions of the Higgs boson mass for the combined CMS analyses [10].

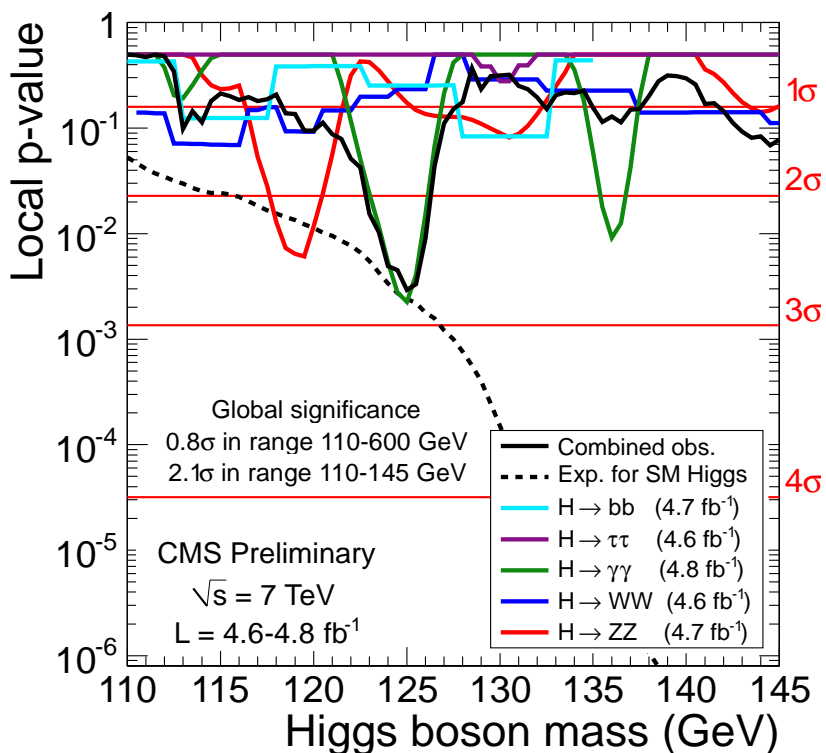


Figure 12: Local p -values for each of CMS’s SM Higgs boson search channels and the combination [10]. The observed p -values are shown with solid curves, and the median expected p -value for the combined search assuming a signal is present at the SM strength is shown with a dashed curve. Horizontal lines indicate the 1σ , 2σ , 3σ , and 4σ thresholds.

for the main channels and the combinations searching for the SM Higgs boson with $m_H = 125$ GeV. The best-fit cross section is close to the SM prediction at the m_H corresponding to the most significant p -value for both LHC experiments. The data samples are not yet large enough to make a significant statement about the balance between the individual channels.

If a SM Higgs boson is discovered, its properties will be studied at the LHC. The decay branching ratios, and more generally, the couplings of the Higgs bosons to fermions and gauge bosons will be constrained by the measurements of the cross sections times branching ratios for the processes searched for above.

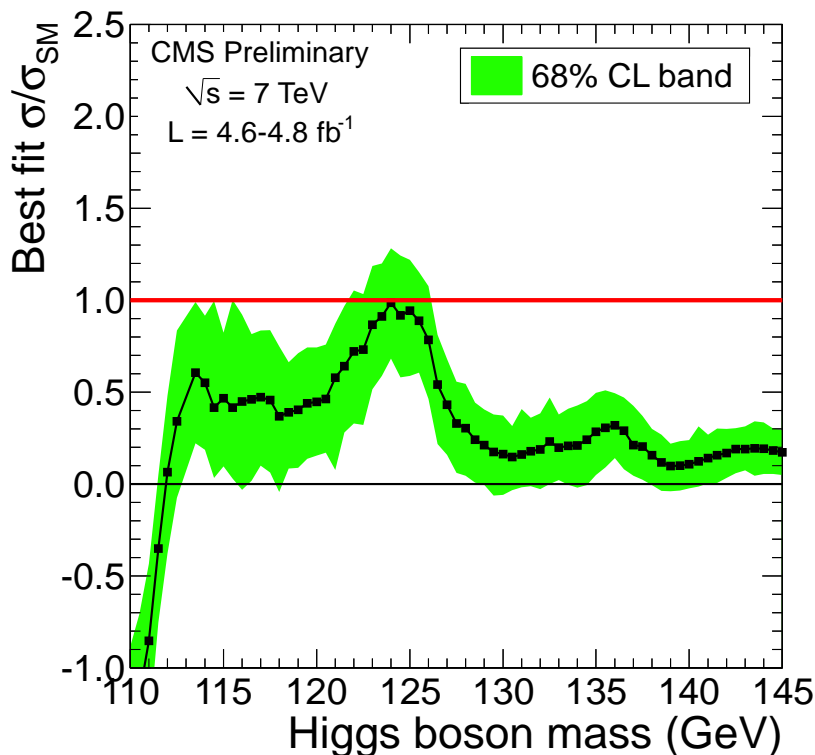


Figure 13: CMS SM best-fit cross sections [10].

The mass of the Higgs boson will be measured by each LHC experiment with a precision of $\sim 0.1\%$, limited by the energy scale, in the currently allowed low mass range [141,142]. This projection is based on the invariant mass reconstruction from electromagnetic calorimeter objects, using the decays $H \rightarrow \gamma\gamma$ or $H \rightarrow ZZ^* \rightarrow 4\ell$. The precision would be degraded at higher masses because of the larger decay width, but even at $m_H \sim 700$ GeV a precision of 1% on m_H is expected to be achievable. The width of the SM Higgs boson may be too narrow to be measured directly. The width could be constrained indirectly using partial width measurements [143,144]. For $300 < m_H < 700$ GeV, a direct measurement of the decay width of an SM-like Higgs boson could be performed with a precision of about 6%.

The possibilities for measuring other properties of the Higgs boson, such as its spin, its CP eigenvalue, its couplings to

Table 1: Observed and expected limits at the 95% C.L. normalized to the SM predictions for the main search channels at the Tevatron and the LHC, evaluated for $m_H = 125$ GeV

Channel	Obs	Exp	Lumi [fb^{-1}]	Ref.
Tevatron				
$H \rightarrow W^+W^-$	2.4	2.2	9.7	[6]
$H \rightarrow b\bar{b}$	3.2	1.4	9.7	[6]
Combined	2.2	1.1	10.0	[6]
ATLAS				
$H \rightarrow \gamma\gamma$ (MVA)	3.5	1.6	4.9	[132]
$H \rightarrow W^+W^- \rightarrow \ell^+\nu\ell^-\bar{\nu}$	1.4	1.2	4.7	[121]
$H \rightarrow ZZ \rightarrow \ell^+\ell^-\ell^+\ell^-$	4.2	2.4	4.8	[125]
Combined	1.5	0.8	4.9	[8]
CMS				
$H \rightarrow \gamma\gamma$ (MVA)	2.9	1.2	4.8	[134]
$H \rightarrow W^+W^- \rightarrow \ell^+\nu\ell^-\bar{\nu}$	1.5	1.1	4.6	[122]
$H \rightarrow ZZ \rightarrow \ell^+\ell^-\ell^+\ell^-$	2.5	1.6	4.7	[126]
Combined	1.6	0.7	4.8	[10]

bosons and fermions, and its self-coupling, have been investigated in numerous studies [141,142,145–148]. Given a sufficiently high integrated luminosity (300 fb^{-1}), most of these properties are expected to be accessible to analysis in the favored mass range $114 \text{ GeV} < m_H < 129 \text{ GeV}$. The measurement of Higgs self-couplings, however, may suffer from poor sensitivity at the LHC, although a luminosity upgrade, the so-called Super-LHC, could allow for a more precise measurement. The results of these measurements could either establish the presence of a SM-like Higgs boson or point the way to new physics.

II.5 Models with a Fourth Generation of SM-Like Fermions

The SM Higgs boson production processes and branching ratios presented above are limited to the case of three genera-

tions of quarks and leptons. The existence of a fourth generation of fermions is compatible with present experimental bounds and would have direct consequences on the SM Higgs boson production and decay branching ratios [149], and hence on Higgs boson searches at LEP, the Tevatron, and the LHC [150,151]. Current experimental searches bound the fourth generation quark masses to be above the top quark mass [152]. These additional heavy quarks lead to new contributions in the loop-induced couplings of the Higgs boson to gluons and to photons. In particular, they lead to a strong enhancement of the gluon fusion production rate and of the branching ratio of the Higgs boson decay into a pair of gluons. As a result, the branching ratios of Higgs boson decay to $b\bar{b}$, tau pairs, and pairs of W and Z bosons are reduced, although near $m_H \sim 2M_W$, the decay to a pair of W bosons still nearly saturates the decay width, even with the enhanced gluon decay. Due to a cancellation between the W and heavy fermion contributions, the photon decay channels may be further suppressed. The enhancement of the gluon fusion production rate makes the search channels using Higgs boson decays into tau leptons and W and Z bosons promising for a light Higgs boson. In addition, in the case of a fourth generation Majorana neutrino, exotic signals such as Higgs boson decay into same-sign dileptons may be possible. Interpretations of the experimental searches optimized for a minimal fourth-generation model (SM4) are available from the Tevatron [153] and CMS [10]. CMS excludes the Higgs boson in the SM4 model in the mass range $120 \text{ GeV} < m_H < 600 \text{ GeV}$ at the 95% C.L.

III. Higgs Bosons in the Minimal Supersymmetric Standard Model (MSSM)

Electroweak symmetry breaking driven by a weakly-coupled elementary scalar sector requires a mechanism to explain the smallness of the breaking scale compared with the Planck scale [154]. In addition, within supersymmetric extensions of the SM, the supersymmetry-breaking effects, whose origins may lie at energy scales much larger than 1 TeV, can induce a radiative breaking of the electroweak symmetry due to the effects of

the large Higgs-top quark Yukawa coupling [155]. In this way, the electroweak symmetry breaking scale is intimately tied to the scale of supersymmetry breaking masses. Supersymmetry provides an explanation for the stability of the hierarchy of scales, provided that the supersymmetry-breaking masses, in particular those related to the stop sector, are at most in the TeV range [154].

A fundamental theory of supersymmetry breaking is unknown at this time. Nevertheless, one can parameterize the low-energy theory in terms of the most general set of soft supersymmetry-breaking renormalizable operators [156]. The Minimal Supersymmetric extension of the Standard Model (MSSM) [12,157] associates a supersymmetric partner to each gauge boson and chiral fermion of the SM, and provides a realistic model of physics at the weak scale. However, even in this minimal model with the most general set of soft supersymmetry-breaking terms, more than 100 new parameters are introduced [158]. Fortunately, only a subset of these parameters impact the Higgs phenomenology through tree-level and quantum effects. Reviews of the properties and phenomenology of the Higgs bosons of the MSSM can be found for example in Refs. [44] and [159].

The MSSM contains the particle spectrum of a two-Higgs-doublet model (2HDM) extension of the SM and the corresponding supersymmetric partners. Two Higgs doublets, H_u and H_d , are required to ensure an anomaly-free SUSY extension of the SM and to generate mass for both “up”-type and “down”-type quarks and charged leptons [13]. After the spontaneous breaking of the electroweak symmetry, five physical Higgs particles are left in the spectrum: one charged Higgs pair, H^\pm , one CP -odd scalar, A , and two CP -even states, H and h .

The supersymmetric structure of the theory imposes constraints on the Higgs sector of the model. In particular, the parameters of the Higgs self-interaction are given by the gauge coupling constants. As a result, all Higgs sector parameters at tree level are determined by only two free parameters: the ratio of the H_u and H_d vacuum expectation values, $\tan\beta = v_u/v_d$,

with $v_u^2 + v_d^2 \approx (246 \text{ GeV})^2$; and one Higgs boson mass, conventionally chosen to be m_A . The other tree-level Higgs boson masses are then given in terms of these parameters

$$m_{H^\pm}^2 = m_A^2 + M_W^2$$

$$m_{H,h}^2 = \frac{1}{2} \left[m_A^2 + M_Z^2 \pm \sqrt{(m_A^2 + M_Z^2)^2 - 4(M_Z m_A \cos 2\beta)^2} \right]$$

and α is the angle that diagonalizes the CP -even Higgs squared-mass matrix. An important consequence of these mass formulae is that the mass of the lightest CP -even Higgs boson is bounded from above:

$$m_h \leq M_Z |\cos 2\beta|.$$

This contrasts sharply with the SM, in which the Higgs boson mass is bounded from above only by perturbativity and unitarity considerations. In the large m_A limit, also called the decoupling limit [160], one finds $m_h^2 \simeq (M_Z \cos 2\beta)^2$ and $m_A \simeq m_H \simeq m_{H^\pm}$, up to corrections of $\mathcal{O}(M_Z^2/m_A)$. Below the scale m_A , the Higgs sector of the effective low-energy theory consists only of h , which behaves as the SM Higgs boson.

The phenomenology of the Higgs sector depends on the couplings of the Higgs bosons to gauge bosons, and fermions. The couplings of the two CP -even Higgs bosons to W^\pm and Z bosons are given in terms of the angles α and β by

$$g_{hVV} = g_V m_V \sin(\beta - \alpha) \quad g_{HVV} = g_V m_V \cos(\beta - \alpha),$$

where $g_V \equiv 2m_V/v$. There are no tree-level couplings of A or H^\pm to VV . The couplings of the Z boson to two neutral Higgs bosons, which must have opposite CP -quantum numbers, are given by

$$g_{hAZ} = g_Z \cos(\beta - \alpha)/2 \quad g_{HAZ} = -g_Z \sin(\beta - \alpha)/2.$$

Charged Higgs- W boson couplings to neutral Higgs bosons and four-point couplings of vector bosons and Higgs bosons can be found in Ref. 13.

The tree-level Higgs couplings to fermions obey the following property: the neutral components of one Higgs doublet couple

exclusively to down-type fermion pairs while the neutral components of the other doublet couple exclusively to up-type fermion pairs [13,161]. This Higgs-fermion coupling structure defines the Type-II 2HDM [162], and differs from Type-I 2HDM [163] in which one Higgs field couples to all fermions while the other field is decoupled from them. In the MSSM, fermion masses are generated when both neutral Higgs components acquire vacuum expectation values, and the relations between Yukawa couplings and fermion masses are (in third-generation notation)

$$h_b = \sqrt{2} m_b / v_d = \sqrt{2} m_b / (v \cos \beta)$$

$$h_t = \sqrt{2} m_t / v_u = \sqrt{2} m_t / (v \sin \beta).$$

Similarly, one can define the Yukawa coupling of the Higgs boson to τ -leptons (the latter is a down-type fermion).

The couplings of the neutral Higgs bosons to $f\bar{f}$ relative to the SM value, $g m_f / 2M_W$, are given by

$$h\bar{b}b : \quad -\sin \alpha / \cos \beta = \sin(\beta - \alpha) - \tan \beta \cos(\beta - \alpha),$$

$$h\bar{t}t : \quad \cos \alpha / \sin \beta = \sin(\beta - \alpha) + \cot \beta \cos(\beta - \alpha),$$

$$H\bar{b}b : \quad \cos \alpha / \cos \beta = \cos(\beta - \alpha) + \tan \beta \sin(\beta - \alpha),$$

$$H\bar{t}t : \quad \sin \alpha / \sin \beta = \cos(\beta - \alpha) - \cot \beta \sin(\beta - \alpha),$$

$$A\bar{b}b : \quad \gamma_5 \tan \beta, \quad A\bar{t}t : \quad \gamma_5 \cot \beta,$$

where the γ_5 indicates a pseudoscalar coupling. In each relation above, the factor listed for $b\bar{b}$ also pertains to $\tau^+\tau^-$. The charged Higgs boson couplings to fermion pairs are given by

$$g_{H^-t\bar{b}} = \frac{g}{\sqrt{2}M_W} [m_t \cot \beta P_R + m_b \tan \beta P_L],$$

$$g_{H^- \tau^+ \nu} = \frac{g}{\sqrt{2}M_W} [m_\tau \tan \beta P_L],$$

with $P_{L,R} = (1 \mp \gamma_5)/2$.

The Higgs couplings to down-type fermions can be significantly enhanced at large $\tan \beta$ in the following two cases: (i) If $m_A \gg M_Z$, then $|\cos(\beta - \alpha)| \ll 1$, $m_H \simeq m_A$, and the $b\bar{b}H$ and $b\bar{b}A$ couplings have equal strength and are significantly enhanced by a factor of $\tan \beta$ relative to the corresponding SM

coupling, whereas the VVH coupling is negligibly small. The values of the VVh and $b\bar{b}h$ couplings are equal to the corresponding couplings of the SM Higgs boson. (ii) If $m_A < M_Z$ and $\tan\beta \gg 1$, then $|\cos(\beta - \alpha)| \approx 1$ and $m_h \simeq m_A$. In this case, the $b\bar{b}h$ and $b\bar{b}A$ couplings have equal strength and are significantly enhanced by a factor of $\tan\beta$ relative to the corresponding SM coupling, while the VVh coupling is negligibly small. In addition, the VVH coupling is equal in strength to the corresponding SM VVH coupling and one can refer to H as a SM-like Higgs boson. The value of the $b\bar{b}H$ coupling can differ from the corresponding SM coupling and converges to it only for $m_A \ll M_Z$ for which $\tan\beta \sin(\beta - \alpha) \rightarrow 0$. Note that in both cases (i) and (ii) above, only two of the three neutral Higgs bosons have significantly enhanced couplings to $b\bar{b}$.

III.1. Radiatively-Corrected MSSM Higgs Masses and Couplings

Radiative corrections have a significant impact on the values of Higgs boson masses and couplings in the MSSM. Important contributions come from loops of third generation SM particles as well as their supersymmetric partners. The dominant effects to the Higgs mass arise from the incomplete cancellation between top and scalar-top (stop) loops and at large $\tan\beta$ also from sbottom and stau loops. The stop, sbottom and stau masses and mixing angles depend on the supersymmetric Higgsino mass parameter μ and on the soft-supersymmetry-breaking parameters [12,157]: M_Q , M_U , M_D , M_L , M_E , and A_t , A_b , A_τ . The first three of these are the left-chiral and the two right-chiral top and bottom scalar quark mass parameters. The next two are the left-chiral stau/sneutrino and the right-chiral stau mass parameters, and the last three are the trilinear parameters that enter in the off-diagonal squark/slepton mixing elements: $X_t \equiv A_t - \mu \cot\beta$ and $X_{b,\tau} \equiv A_{b,\tau} - \mu \tan\beta$. The corrections affecting the Higgs boson masses, production, and decay properties depend on all of these parameters in various ways. At the two-loop level, also the masses of the gluino and the electroweak gaugino enter in the calculations. For simplicity, we shall initially assume that A_t , A_b , A_τ , μ , and the gluino

and electroweak gaugino masses are real parameters. The impact of complex phases on MSSM parameters, which will induce CP -violation in the Higgs sector, is addressed below.

Radiative corrections to the Higgs boson masses have been computed using a number of techniques, with a variety of approximations; see Refs. [165–176]. They depend strongly on the top quark mass ($\sim m_t^4$) and the stop mixing parameter X_t , and there is also a logarithmic dependence on the stop masses. One of the most striking effects is the increase of the upper bound of the light CP -even Higgs boson mass, as first noted in Refs. [165,166]. The value of m_h is maximized for large $m_A \gg M_Z$, when all other MSSM parameters are fixed. Moreover, $\tan\beta \gg 1$ also maximizes m_h , when all other parameters are held fixed. Taking m_A large (the decoupling limit) and $\tan\beta \gg 1$, the value of m_h can be further maximized at one-loop level for $X_t \simeq \sqrt{6}M_{\text{SUSY}}$, where $M_{\text{SUSY}} \simeq M_Q \simeq M_U \simeq M_D$ is an assumed common value of the soft SUSY-breaking squark mass parameters. This choice of X_t is called the “maximal-mixing scenario” which will be indicated by m_h -max. Instead, for $X_t = 0$, which is called the “no-mixing scenario,” the value of m_h has its lowest possible value, for fixed m_A and all other MSSM parameters. The value of m_h also depends on the specific value of M_{SUSY} , and, for example, raising M_{SUSY} from 1 TeV to 2 TeV can increase m_h by 2-5 GeV. Variation of the value of m_t by 1 GeV changes the value of m_h by about the same amount. As mentioned above, m_h also depends on μ and more weakly on the electroweak gaugino mass as well as the gluino mass at the two-loop level. For any given scenario defined by a full set of MSSM parameters, we will denote the maximum value of m_h by $m_h^{\text{max}}(\tan\beta)$, for each value of $\tan\beta$. Allowing for the experimental uncertainty on m_t and for the uncertainty inherent in the theoretical analysis, one finds for $M_{\text{SUSY}} \lesssim 2$ TeV, large m_A and $\tan\beta \gg 1$, $m_h^{\text{max}} = 135$ GeV in the m_h -max scenario, and $m_h^{\text{max}} = 122$ GeV in the no-mixing scenario [177,178]. In practice, parameter values leading to maximal mixing are not obtained in most models of supersymmetry breaking, so typical upper limits on m_h will lie between these two extremes [179]. In the large $\tan\beta$ regime light staus and/or sbottoms with

sizable mixing, governed by the μ parameter, yield negative radiative corrections to the mass of the lightest Higgs boson, and can lower it by several GeV [173,180]. Hence, if the Higgs boson were to have a mass of about 125 GeV, a sizable mixing in the stop sector would be required [180,181] ($X_t \geq 1.5M_{\text{SUSY}}$, or even larger if $\tan\beta$ is large). The relatively small mass of the lightest neutral scalar boson is a prediction for both the CP -conserving (CPC) and CP -violating (CPV) [182] MSSM scenarios. This is particularly interesting in the light of the intriguing excesses observed at the Tevatron and the LHC and given that masses above 130 GeV are strongly disfavored by LHC data.

Radiative corrections also modify significantly the values of the Higgs boson couplings to fermion pairs and to vector boson pairs. The tree-level Higgs couplings depend strongly on the value of $\cos(\beta - \alpha)$. In a first approximation, when radiative corrections of the Higgs squared-mass matrix are computed, the diagonalizing angle α is shifted from its tree-level value, and hence one may compute a “radiatively-corrected” value for $\cos(\beta - \alpha)$. This shift provides one important source of the radiative corrections to the Higgs couplings. In particular, depending on the sign of μX_t and the magnitude of X_t/M_{SUSY} , modifications of α can lead to important variations of the SM-like Higgs boson coupling to bottom quarks and tau leptons [175]. Similar corrections to the mixing angle α can come for large $\tan\beta$ from the stau/sbottom sector for sizable $A_{b,\tau}$ [180]. Additional contributions from the one-loop vertex corrections to tree-level Higgs couplings must also be considered [170–189]. These contributions alter significantly the Higgs-fermion Yukawa couplings at large $\tan\beta$, both in the neutral and charged Higgs sector. Moreover, these radiative corrections can modify the basic relationship $g_{h,H,A\bar{b}b}/g_{h,H,A\tau^+\tau^-} \propto m_b/m_\tau$, and change the main features of MSSM Higgs phenomenology.

III.2. Decay Properties and Production Mechanisms of MSSM Higgs Bosons

In the MSSM, neglecting CP -violating effects, one must consider the decay properties of three neutral Higgs bosons and one charged Higgs pair. In the region of parameter space where

$m_A \gg m_Z$ and the masses of supersymmetric particles are large, the decoupling limit applies, and the decay rates of h into SM particles are nearly indistinguishable from those of the SM Higgs boson. Hence, the h boson will decay mainly to fermion pairs, since the mass, less than about 135 GeV, is below the W^+W^- threshold. The SM-like branching ratios of h are modified if decays into supersymmetric particles are kinematically allowed [190]. In addition, if light superpartners exist that can couple to photons and/or gluons, then the effective couplings to gg and $\gamma\gamma$ could deviate from the corresponding SM predictions [180,191,192]. In the decoupling limit, the heavier Higgs states, H , A and H^\pm , are roughly mass degenerate, and their decay branching ratios strongly depend on $\tan\beta$ as discussed below. The AWW and AZZ couplings vanish, and the HWW and HZZ couplings are very small. For values of $m_A \sim \mathcal{O}(M_Z)$, all Higgs boson masses lie below 200 GeV. In this regime, there is a significant area of the parameter space in which none of the neutral Higgs boson decay properties approximates that of the SM Higgs boson. For $\tan\beta \gg 1$, the resulting predictions show marked differences from those for the SM Higgs boson [193]. Significant modifications to the $b\bar{b}$ and/or the $\tau^+\tau^-$ decay rates may occur via radiative effects.

After incorporating the leading radiative corrections to Higgs couplings from both QCD and supersymmetry, the following decay features are relevant in the MSSM. The decay modes $h, H, A \rightarrow b\bar{b}$, $\tau^+\tau^-$ dominate when $\tan\beta$ is large for all values of the Higgs boson masses. For small $\tan\beta$, these modes are significant for neutral Higgs boson masses below $2m_t$ (although there are other competing modes in this mass range), whereas the $t\bar{t}$ decay mode dominates above its kinematic threshold. In contrast to the SM Higgs boson, the vector boson decay modes of H are strongly suppressed at large m_H due to the suppressed HVV couplings in the decoupling limit. For the charged Higgs boson, $H^+ \rightarrow \tau^+\nu_\tau$ dominates below the $t\bar{b}$ threshold, while $H^+ \rightarrow t\bar{b}$ dominates for large values of m_{H^\pm} . For low values of $\tan\beta$ ($\lesssim 1$) and low values of the charged Higgs boson mass ($\lesssim 120$ GeV), the decay mode $H^+ \rightarrow c\bar{s}$ becomes relevant.

In addition to the decay modes of the neutral Higgs bosons into fermion and gauge boson final states, additional decay channels may be allowed which involve scalars of the extended Higgs sector, *e.g.*, $h \rightarrow AA$. Supersymmetric final states from Higgs boson decays into charginos, neutralinos and third-generation squarks and sleptons can be important if they are kinematically allowed [194]. One interesting possibility is a significant branching ratio for the decay of a neutral Higgs boson to the invisible mode $\tilde{\chi}_1^0 \tilde{\chi}_1^0$ (where the lightest neutralino $\tilde{\chi}_1^0$ is the lightest supersymmetric particle) [195], which poses a challenge at hadron colliders.

The production mechanisms for the SM Higgs boson at e^+e^- and hadron colliders can also be relevant for the production of the MSSM neutral Higgs bosons. However, one must take into account the possibility of enhanced or suppressed couplings with respect to those of the Standard Model, since these can significantly modify the production cross sections of neutral Higgs bosons. The supersymmetric-QCD corrections due to the exchange of virtual squarks and gluinos may modify the cross sections depending on the values of these supersymmetric particle masses. At both lepton and hadron colliders there are new mechanisms that produce two neutral Higgs bosons, as well as processes that produce charged Higgs bosons singly or in pairs. In the following we summarize the main processes for MSSM Higgs boson production. For a more detailed discussion and consideration of state-of-the-art calculations, see Refs. [44,75,159].

The main production mechanisms for the neutral MSSM Higgs bosons at e^+e^- colliders are Higgs-strahlung ($e^+e^- \rightarrow Zh, ZH$), vector boson fusion ($e^+e^- \rightarrow \nu\bar{\nu}h, \nu\bar{\nu}H$)—with W^+W^- fusion about an order of magnitude larger than ZZ fusion—and s -channel Z boson exchange ($e^+e^- \rightarrow Ah, AH$) [196]. For the Higgs-strahlung process, it is possible to reconstruct the mass and momentum of the Higgs boson recoiling against the particles from the Z boson decay, and hence sensitive searches for Higgs bosons decaying even to invisible final states can be applied.

The main charged Higgs boson production process at e^+e^- colliders is via s -channel γ or Z boson exchange ($e^+e^- \rightarrow H^+H^-$). Charged Higgs bosons can also be produced in top quark decays via $t \rightarrow b + H^+$ if $m_H^\pm < m_t - m_b$ or via the one-loop process $e^+e^- \rightarrow W^\pm H^\mp$ [197,198], which allows the production of a charged Higgs boson with $m_H^\pm > \sqrt{s}/2$, even when H^+H^- production is kinematically forbidden. Other single charged Higgs production mechanisms include $t\bar{b}H^-/\bar{t}bH^+$ production [51], $\tau^+\nu H^-/\tau^-\bar{\nu}H^+$ production [199], and a variety of processes in which H^\pm is produced in association with a one or two other gauge and/or Higgs bosons [200].

At hadron colliders, the dominant neutral Higgs production mechanism over the majority of the MSSM parameter space is gluon-gluon fusion, mediated by triangle loops containing heavy top and bottom quarks and the corresponding supersymmetric partners [201]. Higgs boson radiation from bottom quarks becomes important for large $\tan\beta$, where at least two of the three neutral Higgs bosons have enhanced couplings to bottom-type fermions [202,203]. A more detailed discussion is presented in Sec. (III.3). The vector boson fusion and Higgsstrahlung production of the CP -even Higgs bosons as well as the associated production of neutral Higgs bosons with top quark pairs have lower production cross sections by least an order of magnitude with respect to the dominant ones, depending on the precise region of MSSM parameter space.

Charged Higgs bosons can be produced in several different modes at hadron colliders. If $m_{H^\pm} < m_t - m_b$, the charged Higgs boson can be produced in decays of the top quark via the decay $t \rightarrow bH^+$, which would compete with the SM process $t \rightarrow bW^+$. Relevant QCD and SUSY-QCD corrections to $\text{BR}(t \rightarrow H^+b)$ have been computed [204–207]. For values of m_{H^\pm} near m_t , width effects are important. In addition, the full $2 \rightarrow 3$ processes $pp/p\bar{p} \rightarrow H^+\bar{t}b + X$ and $pp/p\bar{p} \rightarrow H^-\bar{t}b + X$ must be considered. If $m_{H^\pm} > m_t - m_b$, then charged Higgs boson production occurs mainly through radiation from a third generation quark. Charged Higgs bosons may also be produced singly in association with a top quark via the $2 \rightarrow 3$ partonic processes $gg, q\bar{q} \rightarrow t\bar{b}H^-$ (and the charge

conjugate final states). For charged Higgs boson production cross section predictions for the Tevatron and the LHC, see Refs. [12,43,76,208–214]. Charged Higgs bosons can also be produced via associated production with W^\pm bosons through $b\bar{b}$ annihilation and gg -fusion [215]. They can also be produced in pairs via $q\bar{q}$ annihilation [216]. The inclusive H^+H^- cross section is less than the cross section for single charged Higgs associated production [216–218].

III.3. Searches for Neutral Higgs Bosons in the CP-Conserving (CPC) Scenario

Most of the experimental investigations carried out at LEP, the Tevatron, and the LHC, assume CP -conservation (CPC) in the MSSM Higgs sector. In many cases the search results are interpreted in a number of specific benchmark models where a representative set of the relevant SUSY breaking parameters are specified [177].

III.3.1. Searches for Neutral MSSM Higgs Bosons at LEP

In e^+e^- collisions at LEP energies, the main production mechanisms of the neutral MSSM Higgs bosons are the Higgs-strahlung processes $e^+e^- \rightarrow hZ, HZ$ and the pair production processes $e^+e^- \rightarrow hA, HA$, while the fusion processes play a marginal role. Higgs boson decays to $b\bar{b}$ and $\tau^+\tau^-$ are used in these searches.

The searches and limits from the four LEP experiments are described in Refs. [219–222]. The combined LEP data did not contain any excess of events which would imply the production of a Higgs boson, and combined limits were derived [34]. For $m_A \gg M_Z$ the limit on m_h is nearly that of the SM searches, as $\sin^2(\beta - \alpha) \approx 1$. For high values of $\tan\beta$ and low m_A ($m_A \leq m_h^{max}$) the $e^+e^- \rightarrow hA$ searches become the most important, and the lightest Higgs h is non SM-like. In this region, the 95% C.L. mass bounds are $m_h > 92.8$ GeV and $m_A > 93.4$ GeV. In the m_h -max. scenario, values of $\tan\beta$ from 0.7 to 2.0 are excluded taking $m_t = 174.3$ GeV, while a much larger $\tan\beta$ region is excluded for other benchmark scenarios such as the no-mixing one.

Neutral Higgs bosons may also be produced by Yukawa processes $e^+e^- \rightarrow f\bar{f}\phi$, where the Higgs particle $\phi \equiv h, H, A$, is radiated off a massive fermion ($f \equiv b$ or τ^\pm). These processes can be dominant at low masses, and whenever the $e^+e^- \rightarrow hZ$ and hA processes are suppressed. The corresponding ratios of the $f\bar{f}h$ and $f\bar{f}A$ couplings to the SM coupling are $\sin\alpha/\cos\beta$ and $\tan\beta$, respectively. The LEP data have been used to search for $b\bar{b}b\bar{b}$, $b\bar{b}\tau^+\tau^-$, and $\tau^+\tau^-\tau^+\tau^-$ final states [223,224]. Regions of low mass and high enhancement factors are excluded by these searches.

III.3.2. Searches for Neutral MSSM Higgs Bosons at Hadron Colliders

Over a large fraction of the MSSM parameter space, one of the CP -even neutral Higgs bosons (h or H) couples to the vector bosons with SM-like strength and has a mass below 135 GeV. Hence, if the current 95% C.L. exclusion limits for a SM Higgs boson from ATLAS and CMS are interpreted in terms of the SM-like supersymmetric Higgs boson, there is a region of SUSY parameter space beyond that excluded by LEP that is strongly disfavored. In particular, the minimal mixing scenario with $M_{SUSY} \leq 2$ TeV is disfavored considering the LEP and ATLAS data. At the same time, if the excess of events observed in the Higgs boson searches in the diphoton and ZZ channels are confirmed, this could be interpreted as a SM-like MSSM Higgs boson.

Scenarios with enhanced Higgs boson production cross sections are studied at hadron colliders. The best sensitivity is in the regime with low to moderate m_A and with large $\tan\beta$ which enhances the couplings of the Higgs bosons to down-type fermions. The corresponding limits on the Higgs boson production cross section times the branching ratio of the Higgs boson into down-type fermions can be interpreted in MSSM benchmark scenarios [225]. If $\phi = A, H$ for $m_A > m_h^{\max}$, and $\phi = A, h$ for $m_A < m_h^{\max}$, the most promising channels at the Tevatron are $b\bar{b}\phi, \phi \rightarrow b\bar{b}$ or $\phi \rightarrow \tau^+\tau^-$, with three tagged b -jets or $b\tau\tau$ in the final state, respectively, and the inclusive $p\bar{p} \rightarrow \phi \rightarrow \tau^+\tau^-$ process, with contributions from both $gg \rightarrow \phi$ and $b\bar{b}\phi$ production. Although Higgs boson production

via gluon fusion has a higher cross section than via associated production, it cannot be used to study the $\phi \rightarrow b\bar{b}$ decay mode since the signal is overwhelmed by QCD background.

The CDF and DØ collaborations have searched for neutral Higgs bosons produced in association with bottom quarks and which decay into $b\bar{b}$ [226,227], or into $\tau^+\tau^-$ [228,229]. The most recent searches in the $b\bar{b}\phi$ channel with $\phi \rightarrow b\bar{b}$ analyze approximately 2.6 fb^{-1} of data (CDF) and 5.2 fb^{-1} (DØ), seeking events with at least three b -tagged jets. The cross section is defined such that at least one b quark not from ϕ decay is required to have $p_T > 20 \text{ GeV}$ and $|\eta| < 5$. The decay widths of the Higgs bosons are assumed to be much smaller than the experimental resolution. The invariant mass of the two leading jets as well as b -tagging variables are used to discriminate the signal from the backgrounds. The QCD background rates and shapes are inferred from data control samples, in particular, the sample with two b tagged jets and a third, untagged jet. Separate signal hypotheses are tested and limits are placed on $\sigma(p\bar{p} \rightarrow b\bar{b}\phi) \times \text{BR}(\phi \rightarrow b\bar{b})$. CDF sees a local excess of approximately 2.5σ significance in the mass range of 130-160 GeV, but DØ's search is more sensitive and sets stronger limits. The DØ result shown in Fig. 14 displays a ≈ 2 sigma local upward fluctuation in the 110 to 125 GeV mass range.

CDF and DØ have also performed searches for inclusive production of Higgs bosons with subsequent decays to $\tau^+\tau^-$ [230,231,232], although these limits have been superseded by the LHC searches.

In order to interpret the experimental data in terms of MSSM benchmark scenarios, it is necessary to consider carefully the effect of radiative corrections on the production and decay processes. The bounds from the $b\bar{b}\phi, \phi \rightarrow b\bar{b}$ channel depend strongly on the radiative corrections affecting the relation between the bottom quark mass and the bottom Yukawa coupling. In the channels with $\tau^+\tau^-$ final states, however, compensations occur between large corrections in the Higgs boson production and decay. The total production rates of bottom quarks and τ pairs mediated by the production of a CP -odd

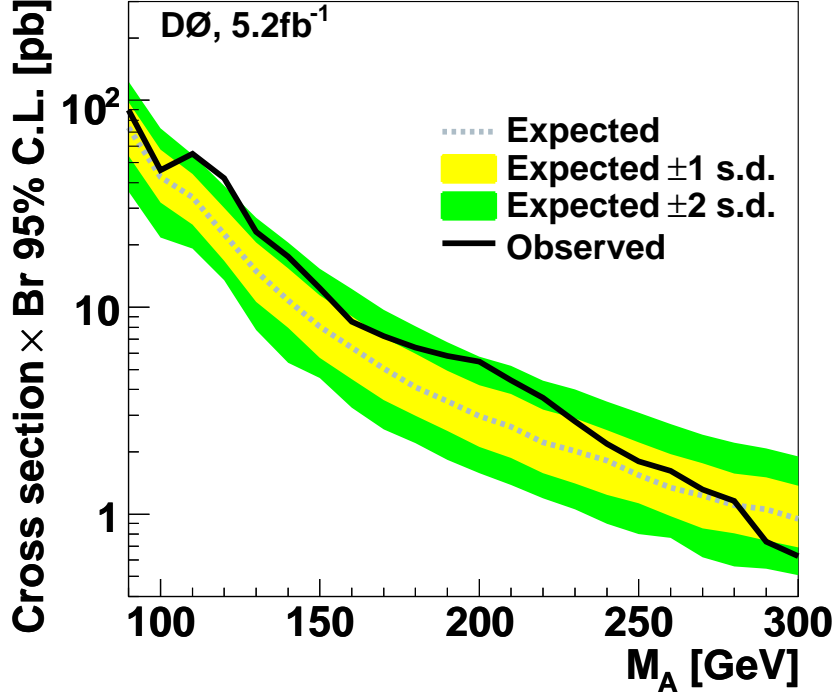


Figure 14: The 95% C.L. limits on $\sigma(p\bar{p} \rightarrow b\phi) \times \text{BR}(\phi \rightarrow b\bar{b})$ from CDF and DØ. The observed limits are indicated with solid lines, and the expected limits are indicated with dashed lines. The limits are to be compared with the sum of signal predictions for Higgs bosons with similar masses.

Higgs boson in the large $\tan\beta$ regime are approximately given by

$$\sigma_{b\bar{b}A} \times \text{BR}(A \rightarrow b\bar{b}) \simeq \sigma_{b\bar{b}A}^{\text{SM}} \frac{\tan^2\beta}{(1 + \Delta_b)^2} \frac{9}{(1 + \Delta_b)^2 + 9},$$

and

$$\sigma_{gg \rightarrow A, b\bar{b}A} \times \text{BR}(A \rightarrow \tau^+\tau^-) \simeq \sigma_{gg \rightarrow A, b\bar{b}A}^{\text{SM}} \frac{\tan^2\beta}{(1 + \Delta_b)^2 + 9},$$

where $\sigma_{b\bar{b}A}^{\text{SM}}$ and $\sigma_{gg \rightarrow A, b\bar{b}A}^{\text{SM}}$ denote the values of the corresponding SM Higgs boson cross sections for a SM Higgs boson mass equal to m_A . The function Δ_b includes the dominant effects of SUSY radiative corrections for large $\tan\beta$ [170,175,187,188], and it depends strongly on $\tan\beta$ and on the SUSY mass parameters.

The $b\bar{b}A$ channel is more sensitive to the value of Δ_b through the factor $1/(1 + \Delta_b)^2$ than the inclusive $\tau^+\tau^-$ channel, for which this leading dependence on Δ_b cancels out. As a consequence, the limits derived from the inclusive $\tau^+\tau^-$ channel depend less on the precise MSSM scenario chosen than those of the $b\bar{b}A$ channel.

The production and decay rates of the CP -even Higgs bosons with $\tan\beta$ -enhanced couplings to down-type fermions— H (or h) for m_A larger (or smaller) than m_h^{\max} , respectively—are governed by formulas similar to the ones presented above. At high $\tan\beta$, one of the CP -even Higgs bosons and the CP -odd Higgs boson are nearly degenerate in mass, enhancing the signal cross section by roughly a factor of two, without complicating the experimental signature except in a small mass region in which the three neutral MSSM Higgs boson masses are close together and each boson contributes to the total production rate. Detailed discussions of the impact of radiative corrections in these search modes are presented in Refs. [225] and [233].

In Fig. 15, the interpretation is shown for DØ’s combination of $\phi \rightarrow b\bar{b}$ and $\phi \rightarrow \tau^+\tau^-$ searches [232] in the $(m_A, \tan\beta)$ plane for the m_h -max benchmark scenario with $\mu = 200$ GeV. The neutral Higgs boson searches consider the contribution of both the CP -odd and the CP -even neutral Higgs bosons with enhanced couplings to bottom quarks. As explained above, considering other benchmark scenarios will not relevantly change the region of SUSY parameter space that can be explored via the inclusive di-tau searches, but different regions of SUSY parameter space will be probed in the case of the $b\bar{b}$ searches.

ATLAS and CMS also search for $\phi \rightarrow \tau^+\tau^-$ in pp collisions at $\sqrt{s} = 7$ TeV. ATLAS seeks tau pairs in 1.06 fb^{-1} of data [234,235], and CMS’s search uses 4.6 fb^{-1} of data [138,139]. The searches are performed in categories of the decays of the two tau leptons: $e\tau_{\text{had}}$, $\mu\tau_{\text{had}}$, $e\mu$, and $\mu\mu$, where τ_{had} denotes a tau lepton which decays to one or more hadrons plus a tau neutrino, e denotes $\tau \rightarrow e\nu\nu$, and μ denotes $\tau \rightarrow \mu\nu\nu$. The dominant background comes from $Z \rightarrow \tau^+\tau^-$ decays, although $t\bar{t}$, W +jets and Z +jets events contribute as

well. Separating events into categories based on the number of b -tagged jets improves the sensitivity in the MSSM. The $b\bar{b}$ annihilation process and radiation of a Higgs boson from a b quark give rise to events in which the Higgs boson is accompanied by a $b\bar{b}$ pair in the final state, sometimes with only one b within the detector acceptance. Requiring the presence of one or more b jets reduces the background from Z +jets. Data control samples are used to constrain background rates. The rates for jets to be identified as a hadronically decaying tau lepton are measured in dijet samples, and W +jets samples provide a measurement of the rate of events that, with a fake hadronic tau, can pass the signal selection requirements. Lepton fake rates are measured using samples of unisolated lepton candidates and same-sign lepton candidates. Constraints from ATLAS's and CMS's searches for $h \rightarrow \tau^+\tau^-$ are also shown in Fig. 15 in the m_h -max benchmark scenario, with $\mu = 200$ GeV. The neutral Higgs boson searches consider the contributions of both the CP -odd and CP -even neutral Higgs bosons with enhanced couplings to bottom quarks, as they were for the Tevatron results. As explained above, the di-tau inclusive search limits do not significantly change by considering other benchmark scenarios.

In addition to $\phi \rightarrow \tau^+\tau^-$ at the LHC, studies indicate that with about 30 fb^{-1} of data one can search for the non-standard neutral Higgs bosons of the MSSM in the $b\bar{b}\phi, \phi \rightarrow b\bar{b}$ channel with three b 's in the final state [233]. Due to the dependence of this production and decay mode on the SUSY radiative corrections there is complementarity between the $3b$ channel and the inclusive tau pair channel in exploring the supersymmetric parameter space.

The LHC has the potential to explore a broad range of SUSY parameter space through the search for non-SM-like Higgs bosons. Nevertheless, Fig. 15 shows a broad region with intermediate $\tan\beta$ and large values of m_A that is not tested by present neutral or charged Higgs boson searches, and which might be difficult to cover completely via these searches, even with much larger data sets. In this region of parameter space it is possible that only the SM-like Higgs boson can be within the LHC's reach. If a SM-like Higgs boson is discovered, it may

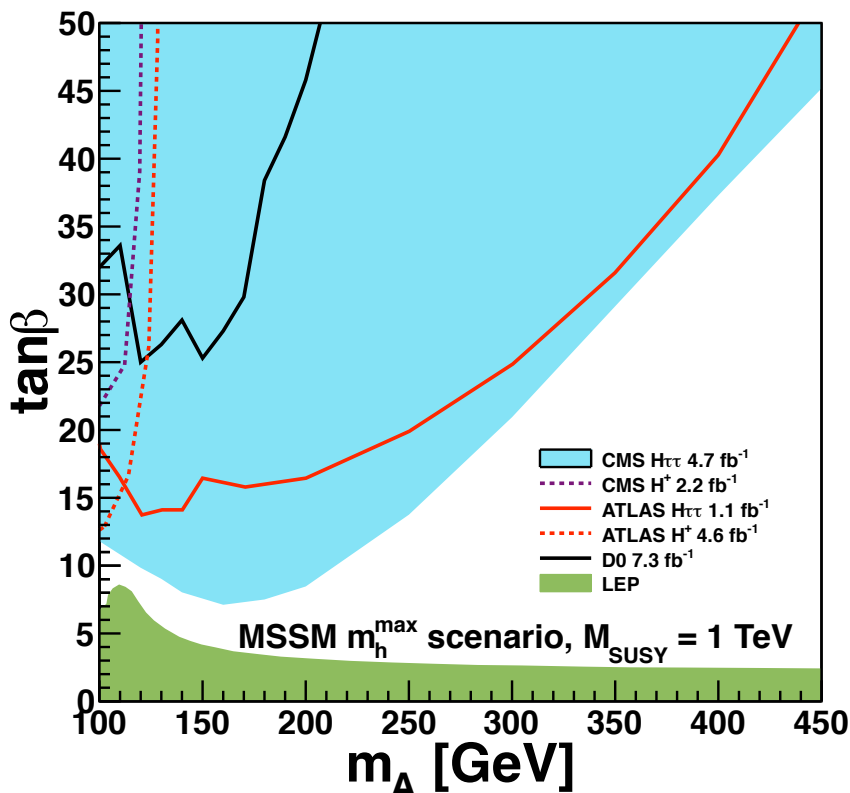


Figure 15: The 95% C.L. MSSM exclusion contours m_h -max benchmark scenario obtained by the ATLAS [234], CMS [138], and DØ [232] collaborations. The LHC collaborations contribute searches for $H \rightarrow \tau^+\tau^-$ and $H^\pm \rightarrow \tau\nu_\tau$ while DØ combines $H \rightarrow \tau^+\tau^-$ with $H \rightarrow b\bar{b}$ searches for these results. Also shown is the region excluded by LEP searches [34], assuming a top quark mass of 174.3 GeV.

be challenging to determine only from the Higgs sector whether there is a supersymmetric extension of the SM in nature.

III.4. Searches for Charged MSSM Higgs Bosons

Searches for the charged Higgs bosons predicted by 2HDMs have been conducted at LEP, the Tevatron, and the LHC, and the results of these searches have been interpreted in terms of the MSSM. Due to the correlations among Higgs boson masses in the MSSM, the experimental results do not yet significantly constrain the MSSM parameter space beyond what is already obtained from the searches for neutral Higgs bosons. In the

near future, however, the LHC experiments will be sensitive to charged Higgs boson decays up to ≈ 170 GeV for all values of $\tan\beta$ [236].

At LEP, searches were performed for pair-produced charged Higgs bosons. In the MSSM and in more general Type-II 2HDMs, for masses which are accessible at LEP energies, the decays $H^+ \rightarrow c\bar{s}$ and $\tau^+\nu_\tau$ dominate. The final states $H^+H^- \rightarrow (c\bar{s})(\bar{c}s)$, $(\tau^+\nu_\tau)(\tau^-\bar{\nu}_\tau)$, and $(c\bar{s})(\tau^-\bar{\nu}_\tau) + (\bar{c}s)(\tau^+\nu_\tau)$ were considered, and the search results are usually presented as functions of $\text{BR}(H^+ \rightarrow \tau^+\nu)$. The sensitivity of the LEP searches was limited to $m_{H^\pm} < 90$ GeV, due to the background from $e^+e^- \rightarrow W^+W^-$ [237], and the kinematic limitation on the production cross section. The combined LEP data constrain $m_{H^\pm} > 78.6$ GeV independently of $\text{BR}(H^+ \rightarrow \tau^+\nu_\tau)$ [238].

At the Tevatron, the CDF and DØ collaborations have searched for charged Higgs bosons in top quark decays with subsequent decays of the charged Higgs boson to $\tau\nu$ or to $c\bar{s}$ [239,240,241]. Assuming $\text{BR}(H^+ \rightarrow c\bar{s}) = 100\%$, the limits on $\text{BR}(t \rightarrow H^+b)$ from CDF and DØ are $\approx 20\%$ in the mass range $90 \text{ GeV} < m_{H^+} < 160 \text{ GeV}$. Assuming $\text{BR}(H^+ \rightarrow \tau^+\nu_\tau) = 100\%$, DØ's limits on $\text{BR}(t \rightarrow H^+b)$ are also $\approx 20\%$ in the same mass range. These limits are valid in general 2HDMs, and they have also been interpreted in terms of the MSSM in the references.

The ATLAS collaboration has also searched for charged Higgs bosons produced in the decay of top quarks in $t\bar{t}$ events. ATLAS has searched for the decay $H^+ \rightarrow \tau^+\nu_\tau$ in three final state topologies: 1) lepton+jets: with $t\bar{t} \rightarrow \bar{b}WH^+ \rightarrow b\bar{b}(q\bar{q}')(\tau_{\text{lep}}\nu)$, i.e., the W boson decays hadronically and the tau decays into an electron or a muon, with two neutrinos; 2) τ +lepton: with $t\bar{t} \rightarrow \bar{b}WH^+ \rightarrow b\bar{b}(l\nu)(\tau_{\text{had}}\nu)$ i.e., the W boson decays leptonically (with $\ell = e, \mu$) and the tau decays hadronically; 3) τ +jets: $t\bar{t} \rightarrow \bar{b}WH^+ \rightarrow b\bar{b}(q\bar{q}')(\tau_{\text{had}}\nu)$, i.e., both the W boson and the τ decay hadronically [242]. Assuming $\text{BR}(H^+ \rightarrow \tau^+\nu_\tau) = 100\%$, ATLAS sets upper limits on $\text{BR}(t \rightarrow H^+b)$ between 5% and 1% for charged Higgs boson masses between 90 GeV to 160 GeV, respectively. These limits are shown in Fig. 16. When interpreted in the context of the

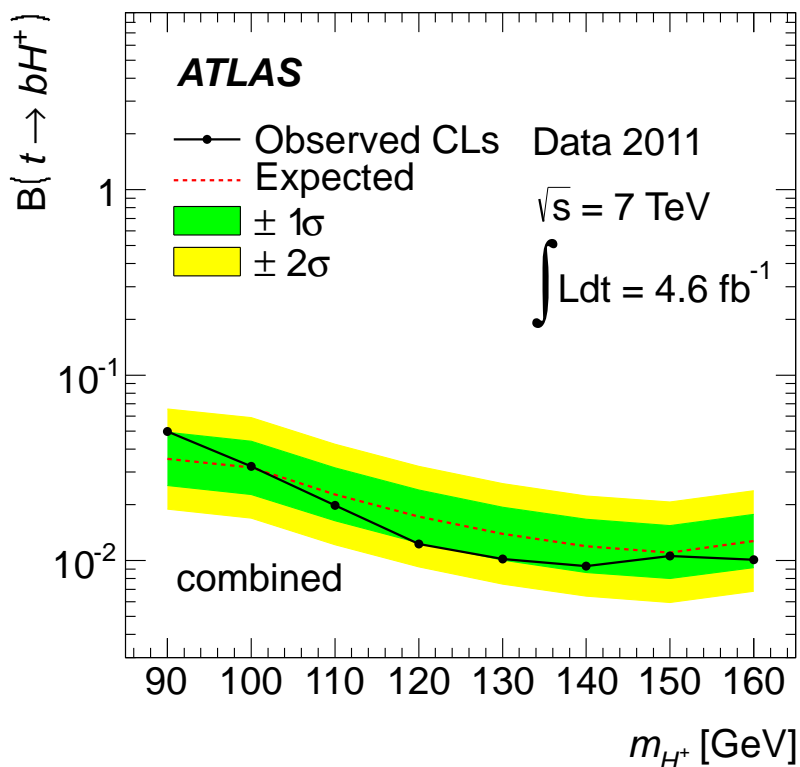


Figure 16: 95% C.L. limit on $\text{BR}(t \rightarrow H^+b)$ assuming $\text{BR}(H^+ \rightarrow \tau\nu) = 100\%$ from the ATLAS collaboration [242].

m_h^{\max} scenario of the MSSM, these bounds exclude $\tan\beta$ values above 20 in this range of charged Higgs boson masses, but also provide sensitivity for $\tan\beta < 4$ due to the increasing predicted decay rate for $t \rightarrow H^+b$ at low $\tan\beta$. The high- $\tan\beta$ interpretation of this result is shown in Fig. 15. ATLAS has also searched for charged Higgs bosons in top quark decays assuming $\text{BR}(H^+ \rightarrow c\bar{s}) = 100\%$ [243], and sets limits of $\approx 20\%$ on $\text{BR}(t \rightarrow H^+b)$ in the $90 \text{ GeV} < m_{H^+} < 160 \text{ GeV}$ mass range.

The CMS collaboration has also searched for the charged Higgs boson in the decay products of top quark pairs: $t\bar{t} \rightarrow H^\pm W^\mp b\bar{b}$ and $t\bar{t} \rightarrow H^+H^-b\bar{b}$ [244]. Three types of final states with large missing transverse energy and jets originating from b -quark hadronization have been analyzed: the fully-hadronic channel with a hadronically decaying tau in association with jets, the di-lepton channel with a hadronically decaying tau

in association with an electron or muon and the di-lepton channel with an electron-muon pair. Combining the results of these three analyses and assuming $\text{BR}(H^\pm \rightarrow \tau\nu)=1$, the upper limits on $\text{BR}(t \rightarrow H^+b)$ are less than 2% to 3% depending on the charged Higgs boson mass in the interval $80 \text{ GeV} < m_{H^\pm} < 160 \text{ GeV}$. The results of this search have been translated into limits in the $(M_A, \tan\beta)$ plane for the m_h -max benchmark scenario and are shown in Fig. 15.

III.5. Effects of CP Violation on the MSSM Higgs Spectrum

In the Standard Model, CP -violation (CPV) is induced by phases in the Yukawa couplings of the quarks to the Higgs field, which results in one non-trivial phase in the CKM mixing matrix. SUSY scenarios with new CPV phases are theoretically appealing, since additional CPV beyond that observed in the K , D , and B meson systems is required to explain the observed cosmic matter-antimatter asymmetry [245,246]. In the MSSM, there are additional sources of CPV from phases in the various mass parameters. In particular, the gaugino mass parameters (M_i , $i = 1, 2, 3$), the Higgsino mass parameter, μ , the bilinear Higgs squared-mass parameter, m_{12}^2 , and the trilinear couplings of the squark and slepton fields to the Higgs fields, A_f , may carry non-trivial phases. The two parameter combinations $\arg[\mu A_f(m_{12}^2)^*]$ and $\arg[\mu M_i(m_{12}^2)^*]$ are invariant under phase redefinitions of the MSSM fields [247,248]. Therefore, if one of these quantities is non-zero, there would be new sources of CP -violation, which affects the MSSM Higgs sector through radiative corrections [182,248–253]. The mixing of the neutral CP -odd and CP -even Higgs boson states is no longer forbidden. Hence, m_A is no longer a physical parameter. However, the charged Higgs boson mass m_{H^\pm} is still physical and can be used as an input for the computation of the neutral Higgs spectrum of the theory.

For large values of m_{H^\pm} , corresponding to the decoupling limit, the properties of the lightest neutral Higgs boson state approach those of the SM Higgs boson. That is, for $m_{H^\pm} \gg M_W$, the lightest neutral Higgs boson is approximately a CP -even state, with CPV couplings that are suppressed by terms of

$\mathcal{O}(m_W^2/m_{H^\pm}^2)$. In particular, the upper bound on the lightest neutral Higgs boson mass, takes the same value as in the CP -conserving case [248]. Nevertheless, there still can be significant mixing between the two heavier neutral mass eigenstates. For a detailed study of the Higgs boson mass spectrum and parametric dependence of the associated radiative corrections, see Refs. [249,252].

Major variations to the MSSM Higgs phenomenology occur in the presence of explicit CPV phases. In the CPV case, vector boson pairs couple to all three neutral Higgs boson mass eigenstates, H_i ($i = 1, 2, 3$), with couplings

$$g_{H_i V V} = \cos \beta \mathcal{O}_{1i} + \sin \beta \mathcal{O}_{2i}$$

$$g_{H_i H_j Z} = \mathcal{O}_{3i}(\cos \beta \mathcal{O}_{2j} - \sin \beta \mathcal{O}_{1j}) - \mathcal{O}_{3j}(\cos \beta \mathcal{O}_{2i} - \sin \beta \mathcal{O}_{1i})$$

where the $g_{H_i V V}$ couplings are normalized to the analogous SM coupling and the $g_{H_i H_j Z}$ have been normalized to $g_Z^{\text{SM}}/2$. \mathcal{O}_{ij} is the orthogonal matrix relating the weak eigenstates to the mass eigenstates. It has non-zero off-diagonal entries mixing the CP -even and CP -odd components of the weak eigenstates. The above couplings obey the relations

$$\sum_{i=1}^3 g_{H_i Z Z}^2 = 1 \quad \text{and} \quad g_{H_k Z Z} = \varepsilon_{ijk} g_{H_i H_j Z}$$

where ε_{ijk} is the Levi-Civita symbol.

Another consequence of CPV effects in the scalar sector is that all neutral Higgs bosons can couple to both scalar and pseudoscalar fermion bilinear densities. The couplings of the mass eigenstates H_i to fermions depend on the loop-corrected fermion Yukawa couplings (similarly to the CPC case), on $\tan \beta$ and on the \mathcal{O}_{ji} . The resulting expressions for the scalar and pseudoscalar components of the neutral Higgs boson mass eigenstates to fermions and the charged Higgs boson to fermions are given in Refs. [249,254].

The production processes of neutral MSSM Higgs bosons in the CPV scenario are similar to those in the CPC scenario, except for the fact that in any process, the CP eigenstates h , H , and A can be replaced by any of the three neutral Higgs

mass eigenstates H_i . This is the case, since, in the presence of CP violation, the H_i 's do not have well-defined CP quantum numbers. Regarding the decay properties, the lightest mass eigenstate, H_1 , predominantly decays to $b\bar{b}$ if kinematically allowed, with a smaller fraction decaying to $\tau^+\tau^-$, similar to the CPC case. If kinematically allowed, a SM-like neutral Higgs boson, H_2 or H_3 can decay predominantly to H_1H_1 leading to many new interesting signals both at lepton and hadron colliders; otherwise it will decay preferentially to $b\bar{b}$.

III.6. Searches for Neutral Higgs Bosons in CPV Scenarios

At LEP, all three neutral Higgs eigenstates could have been produced by Higgs-strahlung, $e^+e^- \rightarrow H_i Z$, and in pairs, $e^+e^- \rightarrow Z^* \rightarrow H_i H_j$, with $i \neq j$. The production rates depend on the details of the CPV scenario. Possible cascade decays such as H_2 or $H_3 \rightarrow H_1 H_1$ can lead to interesting experimental signatures in the Higgs-strahlung processes, $e^+e^- \rightarrow H_2 Z$ or $H_3 Z$, however, the searches in the CPV MSSM scenario are experimentally more difficult. The cross sections for the Higgs-strahlung and pair production processes are given in Refs [182,248,249,253].

The Higgs boson searches at LEP were interpreted [34] in a CPV benchmark scenario [182] for which the parameters were chosen so as to maximize the phenomenological differences with respect to the CPC scenario. Using the most conservative theoretical calculations available at each point in the $(m_{H_1}, \tan\beta)$ plane, parts of the region $m_{H_1} < 60$ GeV and $\tan\beta < 40$ were excluded, and values of $\tan\beta$ lower than 3 were excluded for all values of $m_{H_1} < 114$ GeV. The Tevatron CP -conserving results and projections for MSSM Higgs searches, as well as the existing projections for LHC MSSM CP -conserving searches have been reinterpreted in the framework of CP -violating MSSM Higgs in Ref. 255.

III.7. Indirect Constraints on Supersymmetric Higgs Bosons

Indirect bounds from a global fit to precision measurements of electroweak observables can be derived in terms of MSSM

parameters [256] in a way similar to what was done in the SM. Given the MSSM and SM predictions for M_W as a function of m_t , and varying the Higgs boson mass and the SUSY spectrum, one finds that the MSSM overlaps with the SM when SUSY masses are large, of $\mathcal{O}(2 \text{ TeV})$, and the light SM-like Higgs boson has a mass in the experimentally preferred mass range: $m_h \tilde{114}\text{--}129 \text{ GeV}$. The MSSM Higgs boson mass expectations are compatible with the constraints provided by the measurements of m_t and M_W [257]. A global fit for m_h in the Constrained MSSM, for example, yields $m_h = 119.1_{-2.9}^{+3.4} \text{ GeV}$ after including the constraints from LHC data, instead of the pre-LHC value of $m_h = 111.5_{-1.2}^{+3.5} \text{ GeV}$, improving the consistency of the model predictions with the LEP exclusion [258]⁴. These global fit studies show that a SM-like Higgs with mass 125 GeV or larger would start to build up some tension with $g_\mu - 2$ that may ultimately lead to exclude the CMSSM or other types of constrained SUSY scenarios for which similar results can be obtained.

Improvements in our understanding of B -physics observables put indirect constraints on MSSM scenarios in regions in which Higgs boson searches at the Tevatron and the LHC are sensitive. In particular, $\text{BR}(B_s \rightarrow \mu^+ \mu^-)$, $\text{BR}(b \rightarrow s\gamma)$, and $\text{BR}(B_u \rightarrow \tau\nu)$ play an important role within minimal flavor-violating (MFV) models [259], in which flavor effects proportional to the CKM matrix elements are induced, as in the SM. For example, see Refs. [260–263]. The supersymmetric contributions to these observables come both at the tree- and loop-level, and have a different parametric dependence, but share the property that they become significant for large values of $\tan\beta$, which is also the regime in which searches for non-standard MSSM Higgs bosons at hadron colliders are the most powerful.

In the SM, the relevant contributions to the rare decay $B_s \rightarrow \mu^+ \mu^-$ come through the Z -penguin and the W^\pm -box diagrams [264]. In supersymmetry with large $\tan\beta$, there are

⁴ This fit does not include the direct limits on the Higgs boson mass from any collider.

also significant contributions from Higgs-mediated neutral currents [265–268], which depend on the SUSY spectra, and grow with the sixth power of $\tan\beta$ and decrease with the fourth power of the CP -odd Higgs boson mass m_A . Therefore, the upper limits from the Tevatron and the LHC [269] put strong restrictions on possible flavor-changing neutral currents (FCNC) in the MSSM at large $\tan\beta$ [270].

Further constraints are obtained from the rare decay $b \rightarrow s\gamma$. The SM rate is known up to NNLO corrections [271,272] and is in good agreement with measurements [273]. In the Type-II 2HDM and in the absence of other sources of new physics at the electroweak scale, a bound $m_{H^\pm} > 295$ GeV has been derived [271]. Although this indirect bound appears much stronger than the results from direct charged Higgs searches, it can be invalidated by new physics contributions, such as those which can be present in the MSSM. In the minimal flavor-violating MSSM, there are new contributions from charged Higgs as well as chargino-stop and gluino-sbottom diagrams. The charged Higgs boson’s contribution is enhanced for small values of its mass and can be partially canceled by the chargino and gluino contributions or by higher-order $\tan\beta$ -enhanced loop effects.

The branching ratio $B_u \rightarrow \tau\nu$, measured by the Belle [274,275] and BaBar [276,277] collaborations, also constrains the MSSM. The SM expectation is in slight tension with the latest experimental results [278]. In the MSSM, there is an extra tree-level contribution from the charged Higgs which interferes destructively with the SM contribution, and which increases for small values of the charged Higgs boson mass and large values of $\tan\beta$ [279]. Charged Higgs effects on $B \rightarrow D\tau\nu$ decays [280], constrain in an important way the parameter space for small values of the charged Higgs boson mass and large values of $\tan\beta$, and exclude a region that is otherwise allowed by values of $B_u \rightarrow \tau\nu$ [278,281,282]. These two observables are only mildly dependent on the SUSY spectra.

Charged Higgs bosons can play a role in explaining the evidence for CP violation in $D^0 \rightarrow \pi^+\pi^-$, K^+K^- decays recently presented by LHCb [283] and CDF [284]. In a

particular minimal flavor violating 2HDM, tree-level charged Higgs insertions can give large contributions to CP violation in D^0 decays while also being consistent with stringent bounds from $D^0 - \bar{D}^0$ mixing, $\text{BR}(b \rightarrow s\gamma)$, and $\text{BR}(B_u \rightarrow \tau\nu)$, as well as direct searches such as $H \rightarrow \tau^+\tau^-$ [285].

Several studies [260–263,286,287] have shown that, in extended regions of parameter space, the combined B -physics measurements impose strong constraints on the MSSM models to which Higgs boson searches at the Tevatron and the LHC are sensitive. Consequently, the observation of a non-SM Higgs boson at the Tevatron or the LHC would point to a rather narrow, well-defined region of MSSM parameter space [260,288] or to something beyond the minimal flavor violation framework.

Another indirect constraint on the Higgs sector comes from the search for dark matter. If dark matter particles are weakly interacting and massive, then particle physics can provide models which predict the correct relic density of the universe. In particular, the lightest supersymmetric particle, typically the lightest neutralino, is an excellent dark matter particle candidate [289]. Within the MSSM, the measured relic density places constraints in the parameter space, which in turn - for specific SUSY low energy spectra- have implications for Higgs searches at colliders, and also for experiments looking for direct evidence of dark matter particles in elastic scattering with atomic nuclei. Large values of $\tan\beta$ and small m_A are relevant for the $b\bar{b}A/H$ and $A/H \rightarrow \tau^+\tau^-$ searches at the Tevatron and the LHC, and also provide a significant contribution from the CP -even Higgs H exchange to the spin-independent cross sections for direct detection experiments such as CDMS or Xenon, for example. Consequently, a signal at colliders would raise prospects for a signal in indirect detection experiments and vice-versa [286,288,290–292]. However, there are theoretical uncertainties in the calculation of dark matter scattering cross sections, and in the precise value of the local dark matter density and velocity distributions, which may dilute these model-dependent correlations.

IV. Other Model Extensions

There are many ways to extend the minimal Higgs sector of the Standard Model. In the preceding sections we have considered the phenomenology of the MSSM Higgs sector⁵, which at tree level is a constrained Type-II 2HDM (with restrictions on the Higgs boson masses and couplings). One can consider general Type-II 2HDMs [13,44,162], with no correlations between masses and couplings, or Type-I 2HDMs [163]. The different patterns of Higgs-fermion couplings in each case will lead to different phenomenology. It is also possible to consider models with a SM Higgs boson and one or more additional scalar SU(2) doublets that acquire no vacuum expectation value (vev) and hence play no role in the EWSB mechanism. These models are dubbed Inert Higgs Doublet Models [293]. Due to the lack of vev, the inert Higgs bosons cannot decay into a pair of gauge bosons, and imposing a Z_2 symmetry that prevents them from coupling to the fermions it follows that if the lightest inert Higgs boson is neutral it becomes a good dark matter candidate with interesting associated collider signals.

Other extensions of the Higgs sector can include [15,164] multiple copies of SU(2)_L doublets, additional Higgs singlets, triplets or more complicated combinations of Higgs multiplets. It is also possible to enlarge the gauge symmetry beyond SU(2)_L × U(1)_Y along with the necessary Higgs structure to generate gauge boson and fermion masses. There are two main experimental constraints that govern these extensions: (i) precision measurements which constrain $\rho = m_W^2 / (m_Z^2 \cos^2 \theta_W)$ to be very close to 1 and (ii) flavor changing neutral current (FCNC) effects. In electroweak models based on the SM gauge group, the tree-level value of ρ is determined by the Higgs multiplet structure. By suitable choices for the hypercharges, and in some cases the mass splitting between the charged and neutral Higgs sector or the vacuum expectation values of the Higgs fields, it is possible to obtain a richer combination of singlets,

⁵ In the searches for charged Higgs bosons the results are presented for given branching ratio assumptions within a general 2HDM, and then interpreted in the MSSM.

doublets, triplets and higher multiplets compatible with precision measurements [294]. Concerning the constraints coming from FCNC effects, the Glashow-Weinberg theorem [295] states that, in the presence of multiple Higgs doublets the tree-level FCNC's mediated by neutral Higgs bosons will be absent if all fermions of a given electric charge couple to no more than one Higgs doublet. The Higgs doublet models Type-I and Type-II are two different ways of satisfying this theorem. The coupling pattern of these two types can be arranged by imposing either a discrete symmetry or, in the case of Type-II, supersymmetry. The resulting phenomenology of extended Higgs sectors can differ significantly from that of the SM Higgs boson.

In supersymmetry, the most studied extensions of the MSSM have a scalar singlet and its supersymmetric partner [296–298]. These models have an extended Higgs sector with two additional neutral scalar states, one CP -even and one CP -odd, beyond those present in the MSSM. In these models, the tree-level bound on the lightest Higgs boson, considering arguments of perturbativity of the theory up to the GUT scale, is about 100 GeV. The radiative corrections to the masses are similar to those in the MSSM and yield an upper bound of about 145 GeV for the mass of the lightest neutral CP -even scalar, for stop masses in the TeV range [16,299]. The couplings of the Higgs bosons to the gauge bosons and fermions are weakened somewhat from mixing with the singlet and this can alter significantly the Higgs phenomenology with respect to the MSSM case.

Another extension of the MSSM which can raise the value of the lightest Higgs boson mass to a few hundred GeV is based on gauge extensions of the MSSM [17,18]. The addition of asymptotically-free gauge interactions naturally yields extra contributions to the quartic Higgs couplings. These extended gauge sector models can be combined with the presence of extra singlets or replace the singlet with a pair of triplets [19].

It is also possible that the MSSM is the low energy effective field theory of a more fundamental SUSY theory that includes additional particles with masses at or somewhat above the TeV range, and that couple significantly to the MSSM Higgs sector.

A model-independent analysis of the spectrum and couplings of the MSSM Higgs fields, based on an effective theory of the MSSM degrees of freedom has been studied [18,20,21,300]. In these scenarios the tree-level mass of the lightest CP-even state can easily be above the LEP bound of 114 GeV, thus allowing for a relatively light spectrum of superpartners, restricted only by direct searches. The Higgs spectrum and couplings can be significantly modified compared to the MSSM ones, often allowing for interesting new decay modes. It is also possible to moderately enhance the gluon fusion production cross section of the SM-like Higgs with respect to both the Standard Model and the MSSM.

Many non-SUSY solutions to the problem of electroweak symmetry breaking and the hierarchy problem are being developed. For example, Little Higgs models [25–27] propose additional sets of heavy vector-like quarks, gauge bosons, and scalar particles, with masses in the 100 GeV to a few TeV range. The couplings of the new particles are tuned in such a way that the quadratic divergences induced in the SM by the top, gauge-boson and Higgs loops are canceled at the one-loop level. If the Little Higgs mechanism successfully resolves the hierarchy problem, it should be possible to detect some of these new states at the LHC. For reviews of models and phenomenology, and a more complete list of references, see Refs. [301–303].

In Little Higgs models the production and decays of the Higgs boson are modified. For example, when the dominant production mode of the Higgs is through gluon fusion, the contribution of new fermions in the loop diagrams involved in the effective ϕgg vertex can reduce the production rate. The rate is generally suppressed relative to the SM rate due to the symmetries which protect the Higgs boson mass from quadratic divergences at the one-loop level. As a result, the branching ratio of the Higgs boson to photon pairs can be enhanced in these models [304]. By design, Little Higgs models are valid only up to a scale $\Lambda \sim 5\text{-}10$ TeV. The new physics which would enter above Λ remains unspecified, and will impact the Higgs sector. In general, it can modify Higgs couplings

to third-generation fermions and gauge bosons, though these modifications are suppressed by $1/\Lambda$ [305].

Distinctive features in the Higgs phenomenology of Little Higgs models may also stem from the fact that loop-level electroweak precision bounds on models with a tree-level custodial symmetry allows for a Higgs boson heavier than the one permitted by precision electroweak fits in the SM. This looser bound follows from a cancellation of the effects on the ρ parameter of a higher mass Higgs boson and the heavy partner of the top quark. The Higgs boson can have a mass as high as 800-1000 GeV in some Little Higgs models and still be consistent with electroweak precision data [306]. Lastly, the scalar content of a Little Higgs structure is model dependent. There could be two, or even more scalar doublets in a little Higgs model, or even different representations of the electroweak gauge group [26].

Models of extra space dimensions present an alternative way of avoiding the hierarchy problem [28]. New states, known as Kaluza-Klein (KK) excitations, can appear at the TeV scale, where gravity-mediated interactions may become relevant. They share the quantum numbers of the graviton and/or SM particles. In a particular realization of these models, based on warped extra dimensions, a light Higgs-like particle, the radion, may appear in the spectrum [307]. The mass of the radion, as well as its possible mixing with the light Higgs boson, depends strongly on the mechanism that stabilizes the extra dimension, and on the curvature-Higgs mixing.

The radion couples to the trace of the energy-momentum tensor of the SM particles, leading to effective interactions with quarks, leptons, and weak gauge bosons which are similar to the ones of the Higgs boson, although they are suppressed by the ratio of the weak scale to the characteristic mass of the new excitations. An important characteristic of the radion is its enhanced coupling to gluons. Therefore, if it is light and mixes with the Higgs boson, it may modify the standard Higgs phenomenology at lepton and hadron colliders. A search for the radion conducted by OPAL at LEP gave negative results [308]. Radion masses below 58 GeV are excluded for the mass eigenstate which becomes the Higgs boson in the

no-mixing limit, for all parameters of the Randall-Sundrum model. Most recently there has been a study of the effects of radion-Higgs mixing in Higgs boson searches at the LHC [309].

In models of warped extra dimensions in which the SM particles propagate in the extra dimensions, the KK excitations of the vector-like fermions may be pair-produced at colliders and decay into combinations of two Higgs bosons and jets, or one Higgs boson, a gauge boson, and jets. KK excitations may also be singly-produced. Some of these interesting possible new signatures for SM-like Higgs bosons in association with top or bottom quarks have been studied [27,29]. Most interesting, in models with warped extra dimensions the Kaluza-Klein excitations of the quarks and leptons which can be exchanged as virtual particles in the loops, can significantly change the Higgs production via gluon fusion, as well as its decay into diphotons. These results may depend on the precise localization of the SM-like Higgs in the extra dimension as well as on the precise particle content of the models. There are many studies in the literature that address these issues and compute the effects on the Higgs phenomenology [27,310].

Models of flat extra dimensions, in which SM particles propagate in the extra dimensions, are named Universal Extra Dimensions (UED) [311]. In such models the KK particles affect the Higgs couplings at the 1-loop level. In the minimal UED model, for tree-level masses of the lowest KK particles of order 1 TeV the $gg \rightarrow h$ production rate is increased by $\approx 20\%$ while the $h \rightarrow \gamma\gamma$ decay width is decreased by a factor of $\lesssim 3\%$ [312].

It is also possible to consider a simple description of models in which electroweak symmetry breaking is triggered by a light composite Higgs, which emerges from a strongly-interacting sector as a pseudo-Goldstone boson, by utilizing an effective low-energy Lagrangian approach [31]. Recent studies of the phenomenology relevant for collider searches can be found in Ref. 313.

The Higgs boson can also be a portal to hidden sectors, in particular, the Higgs boson can decay to the particles of a low-mass hidden sector; these models are referred to as hidden

valley models [314,315]. Since a light Higgs boson is a particle with a narrow width, even modest couplings to new states can give rise to a significant modification of Higgs phenomenology through exotic decays. Simple hidden valley models exist in which the Higgs boson decays to an invisible fundamental particle, which has a long lifetime to decay back to SM particles through small mixings with the SM Higgs boson; Ref. 315 describes an example. The Higgs boson may also decay to a pair of hidden valley “v-quarks,” which subsequently hadronize in the hidden sector, forming “v-mesons.” These mesons often prefer to decay to the heaviest state kinematically available, so that a possible signature is $h \rightarrow 4b$. Some of the v-mesons may be stable, implying a mixed missing energy plus heavy flavor final state. In other cases, the v-mesons may decay to leptons, implying the presence of low mass lepton resonances in high H_T events [316]. Other scenarios have been studied [317] in which Higgs bosons decay predominantly into light hidden sector particles, either directly, or through light SUSY states, and with subsequent cascades that increase the multiplicity of hidden sector particles. In such scenarios, the high multiplicity hidden sector particles, after decaying back into the Standard Model, appear in the detector as clusters of collimated leptons known as lepton jets.

If Higgs bosons are not discovered at the Tevatron or the LHC, other studies might be able to test alternative theories of dynamical electroweak symmetry breaking which do not involve a Higgs particle [318].

V. Searches for Higgs Bosons Beyond the MSSM

In extensions of the MSSM with one or more additional scalar singlets, limits have been set at e^+e^- and hadron colliders. The ALEPH [319] and DELPHI [320] collaborations place constraints on such models. Precise LEP 2 bounds on the Higgs boson masses depend on the couplings of the Higgs bosons to the gauge bosons and such couplings tend to be weakened somewhat from mixing with the singlet(s). At hadron colliders, searches for a light pseudoscalar boson predicted by the NMSSM have been performed by DØ [321], CDF [322],

CMS [323], and ATLAS [324]. No significant excesses have been found and limits have been set on these models.

Most of the searches for the processes $e^+e^- \rightarrow hZ$ and hA , which have been discussed in the context of the *CPC*-MSSM, rely on the assumption that the Higgs bosons have a sizable branching ratio to $b\bar{b}$. However, for specific parameters of the MSSM [325], the general 2HDM case, or composite models [175,177,326], decays to non- $b\bar{b}$ final states may be significantly enhanced. Flavor-independent hadronically-decaying Higgs boson searches have been performed at LEP which do not require the experimental signature of a b -jet [327], and a preliminary combination of LEP data has been performed [34,328]. If Higgs bosons are produced at the SM rate and decay only to jets of hadrons, then the 95% C.L. lower limit on the mass of the Higgs boson is 112.9 GeV, independent of the fractions of gluons and b, c, s, u and d -quarks in Higgs boson decay. In conjunction with b -flavor sensitive searches, large domains of the general Type-II 2HDM parameter space have been excluded [329].

In the Type-I 2HDM, if the *CP*-odd neutral Higgs boson A is light (which is not excluded in the general 2HDM case, nor in some extensions of the MSSM), the decay $H^\pm \rightarrow W^{\pm*}A$ may be dominant for masses accessible at LEP, a possibility that was investigated by DELPHI [330] and OPAL [331]. CDF's search for this decay chain in top quark decays [322] may also be interpreted in this scenario.

The LEP collaborations searched for Higgs bosons produced in pairs, in association with Z bosons, b quarks, and τ leptons. The decays considered are $\phi_{i,j} \rightarrow b\bar{b}, \tau^+\tau^-$, and $\phi_j \rightarrow \phi_i\phi_i$, when kinematically allowed, yielding four- b , four- b +jets, six- b and four- τ final states as well as mixed modes with b -quarks and tau leptons. No evidence for a Higgs boson was found [34,224], and mass-dependent coupling limits on a variety of processes, which apply to a large class of models were, set. The limits on the cross sections of Yukawa production of Higgs bosons are typically more than 100 times larger than the SM predictions [224]. Limits on pair-produced Higgs bosons extend up to $m_{\phi_i} + m_{\phi_j}$ in the range 140- 200 GeV for full-strength

production, assuming $b\bar{b}$ and $\tau^+\tau^-$ decays. Limits on Higgs-strahlung production with subsequent decay of the Higgs into lighter Higgs pairs exclude Higgs masses of the Higgs produced in association with the Z up to 114 GeV, if the lighter Higgs bosons decay to $b\bar{b}$. Weaker limits are set if the lighter Higgs pair decays to four tau leptons, or to a mixture of tau leptons and b quarks [34].

Decays of Higgs bosons into invisible (weakly-interacting and neutral) particles may occur in many models⁶. For example, Higgs bosons might decay into pairs of Goldstone bosons or Majorons [332]. In the process $e^+e^- \rightarrow hZ$, the mass of the invisible Higgs boson can be inferred from the kinematics of the reconstructed Z boson by using the beam energy constraint. Results from the LEP experiments can be found in Refs. [219] and [333]. A preliminary combination of LEP data yields a 95% C.L. lower bound of 114.4 GeV for the mass of a Higgs boson, if it is produced with SM production rate, and if it decays exclusively into invisible final states [334].

OPAL's decay-mode independent search for $e^+e^- \rightarrow S^0Z$ [80] provides sensitivity to arbitrarily-decaying scalar particles, as only the recoiling Z boson decaying into leptons is required to be reconstructed. The energy and momentum constraints provided by the e^+e^- collisions allow the S^0 's four-vector to be reconstructed and limits placed on its production independent of its decay characteristics, allowing sensitivity for very light scalar masses. The limits obtained in this search are less than one-tenth of the SM Higgs-strahlung production rate for $1 \text{ keV} < m_{S^0} < 19 \text{ GeV}$, and less than the SM Higgs-strahlung rate for $m_{S^0} < 81 \text{ GeV}$.

Hidden-valley models predict a rich phenomenology of new particles, some of which can be long-lived and hadronize with SM particles to form exotic particles which decay at measurable distances in collider experiments. CDF and DØ have searched for pair-produced long-lived particles produced resonantly and which decay to $b\bar{b}$ pairs, and set limits on Higgs boson production in hidden-valley models [335,336]. The Higgs boson can

⁶ As discussed above, in the MSSM the Higgs can decay into pairs of lightest, stable neutralinos.

also be the portal to high multiplicity hidden sector particles that may produce multiple charged leptons in the final state. A search for additional leptons in events containing a leptonically decaying W or Z boson by CDF [337] is sensitive to such models and others predicting multi-lepton final states; the results are consistent with SM expectations.

Photonic final states from the processes $e^+e^- \rightarrow Z/\gamma^* \rightarrow H\gamma$ and from $H \rightarrow \gamma\gamma$, could be significantly enhanced, over the SM loop induced effects, in models with anomalous couplings [338]. Searches for the processes $e^+e^- \rightarrow (H \rightarrow b\bar{b})\gamma$, $(H \rightarrow \gamma\gamma)q\bar{q}$, and $(H \rightarrow \gamma\gamma)\gamma$ have been used to set limits on such anomalous couplings [339]. These searches also contribute in the combinations of searches for the standard model Higgs boson, although the small predicted signal rates imply that they contribute less than other channels.

Searches with photonic final states are experimentally very appealing and they have been used to constrain fermiophobic Higgs models, in which the Higgs boson has SM-like properties except that its tree-level couplings to fermions are assumed to be absent or very small. Fermiophobic Higgs models are however quite challenging to construct; they are generally strongly fine-tuned and imply new strong dynamics at low energy scales. A Type-I fermiophobic 2HDM could predict an enhanced $h_f \rightarrow \gamma\gamma$ branching ratio, where h_f denotes a fermiophobic Higgs boson. The LEP searches are described in Ref. 340. In a preliminary combination of LEP data [341], a fermiophobic Higgs boson with mass less than 108.2 GeV (95% C.L.) has been excluded. Fermiophobic models would also predict enhanced branching ratios for the decays $h_f \rightarrow W^*W$ and Z^*Z , a possibility that has been addressed by L3 [342] and ALEPH [343]. At hadron colliders, the process $gg \rightarrow h_f$ has a negligible rate in a fermiophobic Higgs model, but the Wh_f , Zh_f , and VBF production cross sections remain close to their SM predictions and the Higgs boson branching ratios to $\gamma\gamma$, W^+W^- , and ZZ are enhanced. A search for the SM Higgs boson at a hadron collider can not therefore be re-interpreted as a search in a fermiophobic model, even if a limit is set on the total production cross section times a specific decay branching ratio, due to the different

kinematic distributions from the different production modes affecting the signal acceptance. CDF and DØ have re-optimized their $h_f \rightarrow \gamma\gamma$ searches for the fermiophobic model, and with results based on 9.7 fb^{-1} of DØ data [344,345] and 10.0 fb^{-1} of CDF data [346,347], combined with $h_f \rightarrow W^+W^-$ and $h_f \rightarrow ZZ$ searches extend the exclusion in the fermiophobic Higgs model to 119 GeV [110,348]. Other production of fermiophobic Higgs bosons, leading to a 3-photons final state, has also been searched for by DØ [349].

ATLAS and CMS search for a fermiophobic Higgs boson in $h_f \rightarrow \gamma\gamma$ searches optimized for the fermiophobic signature [350,351], and CMS combines these with searches for $h_f \rightarrow W^+W^-$ and $h_f \rightarrow ZZ$ assuming fermiophobic production and decay [10]. CMS excludes a fermiophobic Higgs boson in the range $110 \text{ GeV} < m_H < 188 \text{ GeV}$ at the 95% C.L.

Higgs bosons with double electric charge are predicted, for example, by models with additional triplet scalar fields or left-right symmetric models [352]. It has been emphasized that the see-saw mechanism could lead to doubly-charged Higgs bosons with masses which are accessible to current and future colliders [353]. Searches were performed at LEP for the pair-production process $e^+e^- \rightarrow H^{++}H^{--}$ with four prompt leptons in the final state [354–356]. Lower mass bounds between 95 GeV and 100 GeV were obtained for left-right symmetric models (the exact limits depend on the lepton flavors). Doubly-charged Higgs bosons were also searched for in single production [357]. Furthermore, such particles would modify the Bhabha scattering cross section and forward-backward asymmetry via t -channel exchange. The absence of a significant deviation from the SM prediction puts constraints on the Yukawa coupling of $H^{\pm\pm}$ to electrons for Higgs boson masses which reach into the TeV range [356,357].

Searches have also been carried out at the Tevatron for the pair production process $p\bar{p} \rightarrow H^{++}H^{--}$. The DØ search is performed in the $\mu^+\mu^+\mu^-\mu^-$ final state [358], while CDF also considers $e^+e^+e^-e^-$ and $e^+\mu^+e^-\mu^-$, and final states with τ leptons [359]. A search by CDF for a long-lived $H^{\pm\pm}$ boson, which would decay outside the detector, is described in [360].

CMS has searched for doubly-charged Higgs bosons which are either pair produced, $pp \rightarrow H^{++}H^{--}$ or produced in association with a singly-charged Higgs boson via s -channel W^\pm exchange, $pp \rightarrow H^{++}H^-$, assuming decays of the form $\ell^+\ell'^-$, where ℓ, ℓ' are combinations of e, μ , and τ leptons [361]. No significant excess is seen, and limits on the mass of the doubly-charged Higgs boson vary from 165 GeV to 457 GeV, depending on the production and decay mode. ATLAS has searched for doubly charged Higgs bosons in the dimuon decay [362], setting a limit on the mass of 355 GeV assuming a decay branching ratio to dimuons of 100% and coupling to left-handed fermions, and a limit on the mass of 251 GeV assuming coupling to right-handed fermions.

VI. Outlook

The Tevatron has completed its run and is finalizing its Higgs boson search results with up to 10 fb^{-1} of data analyzed. The combination of the preliminary results from CDF and DØ's searches for the SM Higgs boson shows an excess of data events with respect to the background estimation in the mass range $115 \text{ GeV} < m_H < 135 \text{ GeV}$, dominated by the $H \rightarrow b\bar{b}$ channels. The global significance for such an excess anywhere in the full mass range is 2.2 standard deviations.

In 2011, the LHC delivered approximately 5 fb^{-1} of pp collision data at $\sqrt{s} = 7 \text{ TeV}$. A variety of searches targeting the SM Higgs boson in the mass range $100 \text{ GeV} < m_H < 600 \text{ GeV}$ have been performed, excluding all masses except the range between 114 GeV and 129 GeV. Most of the region below 123 GeV is also excluded by the ATLAS experiment but not by other experiments. Within the allowed mass range, both ATLAS and CMS observe independent excesses of events consistent with a SM-like Higgs boson with a mass of $\approx 125 \text{ GeV}$, with global significances of 1.3σ and 2.1σ , respectively. Both experiments observe excesses of data over the corresponding background predictions in searches for Higgs bosons decaying into diphotons and Z bosons pairs. More data, at $\sqrt{s} = 8 \text{ TeV}$, being collected in 2012, are required to understand this excess. The LHC will either exclude the SM Higgs boson or confirm the existence of a SM-like Higgs particle. In the latter case,

accurate measurements of the properties of the Higgs particle as well as searches for new particles will be of most relevance.

Searches at the LHC for additional Higgs bosons: charged Higgs bosons, doubly charged Higgs bosons, the neutral Higgs bosons of the MSSM, and other exotic Higgs particles, have yielded results consistent with background expectations and strong limits have been placed in significant regions of parameter space. An upgrade of the center of mass energy to 13–14 TeV is planned for the near future. This upgrade will allow the LHC to explore a wide variety of extended Higgs sectors and search for new particles expected in models beyond the SM. This upgrade will also allow for increased precision of measurements of the properties of a SM-like Higgs boson, if one exists.

A high-energy e^+e^- linear collider may be built in the future, allowing ultimate high-precision measurements of the properties of Higgs boson(s) and other particles beyond those of the SM. At a $\mu^+\mu^-$ collider, mass measurements with a precision of a few MeV would be possible, and energy scans may distinguish between signals of Higgs particles nearly degenerate in mass, as predicted in many extended Higgs models.

In the theoretical landscape, numerous models are available with novel approaches to the problem of electroweak symmetry breaking. In the next decade, the LHC’s exploration of the multi-TeV energy scale will solidify our understanding of the mechanism of mass generation of the known elementary particles.

VII. Addendum

Updated July 12, 2012.

On July 4, 2012, the ATLAS and CMS collaborations simultaneously announced observation of a new particle produced in pp collision data at high energies [363–366]. The data samples used correspond to between 4.6 and 5.1 fb^{-1} of collision data collected at $\sqrt{s} = 7$ TeV in 2011, and between 5.3 and 5.9 fb^{-1} of collisions collected at $\sqrt{s} = 8$ TeV in 2012. The observed decay modes indicate that the new particle is a boson. The evidence is strong that the new particle decays to $\gamma\gamma$ and ZZ with rates consistent with those predicted for the Standard Model

(SM) Higgs boson. There are indications that the new particle might also decay to W^+W^- , and decays to $b\bar{b}$ and $\tau^+\tau^-$ are being sought as well.

The ATLAS collaboration has updated its SM Higgs boson searches in the $H \rightarrow \gamma\gamma$ and $H \rightarrow ZZ \rightarrow \ell^+\ell^-\ell'^+\ell'^-$ [367] modes with new data collected at $\sqrt{s} = 8$ TeV and improved analysis techniques applied to both the 7 TeV and 8 TeV data. ATLAS has also finalized its $\sqrt{s} = 7$ TeV analyses in the $H \rightarrow ZZ \rightarrow \ell^+\ell^-\nu\bar{\nu}$, $H \rightarrow ZZ \rightarrow \ell^+\ell^-q\bar{q}$, $H \rightarrow W^+W^- \rightarrow \ell^+\nu_\ell\ell'^-\bar{\nu}_{\ell'}$, $H \rightarrow W^+W^- \rightarrow \ell^+\nu_\ell q\bar{q}'$, $H \rightarrow \tau^+\tau^-$, and $WH, ZH \rightarrow Wb\bar{b}, Zb\bar{b}$ channels [368], and includes them in its SM Higgs boson combined results [369,364]. ATLAS's $H \rightarrow \gamma\gamma$ search has been improved with respect to the previous version by separating events with two jets and two photons from other events, which improves the sensitivity for the vector boson fusion (VBF) process, and by improved photon identification and isolation algorithms. ATLAS's $H \rightarrow ZZ \rightarrow \ell^+\ell^-\ell'^+\ell'^-$ search has been improved with respect to the previous results by re-optimizing the kinematic cuts, improving electron reconstruction and identification efficiency at low p_T , and improved robustness to pileup events.

The CMS collaboration has updated its SM Higgs boson searches in the $H \rightarrow \gamma\gamma$, $H \rightarrow ZZ \rightarrow \ell^+\ell^-\ell'^+\ell'^-$, $H \rightarrow ZZ \rightarrow \ell^+\ell^-\nu\bar{\nu}$, $H \rightarrow W^+W^- \rightarrow \ell^+\nu_\ell\ell'^-\bar{\nu}_{\ell'}$, $H \rightarrow b\bar{b}$, and $H \rightarrow \tau^+\tau^-$ channels, all of which include 8 TeV data collected in 2012 [370]. The $t\bar{t}H \rightarrow t\bar{t}b\bar{b}$ [370] search is new and based on 2011 data. The $H \rightarrow W^+W^- \rightarrow \ell^+\nu_\ell q\bar{q}'$ [370] search is included for the first time in the combination.

CMS's $H \rightarrow \gamma\gamma$ search has been improved with respect to its earlier version by dividing the diphoton plus two jet category into two, depending on the dijet invariant mass and the jet p_T , and also by removing jets from pileup collisions. The $H \rightarrow ZZ \rightarrow \ell^+\ell^-\ell'^+\ell'^-$ search has been improved with respect to its previous version, benefiting from improved lepton identification and isolation algorithms, as well as final state radiation recovery. The discriminant variables used now to separate the expected signal from the backgrounds are two-dimensional, plotting the invariant mass of the four leptons versus a matrix-element-based

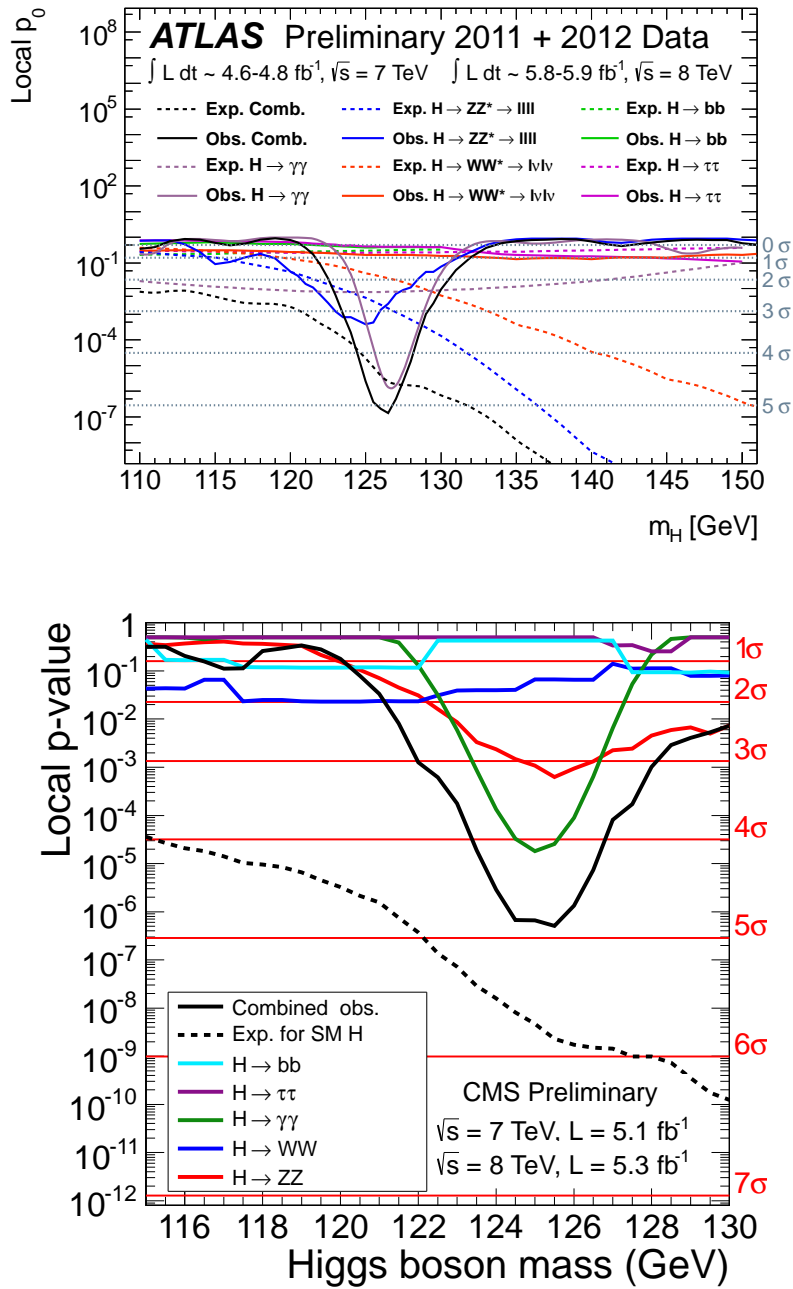


Figure 17: Local p -values for the ATLAS SM Higgs boson search (left), and the CMS SM Higgs boson search (right), separately for each decay mode. The solid lines show the observed p -values and the dashed lines show the median expected p -values, assuming a SM Higgs boson is present, computed at each value of m_H separately.

likelihood discriminant. CMS's $H \rightarrow W^+W^-$ search combines the results from the multivariate analysis (MVA) for the 7 TeV data with the results of a cut-based analysis on the 8 TeV data sample, which is described in Ref. 372. CMS's $VH \rightarrow Vb\bar{b}$ (with $V = W$ or Z) search encompasses five channels: $WH \rightarrow e\nu b\bar{b}$, $WH \rightarrow \mu\nu b\bar{b}$, $ZH \rightarrow e^+e^-b\bar{b}$, $ZH \rightarrow \mu^+\mu^-b\bar{b}$, and $ZH \rightarrow \nu\bar{\nu}b\bar{b}$. CMS's $H \rightarrow \tau^+\tau^-$ search divides the candidate events by tau lepton decay type and subdivides the samples based on number of jets (0,1) or on VBF type. The 0 and 1 jet categories are also further subdivided according to low or high p_T of the τ .

Each experiment, ATLAS and CMS, separately combine their data to obtain independent results of their searches, computing the significance of the observation, measuring the production rates times the decay branching fractions for each channel analyzed, and updating the mass and rate exclusions [364,366]. The separate results provide independent confirmations of the observation. The significance is quantified by a p -value, which is the probability to observe an upward fluctuation of the background which gives a result at least as signal-like as that observed in the data. A p -value of 2.87×10^{-7} corresponds to a five standard deviation excess over the background prediction. The p -values are shown for the analysis channels separately for ATLAS and CMS in Fig. 17. ATLAS observes an excess with a local significance of 5.0σ at a mass $m_H = 126.5$ GeV, with an expected significance of 4.6σ if a SM Higgs boson were present at such mass value. CMS observes an excess with a local significance of 4.9σ at a mass 125.5 GeV, with an expected significance of 5.9σ , and measures the mass of the new boson as $m_H = 125.3 \pm 0.6$ GeV. Fig. 18 shows the best-fit cross sections times the relevant decay branching fractions for the new particle, normalized to the SM predictions for Higgs boson production and decay, assuming it has a mass of 126.5 GeV (ATLAS), and 125 GeV (CMS). ATLAS's combined signal strength fit, assuming SM ratios for the production and decay modes, is $\mu = \sigma/\sigma_{\text{SMH}} = 1.2 \pm 0.3$, and CMS's combined fit is $\mu = 0.80 \pm 0.22$. Within the current experimental uncertainties, the measurements are consistent with SM predictions.

Both ATLAS and CMS separately exclude SM Higgs bosons with masses outside a narrow range near the local excesses.

The Tevatron collaborations updated their Higgs boson search results on July 2, 2012 [373]. The D0 collaboration has updated its $VH \rightarrow Vb\bar{b}$ search results by improving the acceptance of the lepton selection, dividing the events into more categories based on the number and quality of b tags, and improving the MVA treatment [374]. Additional data and analysis improvements also improve the sensitivity of D0's $H \rightarrow W^+W^-$ searches by 5-10% with respect to the previous result [375]. The CDF Higgs boson searches were updated with the full Run II data set and improved b -tagging for the Winter 2012 conferences [376]. CDF and D0 combine their results together, and, with the full suite of SM Higgs boson search analyses, see a broad excess in the range $115 \text{ GeV} < m_H < 135 \text{ GeV}$, with a global signal significance of 2.5σ , and a maximum local significance of 3.0σ . Fig. 19 shows the measured cross sections times the relevant decay branching ratios normalized to those expected for a SM Higgs boson at mass $m_H = 125 \text{ GeV}$ for the combined CDF and D0 searches for $H \rightarrow W^+W^-$, $H \rightarrow \gamma\gamma$, and $VH \rightarrow Vb\bar{b}$ searches. The combined result, assuming SM ratios for the production and decay modes, is $\mu = 1.4 \pm 0.6$. In the dominant decay channel, $VH \rightarrow Vb\bar{b}$, the global significance is 2.9σ , with a maximum local significance of 3.2σ . Assuming the existence of a new particle, this provides the first strong indication for its decay into a fermion pair at a rate consistent with the SM prediction for a Higgs boson of such a mass.

In summary, a new particle has been observed at the LHC. Within the experimental uncertainties, it has characteristics consistent with those expected from the Higgs boson predicted by the Standard Model, with a mass near 125 GeV. Tevatron data also are consistent with the production and decay of a SM-like Higgs boson at this mass. However, the present experimental uncertainties still allow for a wide variety of new physics alternatives.

The LHC will continue to run until early 2013, and it is expected to deliver at least 15 fb^{-1} more data to both ATLAS and CMS, at $\sqrt{s} = 8 \text{ TeV}$. After this run, a shutdown

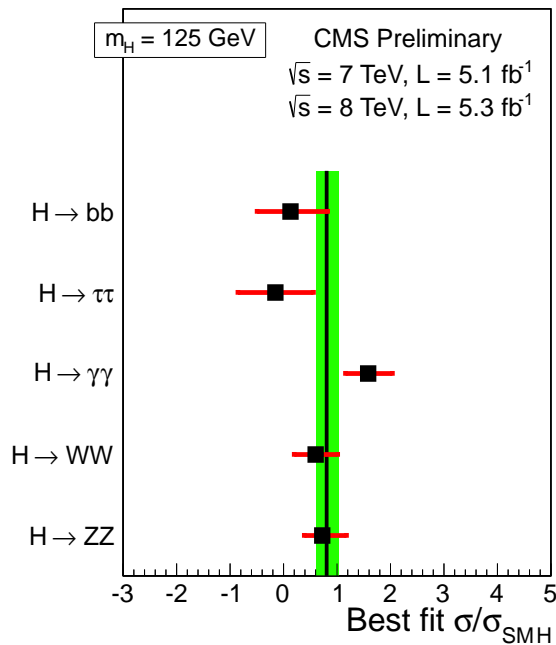
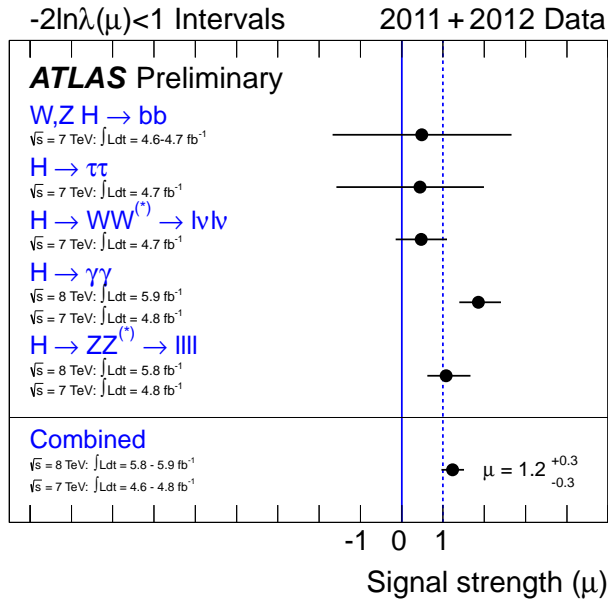


Figure 18: Best-fit production cross sections times branching ratios to $H \rightarrow \gamma\gamma$, $H \rightarrow ZZ$, $H \rightarrow W^+W^-$, $H \rightarrow b\bar{b}$, and $H \rightarrow \tau^+\tau^-$, normalized to the SM predictions for Higgs boson production and decay, assuming it has a mass of 126.5 GeV (ATLAS, left), and 125 GeV (CMS, right). The combined result, assuming SM ratios for the production and decay modes, is shown as a separate point on the ATLAS graph at $\mu = \sigma/\sigma_{\text{SMH}} = 1.2 \pm 0.3$ and is shown with the shaded band on the CMS graph at $\mu = 0.80 \pm 0.22$.

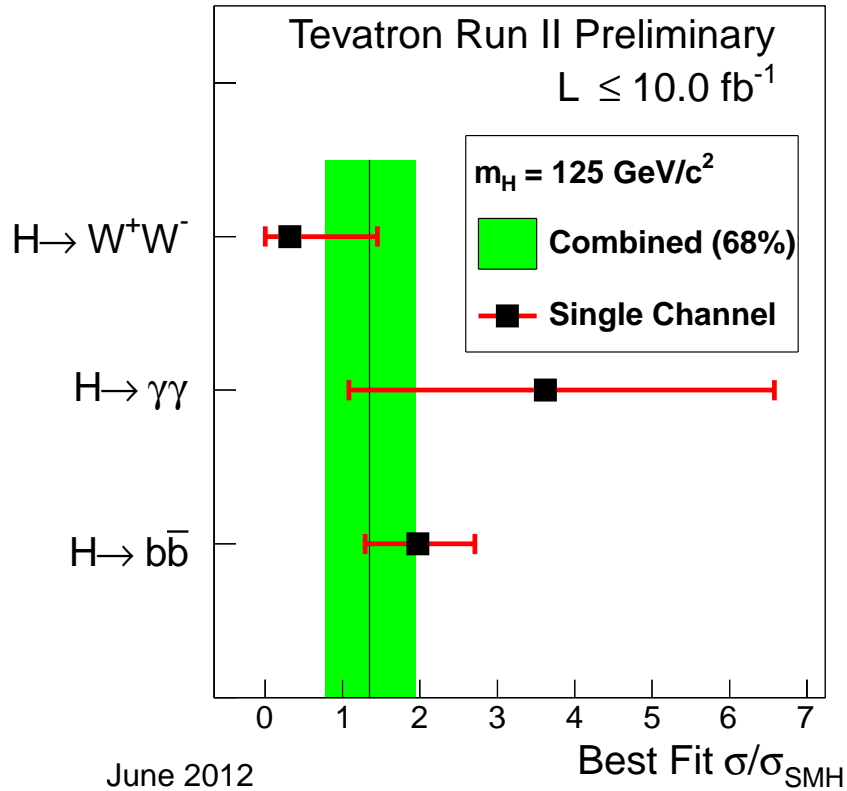


Figure 19: Best-fit cross sections times branching ratios to $H \rightarrow W^+W^-$, $H \rightarrow \gamma\gamma$ and $H \rightarrow b\bar{b}$, normalized to the SM predictions for Higgs boson production and decay, assuming it has a mass of 125 GeV, for the combined CDF and D0 search results. The combined result, assuming SM ratios for the production and decay modes, is shown with a shaded band, at $\mu = \sigma/\sigma_{SMH} = 1.4 \pm 0.6$.

will occur to improve the accelerator components to allow data taking at higher energies. The much larger dataset to be collected will provide the opportunity to make increasingly precise measurements of the properties of the new particle, and test whether it is the SM Higgs boson or point the way to physics beyond the SM.

References

In order to keep this review up to date, some unpublished results are quoted. LEP results are marked with (*) in the reference list and can be accessed conveniently from the public web page <http://lephiggs.web.cern.ch/LEPHIGGS/pdg2008/>. Preliminary results from the CDF Collaboration are marked with (**) and can be obtained from the public web page <http://www-cdf.fnal.gov/physics/physics.html>; those from DØ are marked with (***) and can be obtained at <http://www-d0.fnal.gov/Run2Physics/WWW/results.htm>.

1. P.W. Higgs, Phys. Rev. Lett. **13**, 508 (1964);
idem, Phys. Rev. **145**, 1156 (1966);
F. Englert and R. Brout, Phys. Rev. Lett. **13**, 321 (1964);
G.S. Guralnik, C.R. Hagen, and T.W. Kibble, Phys. Rev. Lett. **13**, 585 (1964).
2. S.L. Glashow, Nucl. Phys. **20**, 579 (1961);
S. Weinberg, Phys. Rev. Lett. **19**, 1264 (1967);
A. Salam, *Elementary Particle Theory*, eds.: Svartholm, Almquist, and Wiksells, Stockholm, 1968;
S. Glashow, J. Iliopoulos, and L. Maiani, Phys. Rev. **D2**, 1285 (1970).
3. J.M. Cornwall, D.N. Levin, and G. Tiktopoulos, Phys. Rev. Lett. **30**, 1286 (1973); Phys. Rev. **D10**, 1145 (1974);
C.H. Llewellyn Smith, Phys. Lett. **B46**, 233 (1973).
4. B.W. Lee, C. Quigg, and H.B. Thacker, Phys. Rev. **D16**, 1519 (1977).
5. LEP Electroweak Working Group, status of March 2012, <http://lepewwg.web.cern.ch/LEPEWWG/>;
The ALEPH, CDF, DØ, DELPHI, L3, OPAL, SLD Collabs., the LEP Electroweak Working Group, the Tevatron Electroweak Working Group, and the SLD Electroweak and Heavy Flavor groups, LEPEWWG/2009-01 (2009);
J. Erler and P. Langacker, *Electroweak Model and Constraints on New Physics*, in this volume.
6. The CDF and DØ Collabs. and the Tevatron New Physics and Higgs Working Group,
[arXiv:1203.3774 \[hep-ex\]](https://arxiv.org/abs/1203.3774) (2012).
7. ATLAS Collab., Phys. Lett. **B710**, 49 (2012).
8. ATLAS Collab., “An update to the combined search for the Standard Model Higgs boson with the ATLAS detector at the LHC using up to 4.9 fb^{-1} of pp collision data at $\sqrt{s} = 7 \text{ TeV}$ ”, ATLAS-CONF-2012-019 (2012).

9. CMS Collab., [arXiv:1202.1488 \[hep-ex\]](#), submitted to Phys. Lett. B (2012).
10. CMS Collab., “Combination of SM, SM4, FP Higgs boson searches”, CMS-PAS-HIG-12-008 (2012).
11. J. Wess and B. Zumino, Nucl. Phys. **B70**, 39 (1974);
idem. Phys. Lett. **49B**, 52 (1974);
 H.P. Nilles, Phys. Rev. **C110**, 1984 (1);
 S.P. Martin, [arXiv:hep-ph/9709356](#) (1997);
 P. Fayet, Phys. Lett. **B69**, 489 (1977);
ibid., **B84**, 421 (1979);
ibid., **B86**, 272 (1979);
idem., Nucl. Phys. **B101**, 81 (2001).
12. H.E. Haber and G.L. Kane, Phys. Rev. **C117**, 75 (1985).
13. J.F. Gunion *et al.*, *The Higgs Hunter’s Guide*, Addison-Wesley (1990).
14. A detailed discussion and list of references is given in subsection III.
15. E. Accomando, *et al.*, [hep-ph/0608079](#).
16. U. Ellwanger and C. Hugonie, Mod. Phys. Lett. **A22**, 1581 (2007).
17. P. Batra *et al.*, JHEP **0402**, 043 (2004);
 P. Batra *et al.*, JHEP **0406**, 032 (2004).
18. M. Dine, N. Seiberg, and S. Thomas, Phys. Rev. **D76**, 095004 (2007) and refs. therein.
19. J.R. Espinosa and M. Quirós, Phys. Rev. Lett. **81**, 516 (1998).
20. M. Carena *et al.*, Phys. Rev. **D81**, 015001 (2010);
 W. Altmannshofer *et al.*, Phys. Rev. **D84**, 095027 (2011).
21. I. Antoniadis *et al.*, Nucl. Phys. **B831**, 133 (2010).
22. L.E. Ibáñez and G.G. Ross, Phys. Lett. **B105**, 439 (1981);
 S. Dimopoulos, S. Raby, and F. Wilczek, Phys. Rev. **D24**, 1681 (1981);
 M.B. Einhorn and D.R.T. Jones, Nucl. Phys. **B196**, 475 (1982);
 W.J. Marciano and G. Senjanovic, Phys. Rev. **D25**, 3092 (1982).
23. J. Ellis, S. Kelley and D.V. Nanopoulos, Phys. Lett. **B249**, 441 (1990);
 P. Langacker and M. Luo, Phys. Rev. **D44**, 817 (1991);
 U. Amaldi, W. de Boer, and H.Fürstenau, Phys. Lett. **B260**, 447 (1991);
 P. Langacker and N. Polonsky, Phys. Rev. **D52**, 3081

- (1995);
 S. Pokorski, *Act. Phys. Pol.* **B30**, 1759 (1999);
 For a recent review, see R.N. Mohapatra, in *Particle Physics 1999, Proceedings of the ICTP Summer School in Particle Physics*, Trieste, Italy, 21 June–9 July, 1999, edited by G. Senjanovic and A.Yu. Smirnov. (World Scientific, Singapore, 2000) pp. 336–394.
24. S. Weinberg, *Phys. Rev.* **D13**, 974 (1979); *Phys. Rev.* **D19**, 1277 (1979);
 L. Susskind, *Phys. Rev.* **D20**, 2619 (1979);
 E. Farhi and L. Susskind, *Phys. Rev.* **74**, 277 (1981);
 R.K. Kaul, *Rev. Mod. Phys.* **55**, 449 (1983);
 C. T. Hill and E. H. Simmons, *Phys. Reports* **381**, 235 (2003) [E: *ibid.*, **390**, 553 (2004)].
25. N. Arkani-Hamed, A.G. Cohen, and H. Georgi, *Phys. Lett.* **B513**, 232 (2001);
 N. Arkani-Hamed *et al.*, *JHEP* **0207**, 034 (2002);
 N. Arkani-Hamed *et al.*, *JHEP* **0208**, 020 (2002);
 N. Arkani-Hamed *et al.*, *JHEP* **0208**, 021 (2002);
 I. Low and A. Vichi, *Phys. Rev.* **D84**, 045019 (2011);
 A. Azatov and J. Galloway, *Phys. Rev.* **D85**, 055013 (2012).
26. I. Low, W. Skiba, and D. Smith, *Phys. Rev.* **D66**, 072001 (2002).
27. A. Falkowski, *Phys. Rev.* **D77**, 055018 (2008).
28. I. Antoniadis, *Phys. Lett.* **B246**, 377 (1990);
 N. Arkani-Hamed, S. Dimopoulos, and G.R. Dvali, *Phys. Lett.* **B429**, 263 (1998);
 L. Randall and R. Sundrum, *Phys. Rev. Lett.* **83**, 3370 (1999) *idem*, **84**, 4690 (1999);
 G.F. Giudice *et al.*, *Nucl. Phys.* **B544**, 3 (1999);
 C. Csáki *et al.*, *Phys. Rev.* **D63**, 065002 (2001).
29. J.A. Aguilar-Saavedra, *JHEP* **0612**, 033 (2006);
 M. Carena *et al.*, *Phys. Rev.* **D76**, 035006 (2007);
 A.D. Medina, N. R. Shah, and C.E.M. Wagner, *Phys. Rev.* **D76**, 095010 (2007);
 A. Djouadi and G. Moreau, *Phys. Lett.* **B660**, 67 (2008);
 H. Davoudiasl, B. Lillie, and T.G. Rizzo, *JHEP* **0608**, 042 (2006);
 R. Contino, Y. Nomura, and A. Pomarol, *Nucl. Phys.* **B671**, 148 (2003);
 K. Agashe, R. Contino, and A. Pomarol, *Nucl. Phys.* **B719**, 165 (2005);
 R. Contino, L. Da Rold, and A. Pomarol, *Phys. Rev.* **D75**, 055014 (2007).

30. M. Carena, E. Ponton, and J. Zurita, Phys. Rev. **D82**, 055025 (2010);
M. Carena, E. Ponton, and J. Zurita, Phys. Rev. **D85**, 035007 (2012).
31. G.F. Giudice *et al.*, JHEP **0706**, 045 (2007);
R. Contino *et al.*, JHEP **1005**, 089 (2010);
J.R. Espinosa, C. Grojean, and M. Mühlleitner, JHEP **1005**, 065 (2010);
J.R. Espinosa, C. Grojean, and M. Mühlleitner, arXiv:1202.1286 [hep-ph] (2012);
G. Panico and A. Wulzer, JHEP **1109**, 135 (2011);
S. De Curtis, M. Redi, and A. Tesi, JHEP **1204**, 042 (2012);
R. Contino *et al.*, JHEP **1110**, 081 (2011);
A. Azatov, R. Contino, and J. Galloway, JHEP **1204**, 127 (2012).
32. P.J. Franzini and P. Taxil, in *Z physics at LEP 1*, CERN 89-08 (1989).
33. ALEPH, DELPHI, L3, and OPAL Collabs., The LEP Working Group for Higgs Boson Searches, Phys. Lett. **B565**, 61 (2003).
34. ALEPH, DELPHI, L3 and OPAL Collabs., The LEP Working Group for Higgs Boson Searches, Eur. Phys. J. **C47**, 547 (2006).
35. T. van Ritbergen and R. G. Stuart, Phys. Rev. Lett. **82**, 488 (1999);
T. van Ritbergen and R. G. Stuart, Nucl. Phys. **B564**, 343 (2000);
M. Steinhauser and T. Seidensticker, Phys. Lett. **B467**, 271 (1999);
D. M. Webber *et al.*, Phys. Rev. Lett. **106**, 041803 (2011).
36. N. Cabibbo *et al.*, Nucl. Phys. **B158**, 295 (1979);
G. Altarelli and G. Isidori, Phys. Lett. **B337**, 141 (1994);
J.A. Casas, J.R. Espinosa, and M. Quirós, Phys. Lett. **B342**, 171 (1995);
idem., Phys. Lett. **B382**, 374 (1996);
T. Hambye and K. Riessellmann, Phys. Rev. **D55**, 7255 (1997).
37. J.R. Espinosa and M. Quirós, Phys. Lett. **B353**, 257 (1995);
G. Isidori *et al.*, Nucl. Phys. **B609**, 387 (2001).
38. J. Elias-Miró *et al.*, Phys. Lett. **B709**, 222 (2012).
39. B.A. Kniehl, Phys. Rept. **240**, 211 (1994).

40. A. Denner *et al.*, Eur. Phys. J. **C71**, 1753 (2011);
A. Djouadi, J. Kalinowski, and M. Spira, Comput. Phys. Commun. **108**, 56 (1998);
A. Djouadi *et al.*, arXiv:1003.1643 [hep-ph] (2010);
A. Bredenstein *et al.*, Phys. Rev. **D74**, 013004 (2006);
A. Bredenstein *et al.*, JHEP **0702**, 80 (2007);
S. Actis *et al.*, Nucl. Phys. **B811**, 182 (2009);
D. Bardin, B. Vilensky, and P. Khristova, Sov. J. Nucl. Phys. **53**, 152 (1991);
A. Dabelstein and W. Hollik, Z. Phys. **C53**, 507 (1992);
B.A. Kniehl, Nucl. Phys. **B376**, 3 (1992);
S.G. Gorishniĭ, A.L. Kataev, and S.A. Larin, Sov. J. Nucl. Phys. **40**, 329 (1984) [Yad. Fiz. **40**, 517 (1984)];
S.G. Gorishniĭ *et al.*, Phys. Rev. **D43**, 1633 (1991);
K.G. Chetyrkin, Phys. Lett. **B390**, 309 (1997);
K.G. Chetyrkin and M. Steinhauser, Phys. Lett. **B408**, 320 (1997);
E. Braaten and J.P. Leveille, Phys. Rev. **D22**, 715 (1980);
N. Sakai, Phys. Rev. **D22**, 2220 (1980);
T. Inami and T. Kubota, Nucl. Phys. **B179**, 171 (1981);
M. Drees and K. Hikasa, Phys. Lett. **B240**, 455 (1990) [E: **B262** 497 (1991)];
M. Drees and K. Hikasa, Phys. Rev. **D41**, 1547 (1990);
R. Harlander and M. Steinhauser, Phys. Rev. **D56**, 3980 (1997);
A. Ghinculov, Phys. Lett. **B337**, 137 (1994);
L. Durand, K. Riesselmann, and B.A. Kniehl, Phys. Rev. Lett. **72**, 2534 (1994);
K. Melnikov and O.I. Yakovlev, Phys. Lett. **B312**, 179 (1993);
M. Inoue *et al.*, Mod. Phys. Lett. **A9**, 1189 (1994);
U. Aglietti *et al.*, JHEP **0701**, 021 (2007);
K.G. Chetyrkin, B.A. Kniehl, and M. Steinhauser, Phys. Rev. Lett. **79**, 353 (1997);
P.A. Baikov and K.G. Chetyrkin, Phys. Rev. Lett. **97**, 061803 (2006);
A. Ghinculov, Nucl. Phys. **B455**, 21 (1995);
A. Frink *et al.*, Phys. Rev. **D54**, 4548 (1996);
E. Gross *et al.*, Z. Phys. **C63**, 417 (1994); [E: *ibid.*, **C66**, 32 (1995)];
A.L. Kataev, Sov. Phys. JETP Lett. **66**, 327 (1997) [Pis'ma Zh. Éksp. Teor. Fiz. **66** (1997) 308].
41. A. Djouadi, M. Spira, and P.M. Zerwas, Z. Phys. **C70**, 675 (1996).
42. M. Spira *et al.*, Nucl. Phys. **B453**, 17 (1995).

43. S. Dittmaier *et al.*, [LHC Higgs Cross Section Working Group], [arXiv:1201.3084](https://arxiv.org/abs/1201.3084) [hep-ph] (2012).
44. M. Carena and H.E. Haber, *Prog. in Part. Nucl. Phys.* **50**, 152 (2003).
45. A. Djouadi, *Phys. Reports* **457**, 1 (2008).
46. J. Ellis, M.K. Gaillard, and D.V. Nanopoulos, *Nucl. Phys.* **B106**, 292 (1976);
B.L. Ioffe and V.A. Khoze. *Sov. J. Nucl. Phys.* **9**, 50 (1978).
47. D.R.T. Jones and S. Petcov, *Phys. Lett.* **B84**, 440 (1979);
R.N. Cahn and S. Dawson, *Phys. Lett.* **B136**, 196 (1984);
G.L. Kane, W.W. Repko, and W.B. Rolnick, *Phys. Lett.* **B148**, 367 (1984);
G. Altarelli, B. Mele, and F. Pitolli. *Nucl. Phys.* **B287**, 205 (1987);
W. Kilian, M. Krämer, and P.M. Zerwas, *Phys. Lett.* **B373**, 135 (1996).
48. B.A. Kniehl, *Z. Phys.* **C55**, 605 (1992).
49. J. Fleischer and F. Jegerlehner, *Nucl. Phys.* **B216**, 469 (1983);
A. Denner *et al.*, *Z. Phys.* **C56**, 261 (1992).
50. B.A. Kniehl, *Int. J. Mod. Phys.* **A17**, 1457 (2002).
51. K.J. Gaemers and G.J. Gounaris, *Phys. Lett.* **B77**, 379 (1978);
A. Djouadi, J. Kalinowski, and P. M. Zerwas, *Z. Phys.* **C54**, 255 (1992);
B.A. Kniehl, F. Madricardo, and M. Steinhauser, *Phys. Rev.* **D66**, 054016 (2002).
52. S. Dittmaier *et al.*, *Phys. Lett.* **B441**, 383 (1998);
S. Dittmaier *et al.*, *Phys. Lett.* **B478**, 247 (2000);
S. Dawson and L. Reina, *Phys. Rev.* **D59**, 054012 (1999).
53. A. Djouadi, M. Spira, and P.M. Zerwas, *Phys. Rev.* **B264**, 440 (1991);
S. Dawson, *Nucl. Phys.* **B359**, 283 (1991);
R.V. Harlander and W.B. Kilgore, *Phys. Rev. Lett.* **88**, 201801 (2002);
C. Anastasiou and K. Melnikov, *Nucl. Phys.* **B646**, 220 (2002);
V. Ravindran, J. Smith, and W.L. van Neerven, *Nucl. Phys.* **B665**, 325 (2003).
54. S. Actis *et al.*, *Phys. Lett.* **B670**, 12 (2008);
U. Aglietti *et al.*, *Phys. Lett.* **B595**, 432 (2004);
G. Degrossi and F. Maltoni, *Phys. Lett.* **B600**, 255 (2004).

55. C. Anastasiou, R. Boughezal, and F. Petriello, JHEP **0904**, 003 (2009).
56. M. Kramer, E. Laenen, and M. Spira, Nucl. Phys. **B511**, 523 (1998);
Chetyrkin et al, Nucl. Phys. **B510**, 61 (1998);
S. Catani *et al.*, JHEP **0307**, 028 (2003);
S. Moch and A. Vogt, Phys. Lett. **B631**, 48 (2005);
E. Laenen and L. Magnea, Phys. Lett. **B632**, 270 (2006);
A. Idilbi *et al.*, Phys. Rev. **D73**, 077501 (2006);
V. Ravindran, Nucl. Phys. **B764**, 291 (2006).
57. D. de Florian and M. Grazzini, Phys. Lett. **B674**, 291 (2009).
58. V. Ahrens *et al.*, Phys. Rev. **D79**, 033013 (2009);
V. Ahrens *et al.*, Eur. Phys. J. **C62**, 333 (2009).
59. V. Ahrens *et al.*, Phys. Lett. **B698**, 271 (2011).
60. C.R. Schmidt, Phys. Lett. **B413**, 391 (1997).
61. D. de Florian, M. Grazzini, and Z. Kunszt, Phys. Rev. Lett. **82**, 5209 (1999).
62. Nucl. Phys. **B634**, 247 (2002).
63. C.J. Glosser and C. R. Schmidt, JHEP **0212**, 016 (2002).
64. J.M. Campbell, R.K. Ellis, and G. Zanderighi, JHEP **0610**, 028 (2006).
65. J.M. Campbell, R.K. Ellis, and C. Williams, Phys. Rev. **D81**, 074023 (2010).
66. S L. Glashow, D.V. Nanopoulos, and A. Yildiz, Phys. Rev. **D18**, 1724 (1978);
T. Han and S. Willenbrock, Phys. Lett. **B273**, 167 (1991);
T. Han, G. Valencia, and S. Willenbrock, Phys. Rev. Lett. **69**, 3274 (1992).
67. A. Stange, W. Marciano, and S. Willenbrock, Phys. Rev. **D49**, 1354 (1994).
68. A. Stange, W. Marciano, and S. Willenbrock, Phys. Rev. **D50**, 4491 (1994).
69. K.A. Assamagan *et al.*, arXiv:hep-ph/0406152 (2004).
70. O. Brein, A. Djouadi, and R. Harlander, Phys. Lett. **B579**, 149 (2004);
M.L. Ciccolini, S. Dittmaier, and M. Krämer, Phys. Rev. **D68**, 073003 (2003);
J. Baglio and A. Djouadi, J. High Energy Phys. **1010**, 064 (2010);
G. Ferrera, M. Grazzini, and F. Tramontano, Phys. Rev. Lett. **107**, 152003 (2011);

- A. Denner *et al.*, JHEP **1203**, 075 (2012);
O. Brein *et al.*, Eur. Phys. J. **C72**, 1868 (2012).
71. T. Figy, S. Palmer, and G. Weiglein, JHEP **1202**, 105 (2012);
P. Bolzoni *et al.*, Phys. Rev. Lett. **105**, 011801 (2010);
M. Ciccolini, A. Denner, and S. Dittmaier, Phys. Rev. Lett. **99**, 161803 (2007);
Ciccolini, A. Denner, and S. Dittmaier, Phys. Rev. **D77**, 103002 (2008);
T. Han, G. Valencia, and S. Willenbrock, Phys. Rev. Lett. **69**, 3274 (1992);
E.L. Berger, J. Campbell, Phys. Rev. **D70**, 073011 (2004);
T. Figy, C. Oleari, and D. Zeppenfeld, Phys. Rev. **D68**, 073005 (2003).
72. W. Beenakker *et al.*, Phys. Rev. Lett. **87**, 201805 (2001);
L. Reina and S. Dawson, Phys. Rev. Lett. **87**, 201804 (2001);
S. Dawson *et al.*, Phys. Rev. **D67**, 071503 (2003);
W. Beenakker *et al.*, Nucl. Phys. **B653**, 151 (2003).
73. R.V. Harlander and W.B. Kilgore, Phys. Rev. **D68**, 013001 (2003);
J. Campbell *et al.*, Phys. Rev. **D67**, 095002 (2003);
S. Dawson *et al.*, Phys. Rev. Lett. **94**, 031802 (2005);
S. Dittmaier, M. Krämer, and M. Spira, Phys. Rev. **D70**, 074010 (2004);
S. Dawson *et al.*, Phys. Rev. **D69**, 074027 (2004).
74. W.J. Stirling and D.J. Summers, Phys. Lett. **B283**, 411 (1992);
F. Maltoni *et al.*, Phys. Rev. **D64**, 094023 (2001).
75. For a compilation of theoretical results for SM and MSSM Higgs cross sections at the LHC see:
<https://twiki.cern.ch/twiki/bin/view/LHCPhysics/CrossSections>.
For the SM Higgs production via gluon fusion using renormalization group improved predictions see:
<http://rghiggs.hepforge.org/>.
The text of this review describes recent updates.
76. S. Dittmaier *et al.*, [LHC Higgs Cross Sections Working Group], arXiv:1101.0593 [hep-ph] (2011).
77. The CDF and DØ Collabs. and the Tevatron Electroweak Working Group, *Combination of the CDF and DØ Results on the Mass of the Top Quark Using up to 5.8 fb⁻¹ of Data*, arXiv:1107.5255 [hep-ex] (2011).

78. P. Janot, *Searching for Higgs Bosons at LEP 1 and LEP 2*, in *Perspectives in Higgs Physics II*, World Scientific, ed. G.L. Kane (1998).
79. See the Review on *Statistics* in this volume.
80. OPAL Collab., *Eur. Phys. J.* **C27**, 311 (2003).
81. CDF Collab., *Phys. Rev.* **D85**, 052002 (2012).
82. DØ Collab., *Phys. Rev. Lett.* **102**, 051803 (2009).
83. (**) CDF Collab., CDF Note 10796, “Search for Standard Model Higgs Boson Production in Association with a W^\pm Boson with 9.45 fb^{-1} of CDF Data”, (2012).
84. (***) DØ Collab., DØ Note 6309-CONF, “Search for Higgs boson in final states with lepton, missing energy, and at least two jets using b-jet identification in 9.7 fb^{-1} of Tevatron data” (2012).
85. (***) DØ Collab., DØ Note 5977-CONF, “Search for the standard model Higgs boson in the $WH \rightarrow \tau\nu b\bar{b}$ channel with 4.0 fb^{-1} of $p\bar{p}$ collisions at $\sqrt{s} = 1.96 \text{ TeV}$ ” (2009).
86. CDF Collab., *Phys. Rev. Lett.* **104**, 141801 (2010).
87. DØ Collab., *Phys. Rev. Lett.* **104**, 071801 (2010).
88. (**) CDF Collab., CDF Note 10798, “Search for the SM Higgs boson in the $\cancel{E}_T + b$ -jets signature with relaxed kinematic cuts in 9.45 fb^{-1} of data at CDF” (2012).
89. (***) DØ Collab., DØ Note 6299-CONF, “Search for the Standard-Model Higgs Boson in the $ZH \rightarrow \nu\bar{\nu} b\bar{b}$ Channel in 9.5 fb^{-1} of $p\bar{p}$ Collisions at $\sqrt{s} = 1.96 \text{ TeV}$ ” (2012).
90. CDF Collab., *Phys. Rev.* **D80**, 071101 (2009);
CDF Collab., *Phys. Rev. Lett.* **105**, 251802 (2010).
91. DØ Collab., *Phys. Lett.* **B655**, 209 (2007).
92. (**) CDF Collab., CDF Note 10799, “A Search for the Standard Model Higgs Boson in the Process $ZH \rightarrow \ell^+\ell^- b\bar{b}$ Using 9.45 fb^{-1} of CDF II Data” (2012).
93. (***) DØ Collab., DØ Note 6296-CONF, “Search for $ZH \rightarrow \ell^+\ell^- b\bar{b}$ production in 9.7 fb^{-1} of $p\bar{p}$ collisions” (2012).
94. CDF Collab., *Phys. Rev.* **D84**, 052010 (2011).
95. (**) CDF Collab., CDF Note 10792, “A search for the Higgs Boson in the All Hadronic Channel using 9.45 fb^{-1} of CDF data” (2012).
96. (**) CDF Collab., CDF Note 10805, “Evidence for WZ and ZZ production in final states with b -tagged jets at CDF” (2012).

97. (***) DØ Collab., DØ Note 6260-CONF, “Evidence for WZ and ZZ production in final states with b -tagged jets” (2011).
98. The CDF and DØ Collabs. and the Tevatron New Physics and Higgs Working Group, [arXiv:1203.3782 \[hep-ex\]](#) (2012).
99. CDF Collab., [arXiv:1201.4880 \[hep-ex\]](#), submitted to Phys. Rev. Lett (2012).
100. (**) CDF Collab., CDF Note 10625, “Search for the Standard Model Higgs Boson in $\tau^+\tau^-$ +jets final state with 8.3 fb^{-1} of CDF Data” (2012).
101. DØ Collab., Phys. Rev. Lett. **102**, 251801 (2009).
102. (***) DØ Collab., DØ Note 6305-CONF, “Search for the standard model Higgs boson in tau lepton pair final states” (2012).
103. CDF Collab., Phys. Rev. Lett. **108**, 011801 (2012).
104. (**) CDF Collab., CDF Note 10737, “Search for a Standard Model Higgs Boson Decaying Into Photons at CDF Using 10.0 fb^{-1} of Data” (2012).
105. DØ Collab., Phys. Rev. Lett. **102**, 231801 (2009).
106. (***) DØ Collab., DØ Note 6295-CONF, “Search for the Standard Model Higgs Boson in $\gamma\gamma + X$ final states at DØ using 9.7 fb^{-1} data” (2012).
107. (**) CDF Collab., CDF Note 10801, “Search for the Higgs Boson Produced in Association with Top Quarks using 9.4 fb^{-1} ” (2012).
108. (**) CDF Collab., CDF Note 10582, “Search for SM Higgs boson production in association with $t\bar{t}$ using no lepton final state” (2011).
109. CDF Collab., Phys. Rev. Lett. **104**, 061803 (2010).
110. (**) CDF Collab., CDF Note 10760, “Search for $H \rightarrow WW^*$ Production at CDF Using 9.7 fb^{-1} Data” (2012).
111. (**) CDF Collab., CDF Note 10781, “Search for $H \rightarrow WW^*$ Production with Leptons and Hadronic Taus in the Final State Using 9.7 fb^{-1} ” (2012).
112. DØ Collab., Phys. Rev. Lett. **104**, 061804 (2010).
113. (***) DØ Collab., DØ Note 6302-CONF, “Search for Higgs boson production in dilepton plus missing transverse energy final states with $8.6\text{--}9.7 \text{ fb}^{-1}$ of $p\bar{p}$ collisions at $\sqrt{s} = 1.96 \text{ TeV}$ ” (2012).
114. DØ Collab., Phys. Rev. Lett. **97**, 151804 (2006).

115. (***) DØ Collab., DØ Note 5873-CONF, “Search for the Associated Higgs Boson Production with Like Sign Leptons in $p\bar{p}$ Collisions $\sqrt{s} = 1.96$ TeV” (2009).
116. (**) CDF Collab., CDF Note 10791, “Search for the SM Higgs in the Four-Lepton Final State” (2012).
117. (**) CDF Collab., CDF Note 10804, “Combination of CDF’s searches for the standard model Higgs boson with up to 10.0 fb^{-1} of data” (2012).
118. (***) DØ Collab., DØ Note 6304-CONF, “Combined Search for the Standard Model Higgs Boson from the DØ Experiment in up to 9.7 fb^{-1} of Data” (2012).
119. L. Lyons, *The Annals of Applied Statistics*, Vol. 2, No. 3, 887 (2008);
L. Demortier, “P-Values and Nuisance Parameters”, *Proceedings of PHYSTAT 2007*, CERN-2008-001, p. 23 (2008).
120. ATLAS Collab., Phys. Rev. Lett. **108**, 111802 (2012).
121. ATLAS Collab., “Search for the Standard Model Higgs boson in the $H \rightarrow W^+W^- \rightarrow \ell^+\nu\ell^-\nu$ decay mode with 4.7 fb^{-1} of ATLAS data at $\sqrt{s} = 7$ TeV”, ATLAS-CONF-2012-012 (2012).
122. CMS Collab., “Search for the standard model Higgs boson decaying to a W pair in the fully leptonic final state in pp collisions at $\sqrt{s} = 7$ TeV”, arXiv:1202.1489 [hep-ex], submitted to Phys. Lett. **B** (2012).
123. CMS Collab., “Search for WH to 3 leptons”, CMS-PAS-HIG-11-034 (2012).
124. ATLAS Collab., “Search for the Higgs boson in the $H \rightarrow W^+W^- \rightarrow \ell\nu jj$ decay channel using 4.7 fb^{-1} of pp collisions at $\sqrt{s} = 7$ TeV with the ATLAS detector”, ATLAS-CONF-2012-018 (2012).
125. ATLAS Collab., Phys. Lett. **B710**, 383 (2012).
126. CMS Collab., Phys. Rev. Lett. **108**, 111804 (2012).
127. ATLAS Collab., “Search for a Standard Model Higgs in the $H \rightarrow ZZ \rightarrow \ell^+\ell^-\nu\bar{\nu}$ decay channel with 4.7 fb^{-1} with the ATLAS detector”, ATLAS-CONF-2012-016 (2012).
128. CMS Collab., arXiv:1202.3478 [hep-ex], submitted to JHEP (2012).
129. ATLAS Collab., “Search for a Standard Model Higgs in the mass range 200-600 GeV in the channel $H \rightarrow ZZ \rightarrow \ell^+\ell^- q\bar{q}$ with with the ATLAS detector”, ATLAS-CONF-2012-017 (2012).

- 130. CMS Collab., [arXiv:1202.1416 \[hep-ex\]](#), submitted to JHEP (2012).
- 131. CMS Collab., [arXiv:1202.3617 \[hep-ex\]](#), submitted to JHEP (2012).
- 132. ATLAS Collab., Phys. Rev. Lett. **108**, 111803 (2012).
- 133. CMS Collab., [arXiv:1202.1487 \[hep-ex\]](#), submitted to Phys. Lett. **B** (2012).
- 134. CMS Collab., “A search using multivariate techniques for a standard model Higgs boson decaying into two photons”, CMS-PAS-HIG-12-001 (2012).
- 135. ATLAS Collab., “Search for the Standard Model Higgs boson produced in association with a vector boson and decaying to a b -quark pair using up to 4.7 fb^{-1} of pp collision data at $\sqrt{s} = 7 \text{ TeV}$ with the ATLAS detector at the LHC”, ATLAS-CONF-2012-015 (2012).
- 136. CMS Collab., [arXiv:1202.4195 \[hep-ex\]](#), submitted to Phys. Lett. **B** (2012).
- 137. ATLAS Collab., “Search for the Standard Model Higgs boson in the $H \rightarrow \tau^+ \tau^-$ decay mode with 4.7 fb^{-1} of ATLAS data at 7 TeV”, ATLAS-CONF-2012-014 (2012).
- 138. CMS Collab., [arXiv:1202.4083 \[hep-ex\]](#), submitted to Phys. Lett. **B** (2012).
- 139. CMS Collab., “Search for Neutral Higgs Bosons Decaying into Tau Leptons in the Dimuon Channel with CMS in pp Collisions at 7 TeV”, CMS-PAS-HIG-12-007 (2012).
- 140. CMS Collab., “Search for WH in Final States with Electrons, Muons, Taus”, CMS-PAS-HIG-12-006 (2012).
- 141. CMS Collab., J. Phys. **G34**, 995 (2007).
- 142. V. Buescher and K. Jakobs, Int. J. Mod. Phys. **A20**, 2523 (2005).
- 143. D. Zeppenfeld *et al.*, Phys. Rev. **D62**, 013009 (2000);
D. Zeppenfeld, “Higgs Couplings at the LHC,” in *Proceedings of the APS/DPF/DPB Summer Study on the Future of Particle Physics* (Snowmass 2001), edited by R. Davidson and C. Quigg, SNOWMASS-2001-P123 [arXiv:hep-ph/0203123](#) (2002).
- 144. M. Dührssen *et al.*, Phys. Rev. **D70**, 113009 (2004).
- 145. T. Plehn, D.L. Rainwater, and D. Zeppenfeld, Phys. Rev. Lett. **88**, 051801 (2002).
- 146. V. Hankele *et al.*, Phys. Rev. **D74**, 095001 (2006).
- 147. C. Ruwiedel, N. Wermes, and M. Schumacher, Eur. Phys. J. **C51**, 385 (2007).
- 148. M. Klute *et al.*, [arXiv:1205.2699 \[hep-ph\]](#) (2012).

- 149. A. Denner *et al.*, [arXiv1111.6395 \[hep-ph\]](#) (2011).
- 150. G.D. Kribs *et al.*, *Phys. Rev.* **D76**, 075016 (2007).
- 151. P. Bechtle *et al.*, *Comput. Phys. Commun.* **181**, 138 (2010).
- 152. C.J. Flacco *et al.*, *Phys. Rev. Lett.* **105**, 111801 (2010).
- 153. The CDF and DØ Collabs. and the Tevatron New Physics and Higgs Working Group, *Phys. Rev.* **D82**, 011102 (2010).
- 154. E. Witten, *Nucl. Phys.* **B188**, 513 (1981);
R.K. Kaul, *Phys. Lett.* **B19**, 19 (1982);
R.K. Kaul, *Pramana* **19**, 183 (1982);
L. Susskind, *Phys. Rev.* **104**, 181 (1984).
- 155. L.E. Ibáñez and G.G. Ross, *Phys. Lett.* **B110**, 215 (1982);
L.E. Ibáñez, *Phys. Lett.* **B118**, 73 (1982);
J. Ellis, D.V. Nanopoulos, and K. Tamvakis, *Phys. Lett.* **B121**, 123 (1983);
L. Alvarez-Gaumé, J. Polchinski, and M.B. Wise, *Nucl. Phys.* **B221**, 495 (1983).
- 156. S. Dimopoulos and H. Georgi, *Nucl. Phys.* **B193**, 150 (1981);
K. Harada and N. Sakai, *Prog. Theor. Phys.* **67**, 1877 (1982);
K. Inoue *et al.*, *Prog. Theor. Phys.* **67**, 1889 (1982);
L. Girardello and M.T. Grisaru, *Nucl. Phys.* **B194**, 65 (1982);
L.J. Hall and L. Randall, *Phys. Rev. Lett.* **65**, 2939 (1990);
I. Jack and D.R.T. Jones, *Phys. Lett.* **B457**, 101 (1999).
- 157. H.E. Haber, *Supersymmetry*, in this volume.
- 158. S. Dimopoulos and D.W. Sutter, *Nucl. Phys.* **B452**, 496 (1995);
D.W. Sutter, Stanford Ph. D. thesis, [hep-ph/9704390](#) (1997);
H.E. Haber, *Nucl. Phys. B* (Proc. Suppl.) **62A-C** (1998) 469.
- 159. A. Djouadi, *Phys. Reports* **459**, 1 (2008).
- 160. H.E. Haber and Y. Nir, *Nucl. Phys.* **B335**, 363 (1990);
A. Dobado, M. J. Herrero, and S. Penaranda, *Eur. Phys. J.* **C17**, 487 (2000);
J.F. Gunion and H.E. Haber, *Phys. Rev.* **D67**, 075019 (2003).
- 161. L.J. Hall and M.B. Wise, *Nucl. Phys.* **B187**, 397 (1981).

162. T.D. Lee, Phys. Rev. **D8**, 1226 (1973);
P. Fayet, Nucl. Phys. **B78**, 14 (1974);
R.D. Peccei and H.R. Quinn, Phys. Rev. Lett. **38**, 1440 (1977);
P. Fayet and S. Ferrara, Phys. Rept. **32**, 249 (1977);
V.D. Barger, J.L. Hewett, and R.J.N. Phillips, Phys. Rev. **D41**, 3421 (1990).
163. S.L. Glashow and S. Weinberg, Phys. Rev. **D15**, 1958 (1977);
E.A. Paschos, Phys. Rev. **D15**, 1966 (1977);
H. Georgi, Hadronic J. **1**, 1227 (1978);
H. Haber, G Kane and T Sterling Nucl. Phys. **B161**, 493 (1979);
A. G. Akeroyd, Phys. Lett. **B368**, 89 (1996);
A.G. Akeroyd, Nucl. Phys. **B544**, 557 (1999);
A. G. Akeroyd, A. Arhrib, and E. Naimi, Eur. Phys. J. **C20**, 51 (2001).
164. V. Barger, H. E. Logan, G. Shaughnessy, Phys. Rev. **D79**, 115018 (2009).
165. Y. Okada, M. Yamaguchi, T. Yanagida, Prog. Theor. Phys. **85**, 1 (1991);
J. Ellis, G. Ridolfi, F. Zwirner, Phys. Lett. **B257**, 83 (1991).
166. H.E. Haber and R. Hempfling, Phys. Rev. Lett. **66**, 1815 (1991).
167. S.P. Li and M. Sher, Phys. Lett. **B140**, 339 (1984);
R. Barbieri and M. Frigeni, Phys. Lett. **B258**, 395 (1991);
M. Drees and M.M. Nojiri, Phys. Rev. **D45**, 2482 (1992);
J.A. Casas *et al.*, Nucl. Phys. **B436**, 3 (1995) [E: **B439** (1995) 466];
J. Ellis, G. Ridolfi, and F. Zwirner, Phys. Lett. **B262**, 477 (1991);
A. Brignole *et al.*, Phys. Lett. **B271**, 123 (1991) [E: **B273** (1991) 550].
168. R.-J. Zhang, Phys. Lett. **B447**, 89 (1999);
J.R. Espinosa and R.-J. Zhang, JHEP **0003**, 026 (2000);
J.R. Espinosa and R.-J. Zhang, Nucl. Phys. **B586**, 3 (2000);
A. Brignole *et al.*, Nucl. Phys. **B631**, 195 (2002), Nucl. Phys. **B643**, 79 (2002);
A. Dedes, G. Degrassi, and P. Slavich, Nucl. Phys. **B672**, 144 (2003).
169. J.F. Gunion and A. Turski, Phys. Rev. **D39**, 2701 (1989),
Phys. Rev. **D40**, 2333 (1989);

- M.S. Berger, Phys. Rev. **D41**, 225 (1990);
A. Brignole, Phys. Lett. **B277**, 313 (1992), Phys. Lett. **B281**, 284 (1992);
M.A. Díaz and H.E. Haber, Phys. Rev. **D45**, 4246 (1992);
P.H. Chankowski, S. Pokorski, and J. Rosiek, Phys. Lett. **B274**, 191 (1992), Nucl. Phys. **B423**, 437 (1994);
A. Yamada, Phys. Lett. **B263**, 233 (1991), Z. Phys. **C61**, 247 (1994);
A. Dabelstein, Z. Phys. **C67**, 496 (1995);
R. Hempfling and A.H. Hoang, Phys. Lett. **B331**, 99 (1994);
S. Heinemeyer, W. Hollik, and G. Weiglein, Phys. Rev. **D58**, 091701 (1998), Phys. Lett. **B440**, 296 (1998), Eur. Phys. J. **C9**, 343 (1999).
170. D.M. Pierce *et al.*, Nucl. Phys. **B491**, 3 (1997).
171. R. Barbieri, M. Frigeni, and F. Caravaglios, Phys. Lett. **B258**, 167 (1991);
Y. Okada, M. Yamaguchi, and T. Yanagida, Phys. Lett. **B262**, 45 (1991);
J.R. Espinosa and M. Quirós, Phys. Lett. **B266**, 389 (1991);
D.M. Pierce, A. Papadopoulos, and S. Johnson, Phys. Rev. Lett. **68**, 3678 (1992);
K. Sasaki, M. Carena, and C.E.M. Wagner, Nucl. Phys. **B381**, 66 (1992);
R. Hempfling, in *Phenomenological Aspects of Supersymmetry*, edited by W. Hollik, R. Rückl, and J. Wess (Springer-Verlag, Berlin, 1992) pp. 260–279;
J. Kodaira, Y. Yasui, and K. Sasaki, Phys. Rev. **D50**, 7035 (1994);
H.E. Haber and R. Hempfling, Phys. Rev. **D48**, 4280 (1993);
M. Carena *et al.*, Phys. Lett. **B355**, 209 (1995).
172. H.E. Haber, R. Hempfling, and A.H. Hoang, Z. Phys. **C75**, 539 (1997);
M. Carena *et al.*, Nucl. Phys. **B580**, 29 (2000).
173. M. Carena, M. Quirós, and C.E.M. Wagner, Nucl. Phys. **B461**, 407 (1996).
174. S. Martin, Phys. Rev. **D67**, 095012 (2003); Phys. Rev. **D71**, 016012 (2005); Phys. Rev. **D75**, 055005 (2007).
175. M. Carena, S. Mrenna, and C.E.M. Wagner, Phys. Rev. **D60**, 075010 (1999);
ibid., Phys. Rev. **D62**, 055008 (2000).

176. S. Heinemeyer, W. Hollik, and G. Weiglein, Phys. Lett. **B455**, 179 (1999);
 J.R. Espinosa and I. Navarro, Nucl. Phys. **B615**, 82 (2001);
 G. Degrassi, P. Slavich, and F. Zwirner, Nucl. Phys. **B611**, 403 (2001);
 S. Heinemeyer *et al.*, Eur. Phys. J. **C39**, 465 (2005).
177. M. Carena *et al.*, hep-ph/9912223 (1999); *idem*, Eur. Phys. J. **C26**, 601 (2003).
178. G. Degrassi *et al.*, Eur. Phys. J. **C28**, 133 (2003).
179. S. Heinemeyer *et al.*, J. High Energy Phys. **0808**, 087 (2008).
180. M. Carena *et al.*, JHEP **1203**, 014 (2012).
181. H. Baer, V. Barger, and A. Mustafayev, Phys. Rev. **D85**, 075010 (2012);
 A. Arbey *et al.*, Phys. Lett. **B708**, 162 (2012);
 L.J. Hall, D. Pinner, and J.T. Ruderman, JHEP **1204**, 131 (2012);
 M. Kadastik *et al.*, arXiv:1112.3647 [hep-ph] (2011);
 P. Draper *et al.*, arXiv:1112.3068 [hep-ph] (2011);
 S. Heinemeyer, O. Stal, and G. Weiglein, Phys. Lett. **B710**, 201 (2012).
182. M. Carena *et al.*, Phys. Lett. **B495**, 155 (2000);
 M. Carena *et al.*, Nucl. Phys. **B625**, 345 (2002).
183. A. Dabelstein, Nucl. Phys. **B456**, 25 (1995);
 F. Borzumati *et al.*, Nucl. Phys. **B555**, 53 (1999);
 H. Eberl *et al.*, Phys. Rev. **D62**, 055006 (2000).
184. J.A. Coarasa, R.A. Jiménez, and J. Solà, Phys. Lett. **B389**, 312 (1996);
 R.A. Jiménez and J. Solà, Phys. Lett. **B389**, 53 (1996);
 A. Bartl *et al.*, Phys. Lett. **B378**, 167 (1996).
185. S. Heinemeyer, W. Hollik, and G. Weiglein, Eur. Phys. J. **C16**, 139 (2000).
186. H.E. Haber *et al.*, Phys. Rev. **D63**, 055004 (2001).
187. L. Hall, R. Rattazzi, and U. Sarid, Phys. Rev. **D50**, 7048 (1994);
 R. Hempfling, Phys. Rev. **D49**, 6168 (1994).
188. M. Carena *et al.*, Nucl. Phys. **B426**, 269 (1994).
189. M. Carena *et al.*, Phys. Lett. **B499**, 141 (2001).
190. E. Berger *et al.*, Phys. Rev. **D66**, 095001 (2002).
191. A. Brignole *et al.*, Nucl. Phys. **B643**, 79 (2002); R. Dermisek and I. Low, Phys. Rev. **D77**, 035012 (2008).
192. A. Djouadi, Phys. Lett. **B435**, 101 (1998).

193. E. Boos *et al.*, Phys. Rev. **D66**, 055004 (2002).
194. A. Djouadi, J. Kalinowski, and P.M. Zerwas, Z. Phys. **C57**, 569 (1993);
H. Baer *et al.*, Phys. Rev. **D47**, 1062 (1993);
A. Djouadi *et al.*, Phys. Lett. **B376**, 220 (1996);
A. Djouadi *et al.*, Z. Phys. **C74**, 93 (1997);
S. Heinemeyer and W. Hollik, Nucl. Phys. **B474**, 32 (1996).
195. J.F. Gunion, Phys. Rev. Lett. **72**, 199 (1994);
D. Choudhury and D.P. Roy, Phys. Lett. **B322**, 368 (1994);
O.J. Eboli and D. Zeppenfeld, Phys. Lett. **B495**, 147 (2000);
B.P. Kersevan, M. Malawski, and E. Richter-Was, Eur. Phys. J. **C29**, 541 (2003).
196. J.F. Gunion *et al.*, Phys. Rev. **D38**, 3444 (1988).
197. S.H. Zhu, hep-ph/9901221 (1999);
S. Kanemura, Eur. Phys. J. **C17**, 473 (2000);
A. Arhrib *et al.*, Nucl. Phys. **B581**, 34 (2000).
198. H.E. Logan and S. Su, Phys. Rev. **D66**, 035001 (2002).
199. A. Gutierrez-Rodriguez and O.A. Sampayo, Phys. Rev. **D62**, 055004 (2000).;
A. Gutierrez-Rodriguez, M.A. Hernandez-Ruiz, and O.A. Sampayo, J. Phys. Soc. Jap. **70**, 2300 (2001);
S. Moretti, EPJdirect **C15**, 1 (2002).
200. S. Kanemura, S. Moretti, and K. Odagiri, JHEP **0102**, 011 (2001).
201. J.F. Gunion and H.E. Haber, Nucl. Phys. **B278**, 449 (1986) [E: **B402**, 567 (1993)];
S. Dawson, A. Djouadi, and M. Spira, Phys. Rev. Lett. **77**, 16 (1996);
A. Djouadi *et al.*, Phys. Lett. **B318**, 347 (1993);
R.V. Harlander and W.B. Kilgore, JHEP **0210**, 017 (2002);
C. Anastasiou and K. Melnikov, Phys. Rev. **D67**, 037501 (2003);
J. Guasch, P. Hafziger and M. Spira, Phys. Rev. **D68**, 115001 (2003);
R.V. Harlander and M. Steinhauser, JHEP **0409**, 066 (2004);
S. Dawson *et al.*, Mod. Phys. Lett. **A21**, 89 (2006);
A. Djouadi and M. Spira, Phys. Rev. **D62**, 014004 (2000);
M. Mühlleitner and M. Spira, Nucl. Phys. **B790**, 1

- (2008);
T. Hahn *et al.*, arXiv:hep-ph/0607308 (2006).
202. D. Dicus *et al.*, Phys. Rev. **D59**, 094016 (1999).
203. C. Balázs, H.-J. He, and C.P. Yuan, Phys. Rev. **D60**, 114001 (1999).
204. J.A. Coarasa *et al.*, Eur. Phys. J. **C2**, 373 (1998).
205. C.S. Li and T.C. Yuan, Phys. Rev. **D42**, 3088 (1990);
[E: Phys. Rev. **D47**, 2156 (1993);
A. Czarnecki and S. Davidson, Phys. Rev. **D47**, 3063 (1993);
C.S. Li, Y.-S. Wei, and J.-M. Yang, Phys. Lett. **B285**, 137 (1992).
206. J. Guasch, R.A. Jiménez. and J. Solà, Phys. Lett. **B360**, 47 (1995).
207. M. Carena *et al.*, Nucl. Phys. **B577**, 88 (2000).
208. M. Guchait and S. Moretti, JHEP **0201**,001 (2002).
209. R.M. Barnett, H.E. Haber, and D.E. Soper, Nucl. Phys. **B306**, 697 (1988).
210. F. Olness and W.-K. Tung, Nucl. Phys. **B308**, 813 (1988).
211. F. Borzumati, J.-L. Kneur, and N. Polonsky, Phys. Rev. **D60**, 115011 (1999).
212. A. Belyaev *et al.*, JHEP **0206**, 059 (2002).
213. L.G. Jin *et al.*, Eur. Phys. J. **C14**, 91 (2000); Phys. Rev. **D62**, 053008 (2000);
A. Belyaev *et al.*, Phys. Rev. **D65**, 031701 (2002);
G. Gao *et al.*, Phys. Rev. **D66**, 015007 (2002).
214. S.-H. Zhu, Phys. Rev. **D67**, 075006 (2005);
T. Plehn, Phys. Rev. **D67**, 014018 (2003).
215. A.A. Barrientos BendeZú and B.A. Kniehl, Phys. Rev. **D59**, 015009 (1999); Phys. Rev. **D61**, 015009 (2000);
Phys. Rev. **D63**, 015009 (2001).
216. A.A. Barrientos BendeZú and B.A. Kniehl, Nucl. Phys. **B568**, 305 (2000).
217. A. Krause *et al.*, Nucl. Phys. **B519**, 85 (1998).
218. O. Brein and W. Hollik, Eur. Phys. J. **C13**, 175 (2000).
219. ALEPH Collab., Phys. Lett. **B526**, 191 (2002).
220. DELPHI Collab., Eur. Phys. J. **C32**, 145 (2004).
221. OPAL Collab., Eur. Phys. J. **C37**, 49 (2004).
222. L3 Collab., Phys. Lett. **B545**, 30 (2002).
223. OPAL Collab., Eur. Phys. J. **C23**, 397 (2002).
224. DELPHI Collab., Eur. Phys. J. **C38**, 1 (2004).

- 225. M. Carena *et al.*, Eur. Phys. J. **C45**, 797 (2006).
- 226. DØ Collab., Phys. Lett. **B698**, 97 (2011).
- 227. CDF Collab., Phys. Rev. **D85**, 032005 (2012).
- 228. DØ Collab., Phys. Rev. Lett. **104**, 151801 (2010);
DØ Collab., Phys. Rev. Lett. **107**, 121801 (2011).
- 229. (***) DØ Collab., DØ Note 5974-CONF, “Search for neutral Higgs bosons $\phi b \rightarrow \tau_e \tau_{\text{had}} b$ with 3.7 fb^{-1} of DØ data” (2011).
- 230. CDF Collab., Phys. Rev. Lett. **103**, 201801 (2009).
- 231. DØ Collab., Phys. Rev. Lett. **101**, 071804 (2008);
DØ Collab., Phys. Lett. **B707**, 323 (2012).
- 232. DØ Collab., Phys. Lett. **B710**, 569 (2012).
- 233. M. Carena *et al.*, arXiv:1203.1041 [hep-ph] (2012).
- 234. ATLAS Collab., “Search for neutral MSSM Higgs bosons decaying to $\tau^+ \tau^-$ pairs in proton-proton collisions at $\sqrt{s} = 7 \text{ TeV}$ with the ATLAS detector”, ATLAS-CONF-2011-132 (2011).
- 235. ATLAS Collab., Phys. Lett. **B705**, 174 (2011).
- 236. ATLAS Collab., arXiv:0901.0512 [hep-ex] (2009).
- 237. ALEPH Collab., Phys. Lett. **B543**, 1 (2002);
DELPHI Collab., Phys. Lett. **B525**, 17 (2002);
L3 Collab., Phys. Lett. **B575**, 208 (2003);
OPAL Collab., Eur. Phys. J. **C7**, 407 (1999).
- 238. (*) ALEPH, DELPHI, L3 and OPAL Collabs., The LEP Working Group for Higgs Boson Searches, *Search for Charged Higgs Bosons: Preliminary ...*, LHWG-Note/2001-05.
- 239. DØ Collab., Phys. Rev. Lett. **82**, 4975 (1999);
idem, **88**, 151803 (2002);
CDF Collab., Phys. Rev. **D62**, 012004 (2000);
idem, Phys. Rev. Lett. **79**, 357 (1997).
- 240. CDF Collab., Phys. Rev. Lett. **96**, 042003 (2006).
- 241. DØ Collab., Phys. Lett. **B682**, 278 (2009).
- 242. ATLAS Collab., arXiv:1204.2760 [hep-ex] (2012).
- 243. ATLAS Collab., “A Search for a light charged Higgs boson decaying to $c\bar{s}$ in pp collisions at $\sqrt{s} = 7 \text{ TeV}$ with the ATLAS detector”, ATLAS-CONF-2011-094 (2011).
- 244. CMS Collab., “Search for the light charged Higgs boson in top quark decays in pp collisions at $\sqrt{s} = 7 \text{ TeV}$ CMS-PAS-HIG-11-019.
- 245. A. D. Sakharov, JETP Lett. **5**, 24 (1967).
- 246. M. Carena *et al.*, Nucl. Phys. **B599**, 158 (2001).

247. S. Dimopoulos and S. Thomas, Nucl. Phys. **B465**, 23, (1996);
S. Thomas, Int. J. Mod. Phys. **A13**, 2307 (1998).
248. A. Pilaftsis and C.E.M. Wagner, Nucl. Phys. **B553**, 3 (1999).
249. M. Carena *et al.*, Nucl. Phys. **B586**, 92 (2000).
250. A. Pilaftsis, Phys. Rev. **D58**, 096010 (1998); Phys. Lett. **B435**, 88 (1998);
K.S. Babu *et al.*, Phys. Rev. **D59**, 016004 (1999).
251. G.L. Kane and L.-T. Wang, Phys. Lett. **B488**, 383 (2000);
S.Y. Choi, M. Drees and J.S. Lee, Phys. Lett. **B481**, 57 (2000);
S.Y. Choi and J.S. Lee, Phys. Rev. **D61**, 015003 (2000);
S.Y. Choi, K. Hagiwara and J.S. Lee, Phys. Rev. **D64**, 032004 (2001); Phys. Lett. **B529**, 212 (2002);
T. Ibrahim and P. Nath, Phys. Rev. **D63**, 035009 (2001);
T. Ibrahim, Phys. Rev. **D64**, 035009 (2001);
S. Heinemeyer, Eur. Phys. J. **C22**, 521 (2001);
S.W. Ham *et al.*, Phys. Rev. **D68**, 055003 (2003).
252. M. Frank *et al.*, JHEP **0702**, 047 (2007);
S. Heinemeyer *et al.*, Phys. Lett. **B652**, 300 (2007);
T. Hahn *et al.*, arXiv:0710.4891 (2007).
253. D.A. Demir, Phys. Rev. **D60**, 055006 (1999);
S. Y. Choi *et al.*, Phys. Lett. **B481**, 57 (2000).
254. E. Christova *et al.*, Nucl. Phys. **B639**, 263 (2002) [E: Nucl. Phys. **B647**, 359 (2002)].
255. P. Draper, T. Liu, and C.E.M. Wagner, Phys. Rev. **D81**, 015014 (2010).
256. W. de Boer and C. Sander, Phys. Lett. **B585**, 276 (2004);
S. Heinemeyer *et al.*, JHEP **0608**, 052 (2006);
A. Djouadi *et al.*, Phys. Rev. Lett. **78**, 3626 (1997);
A. Djouadi *et al.*, Phys. Rev. **D57**, 4179 (1998);
S. Heinemeyer and G. Weiglein, JHEP **10** (2002) 072;
J. Haestier *et al.*, JHEP **0512**, 027, (2005).;
S. Heinemeyer, W. Hollik, and G. Weiglein, Phys. Rept. **425**, 265 (2006);
S. Heinemeyer *et al.*, JHEP **0804**, 039 (2008).
257. O. Buchmueller *et al.*, Phys. Rev. **D81**, 035009 (2010).
258. O. Buchmueller *et al.*, Eur. Phys. J. **C72**, 1878 (2012).
259. G. D'Ambrosio *et al.*, Nucl. Phys. **B645**, 155 (2002).
260. M. Carena, A. Menon, and C.E.M. Wagner, Phys. Rev. **D76**, 035004 (2007);

- P. Draper, T. Liu, and C.E.M. Wagner, Phys. Rev. **D80**, 035025 (2009).
261. J.R. Ellis *et al.*, JHEP **0708**, 083 (2007).
262. E. Lunghi, W. Porod, and O. Vives, Phys. Rev. **D74**, 075003 (2006).
263. M. Carena *et al.*, Phys. Rev. **D74**, 015009 (2006).
264. G. Buchalla, A.J. Buras, and M.E. Lautenbacher, Rev. Mod. Phys. **68**, 1125 (1996).
265. A. Dedes and A. Pilaftsis, Phys. Rev. **D67**, 015012 (2003).
266. A.J. Buras *et al.*, Phys. Lett. **B546**, 96 (2002).
267. A. J. Buras *et al.*, Nucl. Phys. **B659**, 2 (2003).
268. K.S. Babu and C.F. Kolda, Phys. Rev. Lett. **84**, 228 (2000).
269. (**) CDF Collab., “A Search for $B_{s(d)}^0 \rightarrow \mu^+ \mu^-$ Decays using 9.7 fb^{-1} of Data”, CDF Note 10701 (2012); CDF Collab., Phys. Rev. Lett. **107**, 191801 (2011); LHCb Collab., arXiv:1203.4493 [hep-ex] (2012); CMS Collab., “Search for $B_s \rightarrow \mu^+ \mu^-$ and $B^0 \rightarrow \mu^+ \mu^-$ decays”, arXiv:1203.3976 (2012). Submitted to JHEP.
270. A. G. Akeroyd, F. Mahmoudi, and D. Martinez Santos, JHEP **1112**, 088 (2011); A. Arbey, M. Battaglia, and F. Mahmoudi, Eur. Phys. J. **C72**, 1906 (2012).
271. M. Misiak *et al.*, Phys. Rev. Lett. **98**, 022002 (2007), and refs. therein.
272. T. Becher and M. Neubert, Phys. Rev. Lett. **98**, 022003 (2007).
273. Heavy Flavor Averaging Group (HFAG), <http://www.slac.stanford.edu/xorg/hfag/rare/lep-pho09/rad11/btosg.pdf>.
274. Belle Collab., arXiv:0809.3834 [hep-ex] (2008).
275. Belle Collab., Phys. Rev. **D82** 071101 (2010).
276. BaBar Collab., Phys. Rev. D **81**, 051101 (2010).
277. BaBar Collab., arXiv:1008.0104 [hep-ex].
278. M. Bona *et al.* [UTfit Collab.], Phys. Lett. **B687**, 61 (2010), http://ckmfitter.in2p3.fr/www/html/ckm_results.html.
279. G. Isidori and P. Paradisi, Phys. Lett. **B639**, 499 (2006).
280. BaBar Collab., Phys. Rev. Lett. **100**, 021801 (2008); Belle Collab., arXiv:0910.4301 [hep-ex] (2009).

281. U. Nierste, S. Trine and S. Westhoff, Phys. Rev. **D78**, 015006 (2008).
282. S. Trine, arXiv:0810.3633 [hep-ph] (2008).
283. LHCb Collab., Phys. Rev. Lett. **108**, 111602 (2012).
284. CDF Collab., “Improved Measurement of the Difference between Time Integrated CP Asymmetries in $D^0 \rightarrow K^+K^-$ and $D^0 \rightarrow \pi^+\pi^-$ Decays at CDF”, CDF Note 10784 (2012).
285. W. Altmannshofer *et al.*, JHEP **1204**, 049 (2012).
286. M. Carena, A. Menon, and C.E.M. Wagner, Phys. Rev. **D79**, 075025 (2009).
287. W. Altmannshofer and D.M. Straub, JHEP **1009**, 078 (2010).
288. J. Ellis *et al.*, Phys. Lett. **B653**, 292 (2007).
289. N. Cabibbo, G.R. Farrar, and L. Maiani, Phys. Lett. **B105**, 155 (1981);
H. Goldberg, Phys. Rev. Lett. **50**, 1419 (1983);
J. R. Ellis *et al.*, Nucl. Phys. **B238**, 453 (1984);
G. Bertone, D. Hooper, and J. Silk, Phys. Reports **405**, 279 (2005).
290. M. Carena, D. Hooper, and A. Vallinotto, Phys. Rev. **D75**, 055010 (2007);
M. Carena, D. Hooper, and P. Skands, Phys. Rev. Lett. **97**, 051801 (2006).
291. A. Djouadi and Y. Mambrini, JHEP **0612**, 001 (2006).
292. J. Ellis, K.A. Olive, and Y. Santoso, Phys. Rev. **D71**, 095007 (2005).
293. N.G. Deshpande and E. Ma Phys. Rev. **D18**, 2574 (1978);
R. Barbieri, L.J. Hall, and V. Rychkov Phys. Rev. **D74**, 015007 (2006);
L. Lopez-Honorez *et al.*, JCAP **0702**, 028 (2007);
E. Lundstrom, M Gustafsson, and J. Edjo, Phys. Rev. **D79**, 035013 (2009);
E. Dolle *et al.*, Phys. Rev. **D8**, 035003 (2010);
X. Miao, S. Su, and B. Thomas, Phys. Rev. **D82**, 035009 (2010);
L. Lopez-Honorez and C.Yaguna, JCAP **1101**, 002 (2011).
294. H.E. Haber, *Proceedings of the 1990 Theoretical Advanced Study Institute in Elementary Particle Physics*, edited by M. Cvetič and Paul Langacker (World Scientific, Singapore, 1991) pp. 340–475, and references therein.

295. S. Glashow and S. Weinberg, Phys. Rev. **D15**, 1958 (1977).
296. P. Fayet, Phys. Lett. **B90**, 104 (1975);
H.-P. Nilles, M. Srednicki, and D. Wyler, Phys. Lett. **B120**, 346 (1983);
J.-M. Frere, D.R.T. Jones, and S. Raby, Nucl. Phys. **B222**, 11 (1983);
J.-P. Derendinger and C.A. Savoy, Nucl. Phys. **B237**, 307 (1984);
B.R. Greene and P.J. Miron, Phys. Lett. **B168**, 226 (1986);
J. Ellis *et al.*, Phys. Lett. **B176**, 403 (1986);
L. Durand and J.L. Lopez, Phys. Lett. **B217**, 463 (1989);
M. Drees, Int. J. Mod. Phys. **A4**, 3635 (1989);
U. Ellwanger, Phys. Lett. **B303**, 271 (1993);
U. Ellwanger, M. Rausch de Taubenberg, and C.A. Savoy, Phys. Lett. **B315**, 331 (1993); Z. Phys. **C67**, 665 (1995); Phys. Lett. **B492**, 21 (1997);
P.N. Pandita, Phys. Lett. **B318**, 338 (1993); Z. Phys. **C59**, 575 (1993);
T. Elliott, S.F. King, and P.L. White, Phys. Lett. **B305**, 71 (1993); Phys. Lett. **B314**, 56 (1993); Phys. Rev. **D49**, 2435 (1994); Phys. Lett. **B351**, 213 (1995);
K.S. Babu and S.M. Barr, Phys. Rev. **D49**, R2156 (1994);
S.F. King and P.L. White, Phys. Rev. **D52**, 4183 (1995);
N. Haba, M. Matsuda, and M. Tanimoto, Phys. Rev. **D54**, 6928 (1996);
F. Franke and H. Fraas, Int. J. Mod. Phys. **A12**, 479 (1997);
S.W. Ham, S.K. Oh, and H.S. Song, Phys. Rev. **D61**, 055010 (2000);
D.A. Demir, E. Ma, and U. Sarkar, J. Phys. **G26**, L117 (2000);
R. B. Nevzorov and M. A. Trusov, Phys. Atom. Nucl. **64**, 1299 (2001);
U. Ellwanger and C. Hugonie, Eur. Phys. J. **C25**, 297 (2002);
U. Ellwanger *et al.*, arXiv:hep-ph/0305109 (2003);
D.J. Miller and S. Moretti, arXiv:hep-ph/0403137 (2004).
297. A. Dedes *et al.*, Phys. Rev. **D63**, 055009 (2001);
A. Menon, D. Morrissey, and C.E.M. Wagner, Phys. Rev. **D70**, 035005, (2004).
298. R. Dermisek and J.F. Gunion, Phys. Rev. **D76**, 095006 (2007);
R. Dermisek and J.F. Gunion, Phys. Rev. **D81**, 075003

- (2010);
 G. Degrossi and P. Slavich, Nucl. Phys. **B825**, 119 (2010);
 M. Maniatis, Int. J. Mod. Phys. **A25**, 3505 (2010);
 U. Ellwanger, G. Espitalier-Noel and C. Hugonie, JHEP **1109**, 105 (2011);
 U. Ellwanger, JHEP **1203**, 044 (2012);
 J.F. Gunion, Y. Jiang, and S. Kraml, Nucl. Phys. **B710**, 454 (2012);
 S.F. King, M. Muhlleitner, and R. Nevzorov, Nucl. Phys. **B860**, 207 (2012).
299. J. R. Espinosa and M. Quirós, Phys. Lett. **B279**, 92 (1992).
300. P. Batra and E. Ponton, Phys. Rev. **D79**, 035001 (2009).
301. M. Schmaltz and D. Tucker-Smith, Ann. Rev. Nucl. Part. Sci. **55**, 229 (2005).
302. M. Perelstein, Prog. Part. Nucl. Phys. **58**, 247 (2007).
303. H.C Cheng, I. Low, and L.T. Wang, Phys. Rev. **D74**, 055001 (2006).
304. C.R. Chen, K. Tobe, and C. P. Yuan, Phys. Lett. **B640**, 263 (2006).
305. G.F. Giudice *et al.*, JHEP **0706**, 045 (2007).
306. J. Hubisz *et al.*, JHEP **0601**, 135 (2006).
307. G. F. Giudice, R. Rattazzi, and J. D. Wells, Nucl. Phys. **B595**, 250 (2001);
 M. Chaichian *et al.*, Phys. Lett. **B524**, 161 (2002);
 D. Dominici *et al.*, Acta Phys. Polon. **B33**, 2507 (2002);
 J. L. Hewett and T. G. Rizzo, JHEP **0308**, 028 (2003).
308. OPAL Collab., Phys. Lett. **B609**, 20 (2005). [E: *ibid.*, **637**, 374 (2006)].
309. B. Grzadkowski and J. F. Gunion, arXiv:1202.5017 [hep-ph] (2012);
 B. Coleppa, T. Gregoire, and H. Logan, Phys. Rev. **D85**, 055001 (2012).
310. S. Casagrande *et al.*, JHEP **1009**, 014 (2010);
 A. Azatov, M. Toharia, and L. Zhu, Phys. Rev. **D82**, 056004 (2010);
 A. Azatov and J. Galloway, Phys. Rev. **D85**, 055013 (2012);
 F. Goertz, U. Haisch, and M. Neubert, arXiv:1112.5099 [hep-ph] (2012);
 M. Carena *et al.*, arXiv:1204.0008 [hep-ph] (2012).
311. T. Appelquist, H. -C. Cheng, and B. A. Dobrescu, Phys. Rev. **D64**, 035002 (2001).

- 312. F.J. Petriello, JHEP **0205**, 003 (2002).
- 313. A. Azatov *et al.*, arXiv:1204.4817 [hep-ph] (2012);
J. R. Espinosa *et al.*, arXiv:1202.3697 [hep-ph] (2012).
- 314. M. J. Strassler and K. M. Zurek, Phys. Lett. **B651**, 374 (2007).
- 315. M. J. Strassler and K. M. Zurek, Phys. Lett. **B661**, 263 (2008).
- 316. T. Han *et al.*, JHEP **0807**, 008 (2008).
- 317. A. Falkowski *et al.*, JHEP **1005**, 077 (2010);
A. Falkowski *et al.*, Phys. Rev. Lett. **105**, 241801 (2010).
- 318. S. Chivukula *et al.*, *Dynamical Electroweak Symmetry Breaking*, in this volume.
- 319. S. Schael *et al.*, [ALEPH Collab.], JHEP **1005**, 049 (2010).
- 320. (*) DELPHI Collab., Interpretation of the searches for Higgs bosons in the MSSM with an additional scalar singlet, CERN-OPEN-99-438 (1999).
- 321. DØ Collab., Phys. Rev. Lett. **103**, 061801 (2009).
- 322. CDF Collab., Phys. Rev. Lett. **107**, 031801 (2011).
- 323. CMS Collab., “Search for a light pseudoscalar boson in the dimuon channel”, CMS-PAS-HIG-12-004 (2012).
- 324. ATLAS Collab., “A Search for Light CP-Odd Higgs Bosons Decaying to $\mu^+\mu^-$ in ATLAS”, ATLAS-CONF-2011-020 (2012).
- 325. E.L. Berger *et al.*, Phys. Rev. **D66**, 095001 (2002).
- 326. W. Loinaz and J. Wells, Phys. Lett. **B445**, 178 (1998);
X. Calmet and H. Fritzsch, Phys. Lett. **B496**, 190 (2000).
- 327. ALEPH Collab., Phys. Lett. **B544**, 25 (2002);
DELPHI Collab., Eur. Phys. J. **C44**, 147 (2005);
L3 Collab., Phys. Lett. **B583**, 14 (2004);
OPAL Collab., Eur. Phys. J. **C18**, 425 (2001).
- 328. (*) The LEP Working Group for Higgs Boson Searches, *Flavour Independent Search for Hadronically Decaying Neutral Higgs Bosons at LEP*, LHWG Note 2001-07.
- 329. OPAL Collab., Eur. Phys. J. **C18**, 425 (2001);
DELPHI Collab., Eur. Phys. J. **C38**, 1 (2004).
- 330. DELPHI Collab., Eur. Phys. J. **C34**, 399 (2004).
- 331. OPAL Collab., arXiv:0812.0267 [hep-ex] (2008).
- 332. Y. Chikashige *et al.*, Phys. Lett. **B98**, 265 (1981);
A.S. Joshipura and S.D. Rindani, Phys. Rev. Lett. **69**, 3269 (1992);
F. de Campos *et al.*, Phys. Rev. **D55**, 1316 (1997).

333. DELPHI Collab., Eur. Phys. J. **C32**, 475 (2004);
L3 Collab., Phys. Lett. **B609**, 35 (2005);
OPAL Collab., Phys. Lett. **B377**, 273 (1996).
334. (*) ALEPH, DELPHI, L3 and OPAL Collabs., The LEP Working Group for Higgs Boson Searches, *Search for Invisible Higgs Bosons: Preliminary ...*, LHWG-Note/2001-06.
335. (**) CDF Collab., “Search for heavy metastable particles decaying to quark pairs in $p\bar{p}$ collisions at $\sqrt{s} = 1.96$ TeV”, CDF Note 10356 (2010).
336. DØ Collab., Phys. Rev. Lett. **103**, 071801 (2009).
337. (**) CDF Collab., “Search for Anomalous Production of Events with a W or Z boson and Additional Leptons”, CDF Note 10526 (2011).
338. A. Abbasabadi *et al.*, Phys. Rev. **D52**, 3919 (1995);
K. Hagiwara, R. Szalapski, and D. Zeppenfeld, Phys. Lett. **B318**, 155 (1993);
O.J.P. Éboli *et al.*, Phys. Lett. **B434**, 340 (1998).
339. L3 Collab, Phys. Lett. **B589**, 89 (2004).
340. ALEPH Collab., Phys. Lett. **B544**, 16 (2002);
DELPHI Collab., Eur. Phys. J. **C35**, 313 (2004);
L3 Collab., Phys. Lett. **B534**, 28 (2002);
OPAL Collab., Phys. Lett. **B544**, 44 (2002).
341. (*) ALEPH, DELPHI, L3 and OPAL Collabs., The LEP Working Group for Higgs Boson Searches, *Search for Higgs Bosons Decaying into Photons: Combined ...*, LHWG Note/2002-02.
342. L3 Collab., Phys. Lett. **B568**, 191 (2003).
343. ALEPH Collab., Eur. Phys. J. **C49**, 439 (2007).
344. DØ Collab., Phys. Rev. Lett. **107**, 151801 (2011).
345. (***) DØ Collab., DØ Note 6297-CONF, “Search for a Fermiophobic Higgs Boson in the di-photon final state using using 9.7 fb^{-1} of DØ data” (2012).
346. CDF Collab., Phys. Rev. Lett. **103**, 061803 (2009).
347. (**) CDF Collab., CDF Note 10731, “Search for a Fermiophobic Higgs Boson in the Di-photon Final State Using 10.0 fb^{-1} of CDF Data” (2012).
348. The CDF and DØ Collabs. and the Tevatron New Physics and Higgs Working Group, “Combined CDF and DØ upper limits on Fermiophobic Higgs Boson Production with up to 8.2 fb^{-1} of $p\bar{p}$ data”, arXiv:1109.0576 (2011).

- 349. (***) DØ Collab., DØ Note 5067-CONF, “Search for Fermiophobic Higgs Boson in $3\gamma + X$ Events” (2007).
- 350. ATLAS Collab., “Search for a fermiophobic Higgs boson in the diphoton decay channel with 4.9 fb^{-1} of ATLAS data at $\sqrt{s} = 7 \text{ TeV}$ ”, ATLAS-CONF-2012-013 (2012).
- 351. CMS Collab., “Search for the fermiophobic model Higgs boson decaying into two photons”, CMS-PAS-HIG-12-002 (2012).
- 352. G.B. Gelmini and M. Roncadelli, Phys. Lett. **B99**, 411 (1981);
R.N. Mohapatra and J.D. Vergados, Phys. Rev. Lett. **47**, 1713 (1981);
V. Barger *et al.*, Phys. Rev. **D26**, 218 (1982).
- 353. B. Dutta and R.N. Mohapatra, Phys. Rev. **D59**, 015018 (1999);
C.S. Aulakh *et al.*, Phys. Rev. **D58**, 115007 (1998);
C.S. Aulakh, A. Melfo, and G. Senjanovic, Phys. Rev. **D57**, 4174 (1998).
- 354. DELPHI Collab., Phys. Lett. **B552**, 127 (2003).
- 355. OPAL Collab., Phys. Lett. **B295**, 347 (1992);
idem, **B526**, 221 (2002).
- 356. L3 Collab., Phys. Lett. **B576**, 18 (2003).
- 357. OPAL Collab., Phys. Lett. **B577**, 93 (2003).
- 358. DØ Collab., Phys. Rev. Lett. **93**, 141801 (2004);
DØ Collab., Phys. Rev. Lett. **101**, 071803 (2008).
- 359. CDF Collab., Phys. Rev. Lett. **93**, 221802 (2004);
CDF Collab., Phys. Rev. Lett. **101**, 121801 (2008).
- 360. CDF Collab., Phys. Rev. Lett. **95**, 071801 (2005).
- 361. CMS Collab., “Inclusive search for doubly charged Higgs in leptonic final states with the 2011 data at 7 TeV”, CMS-PAS-HIG-12-005 (2012).
- 362. ATLAS Collab., Phys. Rev. **D88**, 032004 (2012).
- 363. F. Gianotti, on behalf of the ATLAS Collaboration, “Status of Standard Model Higgs Searches in ATLAS”, presentation given July 4, 2012 at CERN.
- 364. ATLAS Collab., ATLAS-CONF-2012-093 (2012).
- 365. J. Incandela, on behalf of the CMS Collaboration, “Status of the CMS SM Higgs Search”, presentation given July 4, 2012 at CERN.
- 366. CMS Collab., CMS-PAS-HIG-12-020 (2012).
- 367. ATLAS Collab., ATLAS-CONF-2012-091, ATLAS-CONF-2012-092 (2012).

- 368. ATLAS Collab, [arXiv:1205.6744 \[hep-ex\]](#), submitted to Phys. Lett. B (2012); ATLAS Collab., [arXiv:1206.2443 \[hep-ex\]](#), submitted to Phys. Lett. B (2012); ATLAS Collab., [arXiv:1206.0756 \[hep-ex\]](#), submitted to Phys. Lett. B (2012); ATLAS Collab., [arXiv:1206.0756 \[hep-ex\]](#), submitted to Phys. Lett. B (2012); ATLAS Collab., [arXiv:1206.6074 \[hep-ex\]](#), submitted to Phys. Lett. B (2012); ATLAS Collab., [arXiv:1206.5971 \[hep-ex\]](#), submitted to JHEP (2012); ATLAS Collab., [arXiv:1207.0210 \[hep-ex\]](#), submitted to Phys. Lett. B (2012).
- 369. ATLAS Collab., [arXiv:1207.0319 \[hep-ex\]](#), submitted to Phys. Rev. D (2012).
- 370. CMS Collab., CMS-PAS-HIG-12-015, CMS-PAS-HIG-12-016, CMS-PAS-HIG-12-023, CMS-PAS-HIG-12-023, CMS-PAS-HIG-11-024, CMS-PAS-HIG-12-017, CMS-PAS-HIG-12-003, CMS-PAS-HIG-12-021, CMS-PAS-HIG-12-019, CMS-PAS-HIG-12-018, CMS-PAS-HIG-12-012, CMS-PAS-HIG-12-006, CMS-PAS-HIG-12-025 (2011, 2012).
- 371. CMS Collab., CMS-PAS-HIG-12-001 (2012).
- 372. CMS Collab., Phys. Lett. B **710**, 91 (2012).
- 373. The CDF and D0 Collaborations and the Tevatron New Physics and Higgs Working Group, [arXiv:1207.0449 \[hep-ex\]](#) (2012).
- 374. D0 Collab., [arXiv:1207.0422 \[hep-ex\]](#) (2012).
- 375. D0 Collab., D0 Note 6302-CONF, (2012).
- 376. CDF Collab., CDF Note 10804, (2012); CDF Collab., [arXiv:1207.1707](#), submitted to Phys. Rev. Lett. (2012).